ANL-5787
Reactors-General

ARGONNE NATIONAL LABORATORY
P. O. Box 299
Lemont, Illinois

TWO-PHASE AIR-WATER FLOW PHENOMENA

by

Michael Petrick

Reactor Engineering Division

March, 1958

Submitted in Partial Fulfillment of the Requirements for the Degree Doctor of Philosophy in Chemical Engineering in the Graduate School of Illinois Institute of Technology

Operated by The University of Chicago
under
Contract W-31-109-eng-38

DISCLAIMER

TABLE OF CONTENTS

TABLE OF CONTENTS

LIST OF FIGURES

LIST OF FIGURES

LIST OF FIGURES

ACKNOWLEDGEMENTS

The author wishes to express his appreciation to all members of the Heat Engineering Section for their encouragement and helpful criticisms during the course of his work.

Particular thanks are due to Elmer R. Gunchin, who constructed and operated the experimental apparatus, Sanford E. Cohen and Gerald T. Petersen, who assisted greatly in the reduction of the data, Barton M. Hoglund, for his assistance during the early stages of the program, and to M. Jean Radcliff, for typing the original manuscript.

NOMENCLATURE

General

α	void volume fraction (air, vapor, etc.)
A	cross-sectional flow area, ft^2
G	mass flow rate, $lb/(hr)(ft^2)$
V	fluid velocity, fps
ρ	fluid density, lb/ft^3
W	flow rate, lb/hr
X	mixture quality - ratio of mass flow rate of gas to total mass flow rate of both phases
N	exponent in Eq. (4. 16)
P	pressure, psia
T	absolute temperature, degree Rankine
M	molecular weight
L	length, ft
D_e	equivalent diameter, ft
S	channel spacing, in.
f_0	fanning friction factor
g	acceleration of gravity, ft/sec^2
g_c	conversion factor, $\frac{(lb)(ft)}{sec^2}/lb$ force
μ	viscosity, $lb/(hr)(ft)$
N_{Re}	Reynolds Number

Subscripts

w	liquid phase
g	gaseous phase
st	structure
T	total
w_0	liquid phase flowing alone in conduit
m	two-phase mixture
1,2	refers to a position

NOMENCLATURE

Pressure Drop Ratios

$\left(\frac{\Delta P}{\Delta L}\right)_w$	single-phase frictional pressure drop gradient of liquid phase flowing alone in the conduit.
$\left(\frac{\Delta P}{\Delta L}\right)_g$	single-phase frictional pressure drop gradient of gaseous phase flowing alone in the conduit.
$\left(\frac{\Delta P}{\Delta L}\right)_{w_0}$	single-phase liquid frictional pressure drop gradient at total flow rate.
$\left(\frac{\Delta P}{\Delta L}\right)_{TP}$	two-phase frictional pressure drop gradient.
$\Phi_w^2 = \frac{\left(\frac{\Delta P}{\Delta L}\right)_{TP}}{\left(\frac{\Delta P}{\Delta L}\right)_w}$	Lockhart-Martinelli two-phase friction factor multiplier based on the liquid phase.
$\Phi_g^2 = \frac{\left(\frac{\Delta P}{\Delta L}\right)_{TP}}{\left(\frac{\Delta P}{\Delta L}\right)_g}$	Lockhart-Martinelli two-phase friction factor multiplier based on the gaseous phase.
$\chi^2 = \frac{\left(\frac{\Delta P}{\Delta L}\right)_w}{\left(\frac{\Delta P}{\Delta L}\right)_g}$	Lockhart-Martinelli flow parameter.
$R = \frac{\left(\frac{\Delta P}{\Delta L}\right)_{TP}}{\left(\frac{\Delta P}{\Delta L}\right)_{w_0}}$	local two-phase friction factor multiplier.
$\overline{R} = \frac{\left(\frac{\Delta P}{\Delta L}\right)_{TP}}{\left(\frac{\Delta P}{\Delta L}\right)_{w_0}}$	average two-phase friction factor multiplier over boiling length.

TWO-PHASE AIR-WATER FLOW PHENOMENA

by
Michael Petrick

ABSTRACT

An experimental two-phase flow study was conducted on a series of Lucite rectangular channels with aspect ratios of 2 to 16 using an air-water system at atmospheric pressure. The objectives of the study were: (1) to determine the effect of sudden changes of flow area on the density of two-phase fluids; (2) to investigate the effect of mass flow rate on the two-phase friction factor multiplier; and (3) to develop a sound method of measuring the density of a two-phase fluid in large conduits.

The density of the air-water mixture changed during either an expansion or contraction of flow area; however, the magnitude of the change was not great and was readily predicted by a semi-theoretical equation. A sizeable effect of mass flow rate on the two-phase friction factor multiplier was found which was not accounted for in the widely used Martinelli correlation. A traversing technique was developed for measuring the density of a two-phase fluid which also gave a continuous trace of the phase distribution. The method was tried on Lucite mock-ups of simulated two-phase flow patterns, and excellent agreement was obtained between the measured and calculated voids.

I. INTRODUCTION

During recent years considerable effort has been expended in the field of two-phase flow (simultaneous flow of a liquid and gaseous phase) in an attempt to obtain empirical density relationships and pressure drop friction factors for two-phase mixtures. This information is vitally needed in such diversified fields as the petroleum, chemical and power industries. The development of nuclear boiling reactors has prompted an even more intensified research program because of the intimate inter-relationships between the density of the boiling core coolant, reactor kinetics, and system hydrodynamics.

In a natural circulation, two-phase system the hydrodynamic characteristics are determined primarily by the volume fraction of vapor existing in the two-phase region. In analyzing natural circulation systems

it becomes imperative to predict the effect of a sudden geometry change of flow area on two-phase mixture density, should one occur. An example of such a geometry change is the use of risers in a natural circulation system to increase mass flow rates. The flow area of the riser may be either greater or less than the flow area of the boiling section, depending upon the type of riser added. In certain designs of boiling reactors, where practically the entire "net natural circulation driving head" exists in the riser, knowledge of the volume fraction of vapor in the riser is a prerequisite to a competent hydrodynamic analysis of the system. A search of the literature reveals a complete lack of data on such systems. Therefore, this experimental program was undertaken to provide sufficient information to evaluate the effect of sudden changes of flow area on the densities of two-phase mixtures.

Inherent in the evaluation of the effect of geometrical changes on the densities of two-phase mixtures is the problem of obtaining accurate measurements of the vapor volume fraction or "liquid holdups." The method most commonly used in the past was to isolate a portion of a tube by means of two simultaneously closing valves and, subsequently, to measure the actual quantity of liquid present. However, the volume fraction of vapor obtained in this manner was an average value over a length of tube.

During the past few years the use of radioactive techniques for measurement of two-phase density has become more and more prevalent. The radiation attenuation method of density determination is based on the absorption of gamma rays (from a radioactive source) which can be measured and related to the void volume fraction. This technique is a simple means of obtaining local density measurements and vapor volume fraction distributions.

A major portion of the experimental program for investigating the effect of geometry on two-phase fluid density covers a range of geometries on which radiation attenuation techniques have not been tried (large channel spacings). Therefore, it became necessary to conduct a parallel experimental program to develop a sound technique for measurements of two-phase densities and to evaluate the accuracy of the vapor volume fractions obtained.

A study of two-phase pressure drop was also undertaken in conjunction with the primary investigation of area changes on densities of mixtures. A number of investigators have reported a mass flow rate parameter on the two-phase friction pressure drop which is not accounted for in the Lockhart-Martinelli correlation. Since a wide geometry change was being studied, the effect of mass flow rate could be conveniently investigated. Also, a method of correlating data on two-phase pressure drop with the liquid holdup has been reported by Lottes and Flinn.[1] They suggest the local two-phase pressure drops are directly related to the local gaseous volume fraction. This method of correlation could readily be checked using the extensive liquid holdup measurements of this investigation.

II. EXPERIMENTAL APPARATUS

The experimental apparatus was designed and constructed in accordance with the basic goals of the experimental investigation. The ranges of variables selected for study were: (1) flow area changes, minimum 1.25:1 and a maximum of 8 1, (2) the void volume fraction, α, 0.02 to 0.8; (3) mass flow rate, G, 250,000 to 2,000,000 lb/(hr) (ft^2); (4) water velocity, V_w, 1 to 10 fps.

The experimental apparatus is shown pictorially in Fig. 2.1 and schematically in Fig. 2.2. Basically the loop consisted of a water and air-injection system, the mixing section the test sections and an air-water separator. The metered streams of air and water were injected into the mixer. The two-phase mixture then flowed through the test section and into the overhead separator, where the air was liberated to the atmosphere and the water was diverted back to the make-up tank.

A. Description of Equipment Components

1. Air Supply. The air was obtained from the main laboratory 100-psi supply line. A Bailey air filter was used to remove excessive moisture and foreign matter. The flow rate of air was regulated by a series of three valves and measured at either of two orifices. A constant pressure of 75 psi was maintained upstream of the air orifice by a Nogren air-regulator.

2. Water Supply. De-mineralized water was pumped from the make-up tank through the water orifice and into the bottom of the mixer. The water flow rate was regulated by a bypass system on the pump. After passing through the test section into the overhead separator, the water was diverted back to the make-up tank by gravity flow.

3. Air-Water Mixer. The mixer section is shown schematically in Fig. 2.3. The air entered through the 3-inch pipe at the bottom and merged with the water stream through a series of 350 holes (3/16 in. D), spaced along the periphery and top of the pipe. The mixing section above the pipe consisted of a series of screens and packed beds of stainless steel pads which extended through the transition section to the flange of the lower test section. The 100-mesh screen between the flanges of the transition section and lower test section served to disperse any large air bubbles which might tend to form due to coalescence. The quantity of screening and mesh in the mixing section was varied until there was no effect on the measured air volume fraction at the exit of the lower test section for a given quality of the two-phase mixture. A series of screens with a minimum of packing was found to be the most satisfactory arrangement.

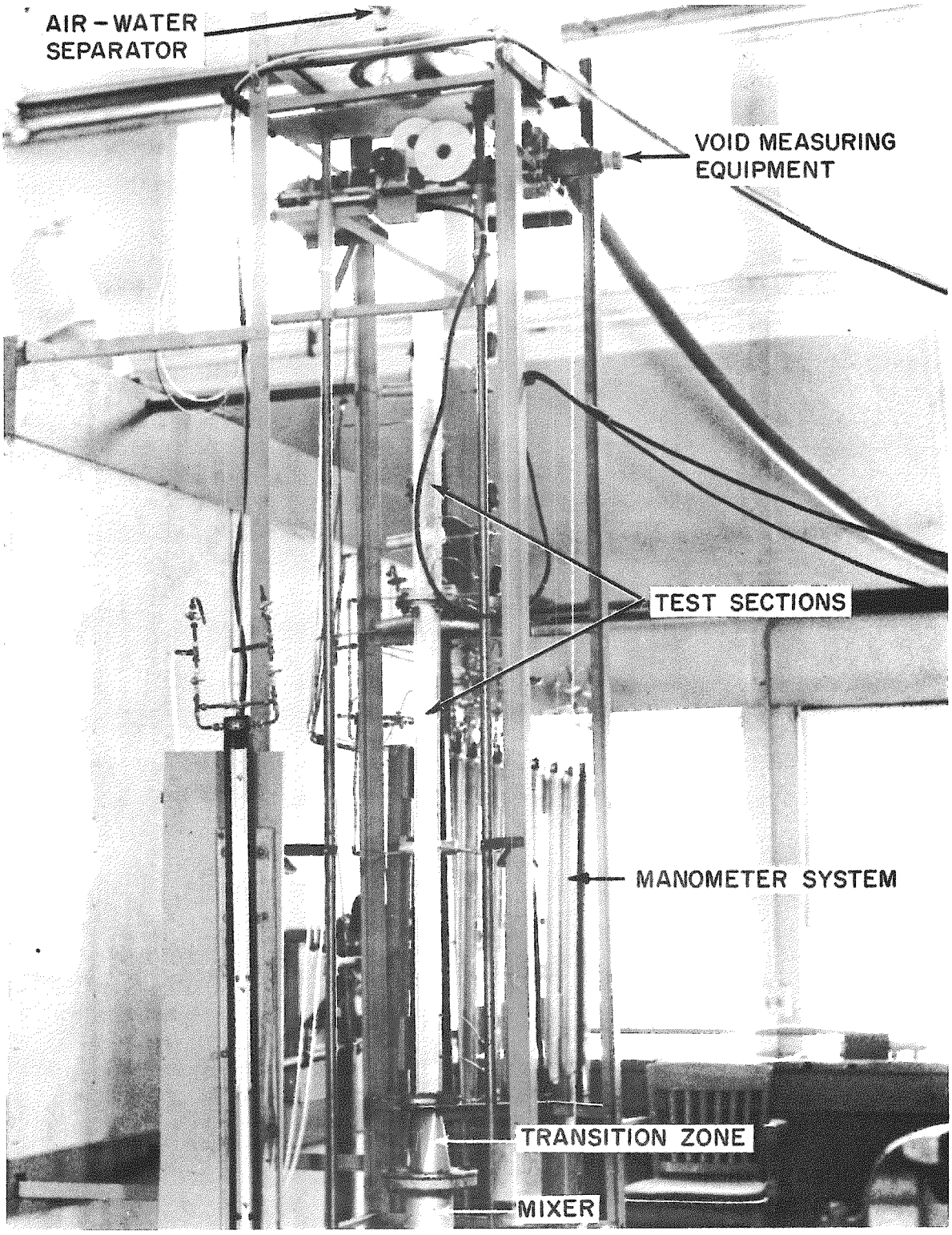

FIG. 2.1 EXPERIMENTAL APPARATUS

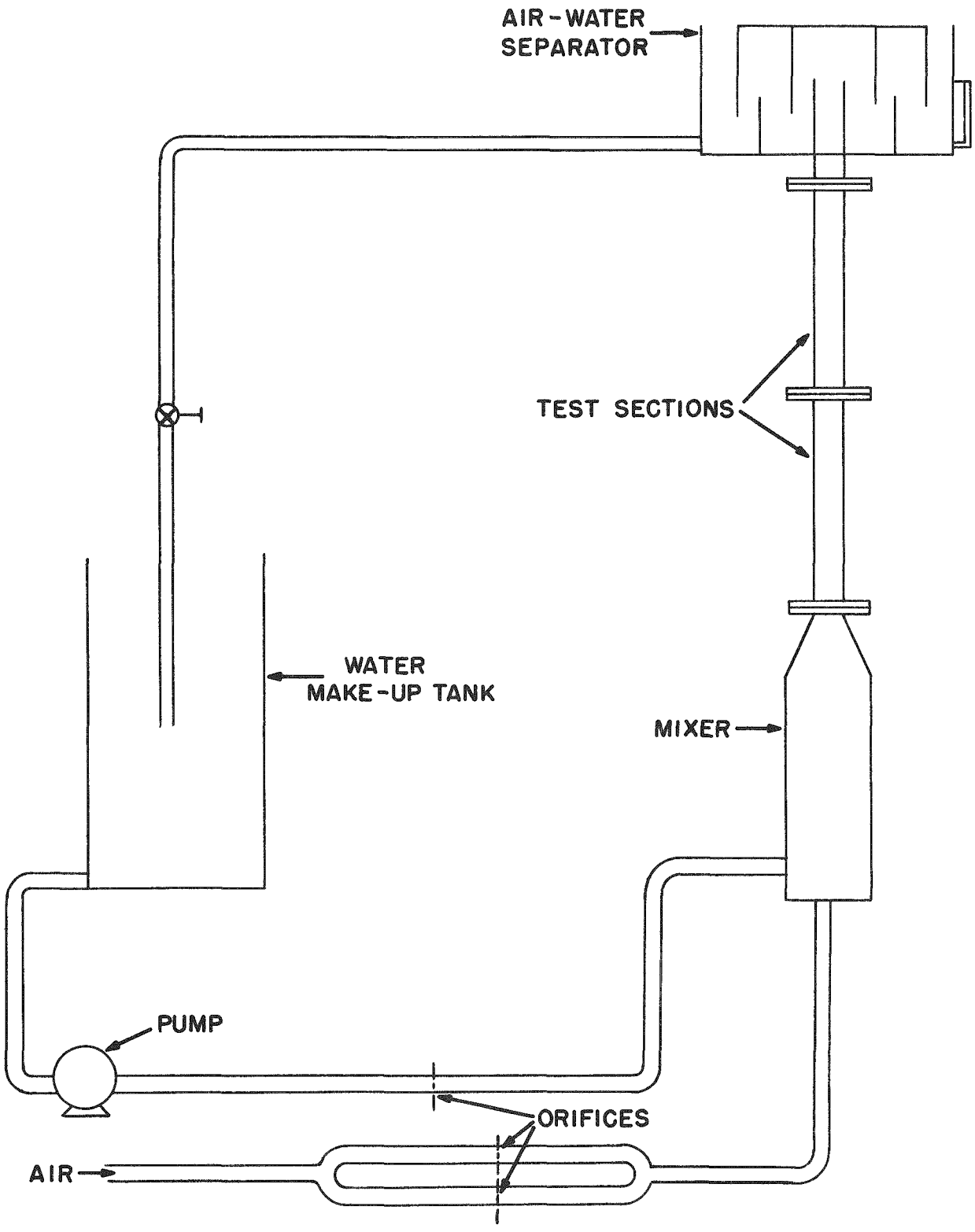

FIG. 2.2 SCHEMATIC DRAWING OF EXPERIMENTAL APPARATUS

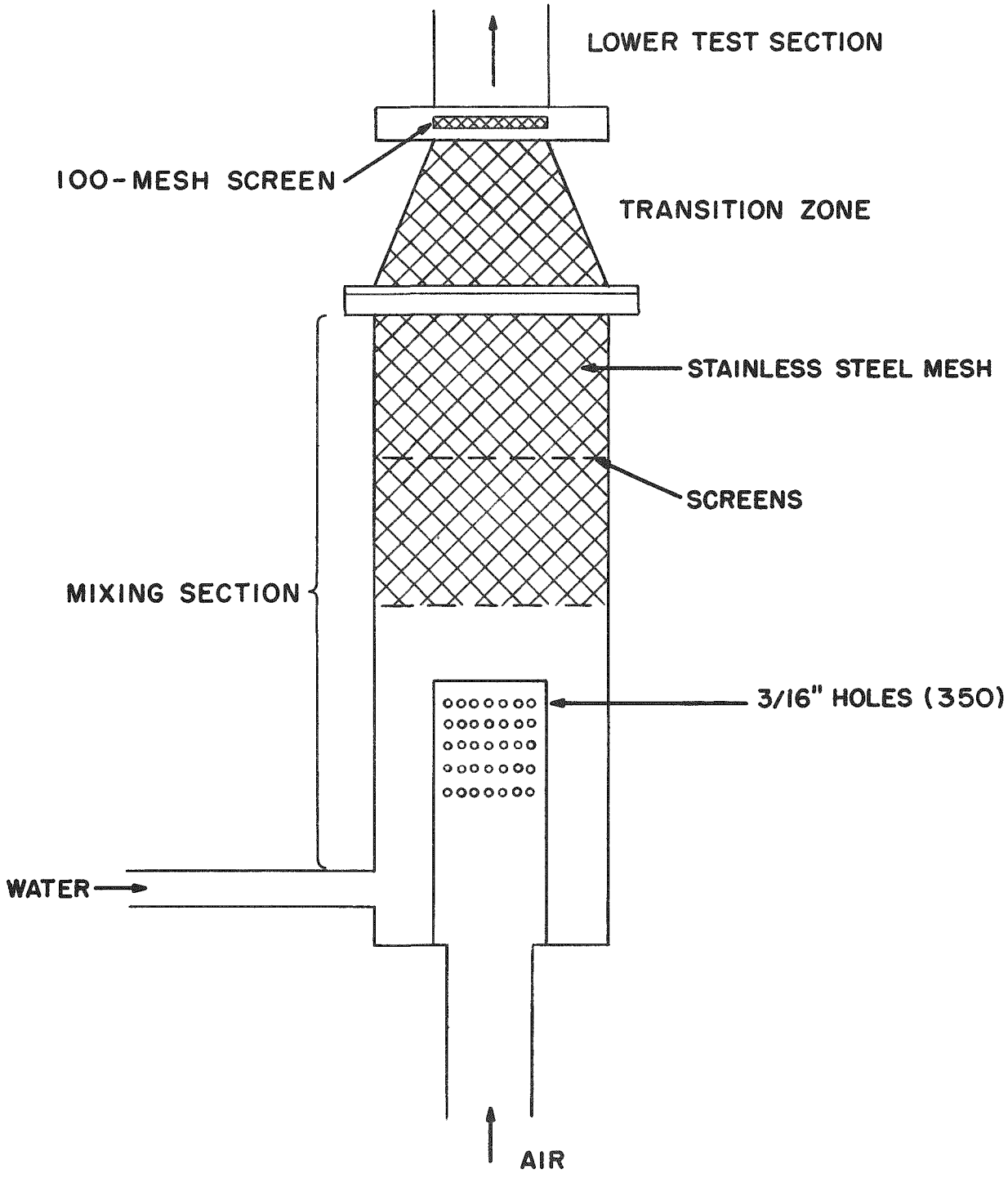

FIG. 2.3 SCHEMATIC DRAWING OF AIR-WATER MIXER

4. Test Section. Five test sections, each 4 ft long and 2 in. wide, with channel spacings of 1/8 in., 1/4 in., 1/2 in., 3/4 in. and 1 in., respectively, were constructed from Lucite. Lucite was used to allow visual observation and photographic studies. The sections could be interchanged to obtain the desired geometrical combinations. A series of pressure taps were inserted into each section for measurements of pressure drop.

B. Instrumentation

1. Density Measurement. The equipment used for measuring the density of the two-phase mixture is shown in Fig. 2.4. It consisted of a 0.085-mev thulium source, a duMont photomultiplier tube with a NaI thallium-activated scintillation crystal, a linear current amplifier and a Brown recorder (0 - 10 mv). The gamma rays were directed through the test section to the photomultiplier tube, where the unattenuated portion of the beam produced a signal. The signal was amplified and transmitted to the recorder. A more detailed description of the procedure for the measurement of density is given in Section III.

The source and photomultiplier tube were mounted on a carriage which could move in either a horizontal or vertical direction. The movement of the carriage was controlled by two constant-speed motors in conjunction with a series of relays and a switch box.

The gamma beam was collimated at the photomultiplier tube by a lead window, 1 in. thick. Cooling coils were placed around the photomultiplier tube to maintain a constant temperature, since both the NaI crystal and the tube are sensitive to temperature changes.

2. Pressure Drop Measurements. The pressure drop manometer system is shown in Fig. 2.1. Different manometer fluids (sp. g. = 1.25, 1.72, 2.95, and 13.6) were used for various operating ranges and test section combinations.

Pressure gauges were installed at various positions along the test sections (Fig. 2.5). Also reservoirs (8-inch sections of 1-inch pipe) were connected to each pressure tap line to collect any air entrained in the water and thus prevent the air from entering the vertical legs in the manometer system.

3. Orifices. The orifices for water and air were made according to the specifications for small diameter orifices by Grace and Lapple.[2] The diameter of the orifice for water was 0.5215 in. The orifice diameters for air were 0.0961 in. and 0.2705 in. The orifices were calibrated with water over the same Reynolds number range as encountered in the experimental investigation. Excellent agreement was obtained between the experimental orifice discharge coefficients and the values of Grace and Lapple for same sizes of orifices.

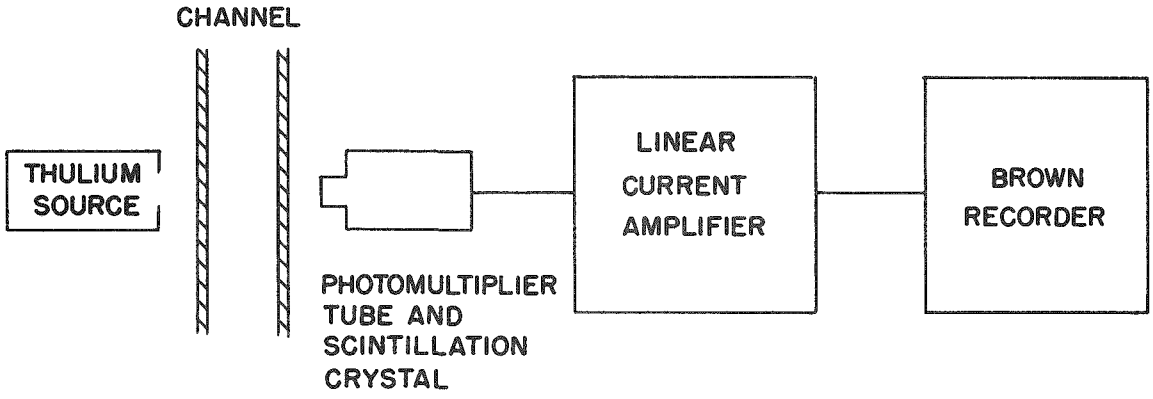

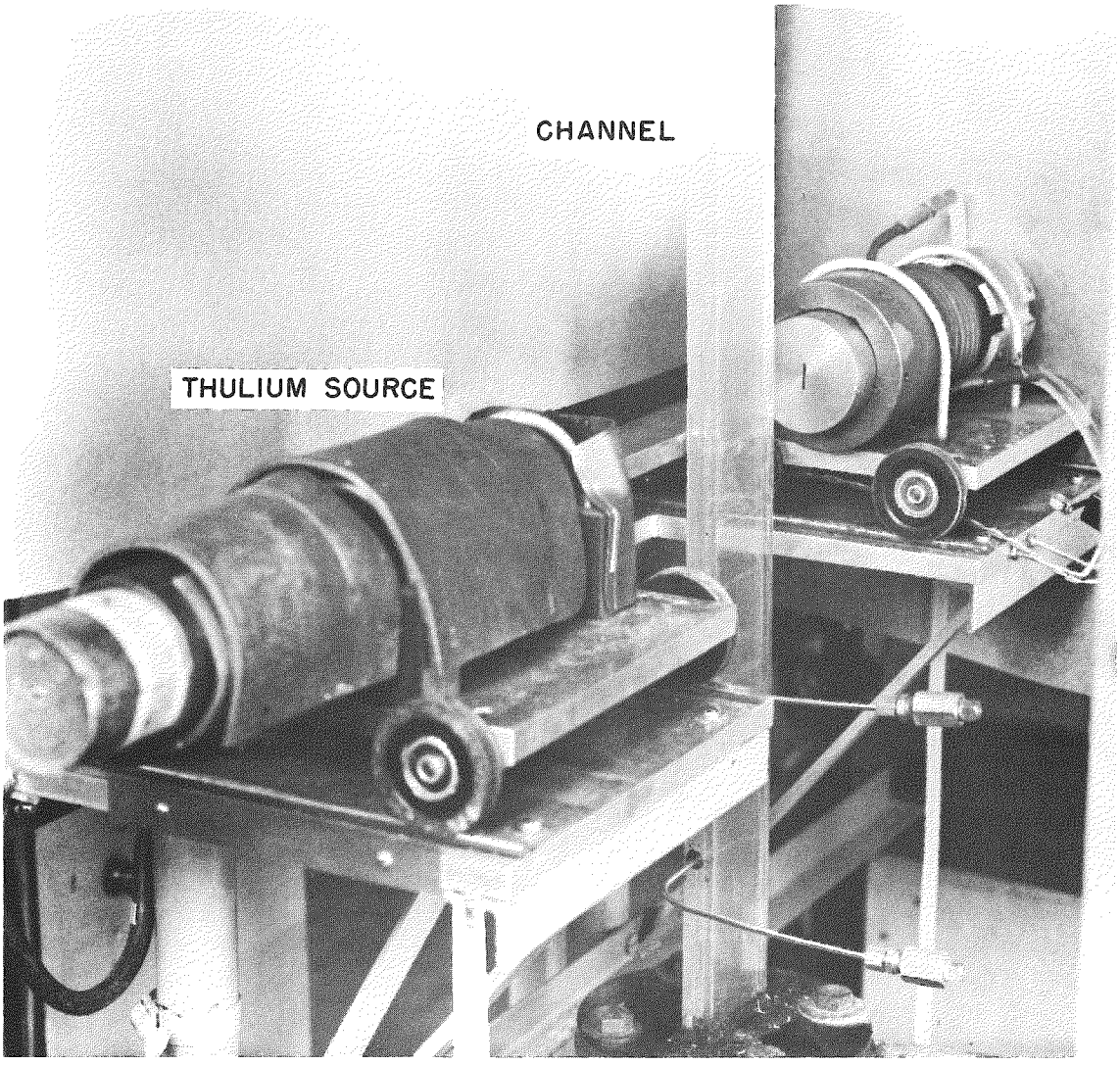

FIG. 2.4 VOID MEASURING APPARATUS

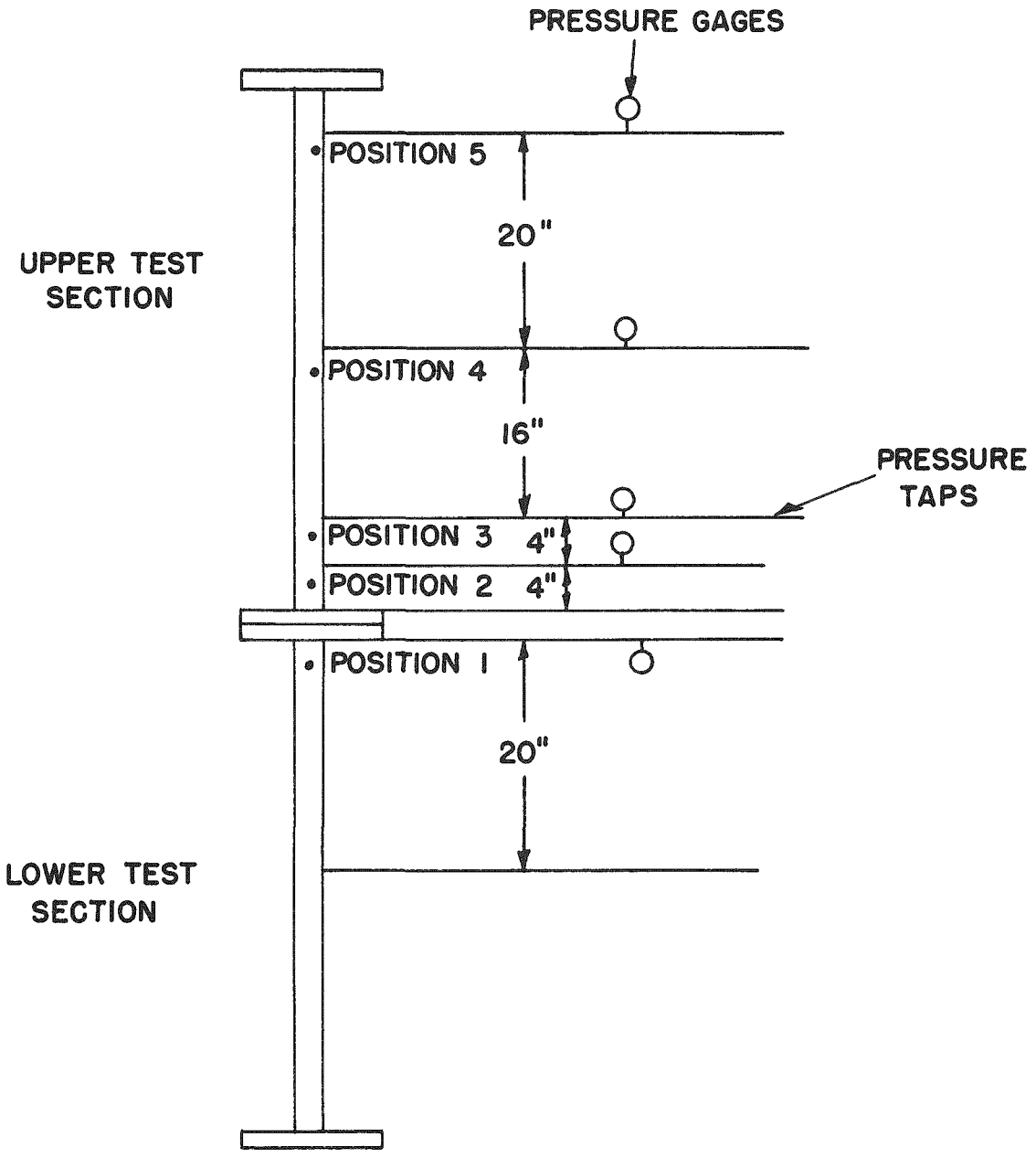

FIG. 2.5 SCHEMATIC DRAWING OF TEST SECTIONS AND PRESSURE TAPS

III. RADIATION ATTENUATION METHOD OF MEASURING DENSITY OF A TWO-PHASE FLUID

A. Introduction

The technique of radiation attenuation is a powerful research tool when applied to fundamental two-phase flow studies, since the local density and the relative velocity of the two phases can be determined readily. The method is essentially very simple; however, the results obtained can be in considerable error unless great care is taken in the experimental technique.

A number of investigators (see Section IV) have recently applied this technique on basic two-phase flow studies. However, only Cook[3] and Egen, et al[4] have reported studies in which the accuracies of the measured values of density were ascertained and the various factors which contributed toward errors were evaluated. Cook[3] conducted a series of tests on Lucite mock-ups to study simulated preferential distribution of two phases, source-channel geometry, and the validity of the assumed exponential attenuation of the gamma beam. His results showed that the error between measured and actual void volume fraction increased as the channel spacing was increased and as the distance between the radioactive source and channel was decreased. Errors of up to 93% were obtained. Egen, et al[4] obtained similar results. However, the Lucite mock-ups studied by Cook and Egen represented extreme cases of preferential distributions of the two phases which would not be encountered in actual two-phase flow, except in the instance of true annular flow.

An experimental study was therefore undertaken to develop a more accurate method of measurement of void volume fraction for wide channels and to evaluate the errors in the measured void volume fraction utilizing Lucite mock-ups which give a more realistic representation of the actual flow patterns encountered in two-phase flow. In addition, a study was made on two-phase fluids in test sections of various channel widths to compare the void fraction measured by a "one-shot" method and a traversing technique. These methods are described on page 28.

B. Theory

The density of a substance is related to the attenuation of a mono-energetic gamma ray by the equation

$$I/I_0 = e^{-\mu x} \quad , \tag{3.1}$$

where

I = intensity of the gamma beam at x, current/cm^2
I_0 = initial intensity of the gamma beam, current/cm^2
μ = linear absorption coefficient, cm^{-1}
x = thickness of the absorber, cm.

The linear absorption coefficient, in turn, is related to the density of the absorber by the expression

$$\mu = (N_0/A)\rho\sigma \quad , \tag{3.2}$$

where

N_0 = Avogadro's number (6.02×10^{23} nuclei/gm-mol)
A = Atomic weight, gm/gm-mol
σ = microscopic absorption cross section, cm^2/nucleus
ρ = density of absorbing medium, gm/cm^3.

The manner in which the two phases are distributed in a fluid can markedly affect the method used to calculate the density or vapor volume fraction. To illustrate this point two extreme cases are considered: Case I - the gamma beam is perpendicular to layers of the two phases present; Case II - the gamma beam is parallel to individual layers of each phase. With reference to Fig. 3.1, let:

L = total length of water-gas mixture
$(\ell_n - \ell_{n-1})$ = length of individual layer (structure, water, or gas)
I_n = intensity of gamma at exit of nth layer
μ_w = mass absorption coefficient of water
μ_g = mass absorption coefficient of gas
μ_{st} = mass absorption coefficient of structure.

Case I - Gamma Beam Perpendicular to Individual Layers

Applying Eq. (3.1) to an individual layer, the general equation for each substance (water, gas, structure, etc.) is

$$I_{st_n} = (I_{n-1}) \exp\left[-\mu_{st} (\ell_n - \ell_{n-1})_{st}\right] \tag{3.3}$$

$$I_{g_n} = (I_{n-1}) \exp\left[-\mu_g (\ell_n - \ell_{n-1})_g\right] \tag{3.4}$$

$$I_{w_n} = (I_{n-1}) \exp\left[-\mu_w (\ell_n - \ell_{n-1})_w\right] \quad . \tag{3.5}$$

Combining Equations (3.3), (3.4), and (3.5) and simplifying:

$$I_{exit} = (I_0) \exp\left[-\mu_w (\ell_n - \ell_{n-1})_w\right] \left[\exp\left\{-\mu_g \Sigma(\ell_n - \ell_{n-1})_g\right\}\right] \left[\exp\left\{-\mu_w \Sigma(\ell_n - \ell_{n-1})_w\right\}\right] \quad . \tag{3.6}$$

Since

$$\Sigma(\ell_n - \ell_{n-1})_w + \Sigma(\ell_n - \ell_{n-1})_g = L, \tag{3.7}$$

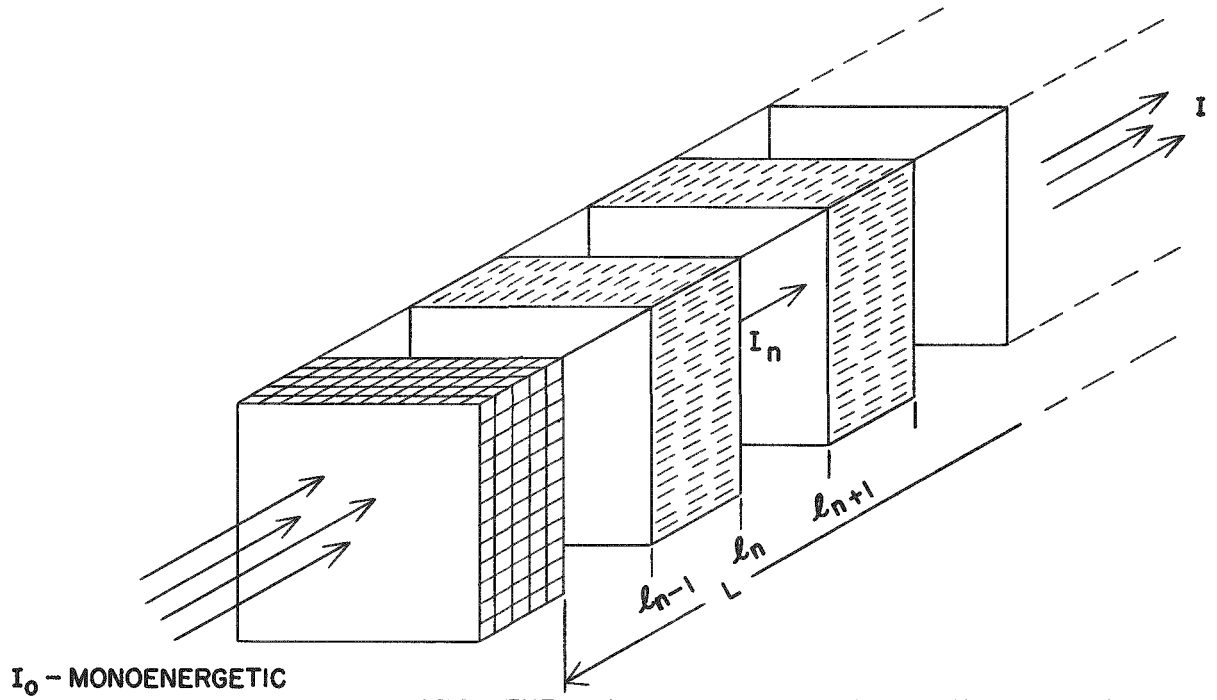

CASE I. THE GAMMA BEAM IS PERPENDICULAR TO LAYERS OF THE TWO PHASES

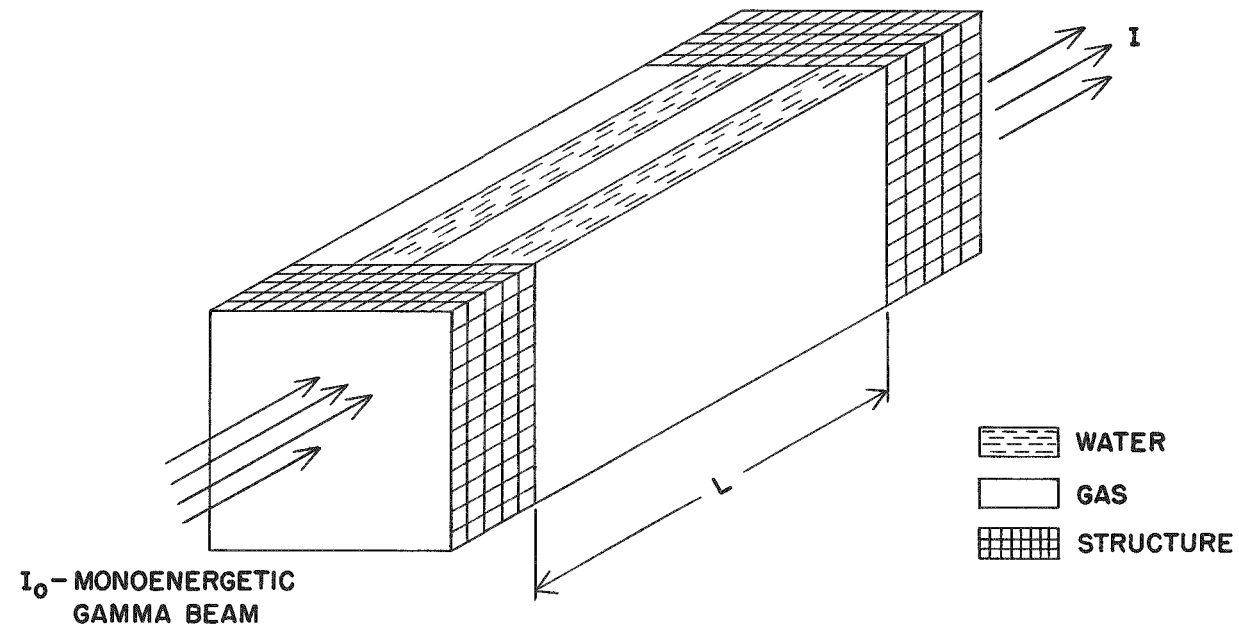

CASE II. THE GAMMA BEAM IS PARALLEL TO INDIVIDUAL LAYERS OF EACH PHASE

FIG. 3.1 SCHEMATIC DRAWING OF TWO TYPES OF PHASE DISTRIBUTION

then

$$\Sigma(\ell_n - \ell_{n-1})_g = L - \Sigma(\ell_n - \ell_{n-1})_w \quad . \tag{3.8}$$

Substituting Eq. (3.8) in Eq. (3.6) and simplifying,

$$I = I_0 \left[\exp\left\{-\mu_{st}(\ell_n - \ell_{n-1})_{st}\right\}\right]\left[\exp(-\mu_g L)\right]\left[\exp\left\{-(\mu_w - \mu_g)\Sigma(\ell_n - \ell_{n-1})_w\right\}\right] \tag{3.9}$$

and for the total gamma flux

$$\Phi = (I_0)(A_T)\left[\exp\left\{-\mu_{st}\,\Sigma(\ell_n - \ell_{n-1})_{st}\right\}\right]\left[\exp(-\mu_g L)\right]\left[\exp\left\{-(\mu_w - \mu_g)\,\Sigma(\ell_n - \ell_{n-1})_w\right\}\right] \tag{3.10}$$

Case II - Gamma Beam Parallel to Layers of Each Phase

Applying Eq. (3.1) as before through layers of gas and water,

$$I_{g_{exit}} = I_0 \left[\exp(-\mu_{st}\,\Sigma\ell_{st})\right]\left[\exp(-\mu_g L)\right] \quad ; \tag{3.11}$$

$$I_{w_{exit}} = I_0 \left[\exp(-\mu_{st}\,\Sigma\ell_{st})\right]\left[\exp(-\mu_w L)\right] \quad . \tag{3.12}$$

The total gamma exit flux Φ is

$$I_g A_g + I_w A_w \quad . \tag{3.13}$$

Combining Eqs. (3.11), (3.12), and (3.13)

$$\Phi = (I_0)\left[\exp(-\mu_{st}\Sigma\ell_{st})\right]\left[(A_g)\exp(-\mu_g L) + (A_w)\exp(-\mu_w L)\right] \quad . \tag{3.14}$$

The gamma fluxes as given by Eqs. (3.10) and (3.14) can be interpreted in terms of voltages, which can be measured and recorded in the following manner.

The gamma flux, Φ, which impinges on the fluorescent crystal and is transformed into light is

$$\Phi_L = K_2 \Phi, \tag{3.15}$$

where

Φ_L = the visible light flux

K_2 = the conversion efficiency of the crystal.

The visible light is then converted to electric current by the photo-cathode of the photomultiplier tube. The current is given by

$$i = K_3 v_h^7 \Phi_L \quad , \tag{3.16}$$

where

i = the photomultiplier tube anode current

v_h = voltage of the photomultiplier tube supply.

The current is transmitted to the linear amplifier whose output voltage is

$$v = k_4 i \tag{3.17}$$

This voltage is measured and recorded. Thus combination of Eqs. (3.15), (3.16) and (3.17) with (3.10) and (3.14) gives

$$v = (K_2)(K_3)(K_4)(v_h)^7(I_0)(A_T)\ [\exp(-\mu_{st}\Sigma(\ell_n - \ell_{n-1})_{st})]\ [\exp(-\mu_g L)]\ \left[\exp\left\{-(\mu_w - \mu_g)\Sigma(\ell_n - \ell_{n-1})_w\right\}\right] \tag{3.18}$$

$$v = (K_2)(K_3)(K_4)(v_h)^7(I_0)\ [\exp(-\mu_{st}\Sigma\ell_{st})]\ [(A_g)\exp(-\mu_g L) + (A_w)\exp(-\mu_w L)] \tag{3.19}$$

Letting

$$K_5 = (K_2)(K_3)(K_4)(v_h)^7(I_0)(A_T)\exp(-\mu_{st}\Sigma(\ell_n - \ell_{n-1})_{st}\exp(-\mu_g L) \tag{3.20}$$

and

$$K_6 = (K_2)(K_3)(K_4)(v_h)^7(I_0)\exp(-\mu_{st}\Sigma\ell_{st})(A_T) \quad , \tag{3.21}$$

Eqs. (3.18) and (3.19) become

$$v = (K_5)\left[\exp\left\{-(\mu_w - \mu_g)\Sigma(\ell_n - \ell_{n-1})_w\right\}\right] \tag{3.22}$$

$$v = K_6\left(\frac{A_g}{A_T}\right)\exp(-\mu_g L) + \left(\frac{A_w}{A_T}\right)\exp(-\mu_w L) \quad . \tag{3.23}$$

From Fig. 3.1, by definition for Case I,

$$\alpha = \left(1 - \frac{\Sigma(\ell_n - \ell_{n-1})_w}{L_T}\right) = \frac{\Sigma(\ell_n - \ell_{n-1})_g}{L_T} \tag{3.24}$$

Substitution of Eq. (3.24) into Eq. (3.22) gives

$$v = (K_5) \exp [- (\mu_w - \mu_g) (1 - \alpha) (L_T)] \quad . \tag{3.25}$$

From Fig. 3.1, by definition for Case II,

$$A_g/A_T = \alpha \quad . \tag{3.26}$$

Substitution of Eq. (3.26) into Eq. (3.23) gives

$$v = (K_6) [(\alpha) \exp (-\mu_g L) + (1 - \alpha) \exp (-\mu_w L)] \quad . \tag{3.27}$$

For each density determination it is necessary to obtain a calibration. Voltages are recorded when the channel is completely devoid of water ($\alpha = 1$) and when the channel is completely filled with water ($\alpha = 0$). Applying these limiting conditions to Eqs. (3.25) and (3.27), namely,

$$v = v_f \text{ when } \alpha = 0 \tag{3.28}$$

and

$$v = v_e \text{ when } \alpha = 1 \quad , \tag{3.29}$$

and simplifying, there is obtained

For Case I:

$$\alpha = \frac{\ln (v/v_f)}{\ln (v_e/v_f)} \quad ; \tag{3.30}$$

For Case II:

$$\alpha = \frac{v - v_f}{v_e - v_f} \quad . \tag{3.31}$$

Thus two equations for calculating the gaseous volume fraction from the measured voltages are obtained from the two extreme types of phase distributions. An actual two-phase mixture would lie between the two cases cited. Since there is a considerable degree of homogeneity in two-phase fluids, the gamma rays would tend to be attenuated exponentially and the gas volume fraction would then be calculated by Eq. (3.30). All air volume fractions in this study were calculated by Eq. (3.30).

In addition to the possible errors which result from preferential phase distribution, a number of other factors tend to introduce substantial error in the technique of radiation attenuation unless adequate corrective measures are taken. However, the manner in which the various errors

are produced is not completely understood. As a result, it is very difficult to attempt a thorough error analysis which would yield the possible limits of errors. A few of the more important factors which must be considered are mentioned briefly. A more complete evaluation of the radiation attenuation technique for density determination and discussion of the errors involved is given by Hooker and Popper.[5]

Some of the factors which tend to produce errors in the radiation attenuation technique are:

(1) Variation in gain of the photomultiplier tube due to changes in the supply voltage. Since the gain is proportional to the supply voltage to the seventh power as shown in Eq. (3.16), a constant supply voltage is mandatory for accurate results. The supply voltage in this investigation could be regulated to within 0.1% of the scale reading.

(2) Variation in gain of the photomultiplier scintillation crystal due to temperature changes. Cooling coils about the photomultiplier tube minimized this error. Thermocouples attached to the crystal surface showed that the temperature was held within $\pm 1/2$ degrees Fahrenheit.

(3) Variation of the transfer characteristics of amplifier due to zero drift over a period of time. This error was eliminated through periodic adjustment.

(4) Accuracy to which strip chart can be read. This is a function of the strength of the source, size of "windows," type of flow being studied, etc.

(5) Decay of source over period during which runs are made. The magnitude of the error depends on the half-life of the source. This factor was eliminated by obtaining calibrations on an empty and a full channel twice daily.

C. Description of Equipment

The basic components of the equipment for measuring density have been described in Section II. Brief supplementary information is presented to give a more complete description.

The thulium source from which the gamma rays emanated was enclosed in a lead shield and collimator as shown in Fig. 3.2(A). The radioactive source was obtained by irradiating a thulium pellet (d = 0.19 in.) encased in an aluminum container until the desired activity was obtained (9 roentgens per hour at a distance of 6 inches in air). The thulium-170 produced has a half-life of approximately 129 days. The energy spectrum of thulium-170 shows two peaks: 0.053 Mev and 0.084 Mev. In order to obtain a monoenergetic radiation, which is a prerequisite for the radiation attenuation

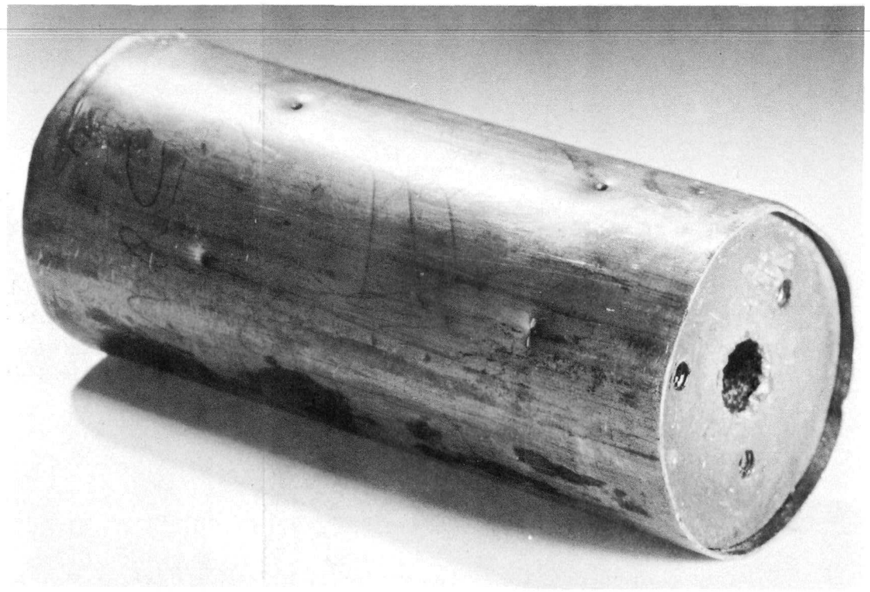

(a)
RADIOACTIVE SOURCE HOLDER

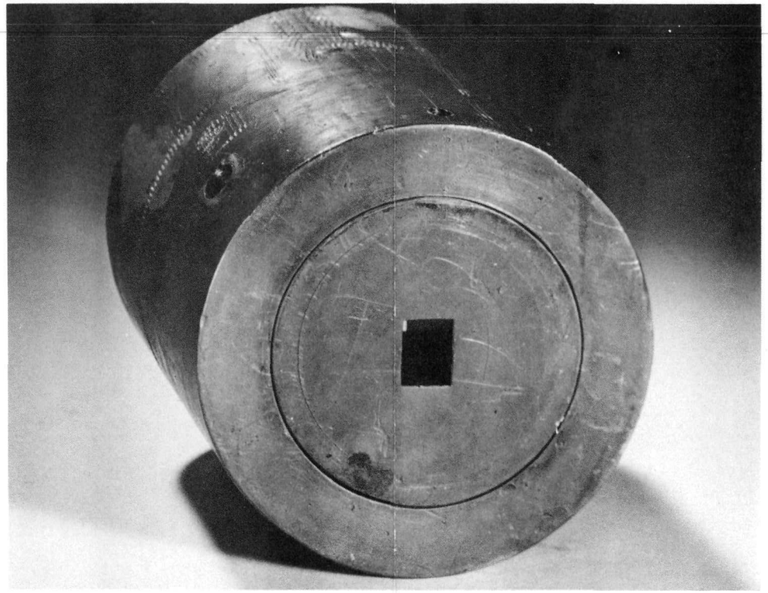

(b)
LEAD SHIELD USED ON SCINTILLATION CRYSTAL

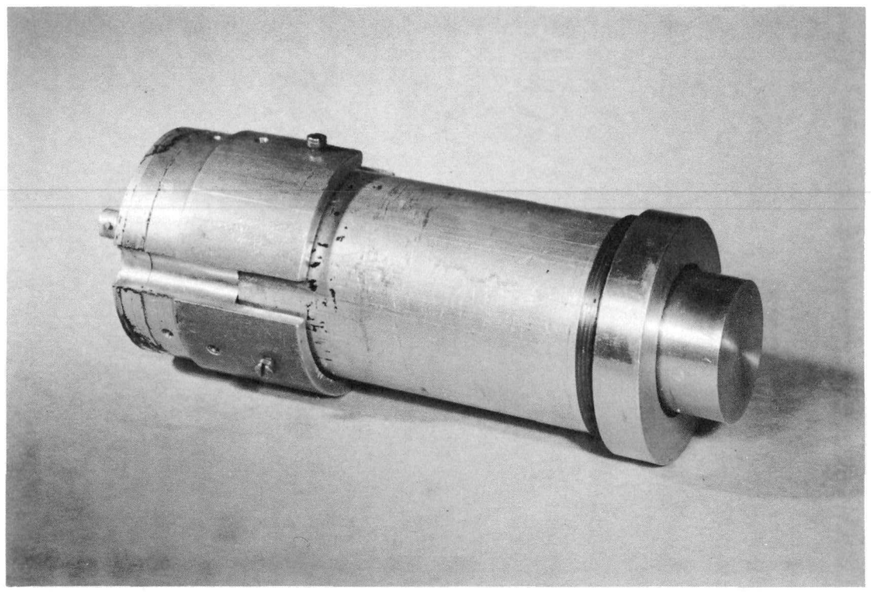

(c)
SCINTILLATION CRYSTAL PHOTOMULTIPLIER TUBE ASSEMBLY

FIG. 3.2 COMPONENTS OF DENSITY MEASURING APPARATUS

technique, the lower peak gamma energy must be absorbed. This was accomplished by inserting a steel plate (0.25 inch thick) between the source and test section.

The scintillation crystal was surrounded by a lead shield (Fig. 3.2(B)) to eliminate any extraneous radiation which might impinge on it. A rectangular window of desired dimensions was cut into the face of the lead shield.

The scintillation crystal-photomultiplier assembly is shown in Fig. 3.2(C). The photomultiplier tube (RCA-5819) was optically coupled to the scintillation crystal by a Lucite light guide. The entire assembly was then sealed in an aluminum can to make it impervious to light.

A comprehensive description of the equipment for measuring density is also given by Hooker and Popper.[5]

D. Procedure

In previous studies the void volume fraction has been measured by the "one-shot" radiation attenuation method. However, as mentioned previously, initial Lucite mock-up studies showed that the measured values of the void volume fraction can be in considerable error for the larger channel widths. Therefore a traverse technique was tried on a series of Lucite mock-ups in an attempt to develop a more accurate method of density measurement and to compare the results with the "one-shot" method.

In the "one-shot" method a window slightly wider than the test section channel to be studied was cut into the lead shield placed on the scintillation crystal (see Fig. 3.2(B)). The window width was made 1/32 in. greater than the channel width to facilitate alignment of the source, test section and photomultiplier tube assembly. The test section was calibrated when completely empty and when completely full of water (or Lucite for the mock-up studies) to give values of v_e and v_f. A reading was then taken during the actual run (which represents the two-phase fluid or Lucite mock-up) and the void volume fraction calculated from Eq. (3.30).

In the traversing method a continuous trace of the density variation (phase distribution) across the channel is obtained by traversing the channel horizontally with the narrow slot (1/32 in. wide, or less) in the scintillation crystal lead shield.

The manner in which the data was taken and reduced is shown by schematic strip charts in Fig. 3.3. Calibration traverses were made as for the "one-shot" method to obtain empty and full readings, v_e and v_f. The traverse started in the air beyond the test section to obtain a reference starting point that could easily be fixed on the strip charts for each traverse.

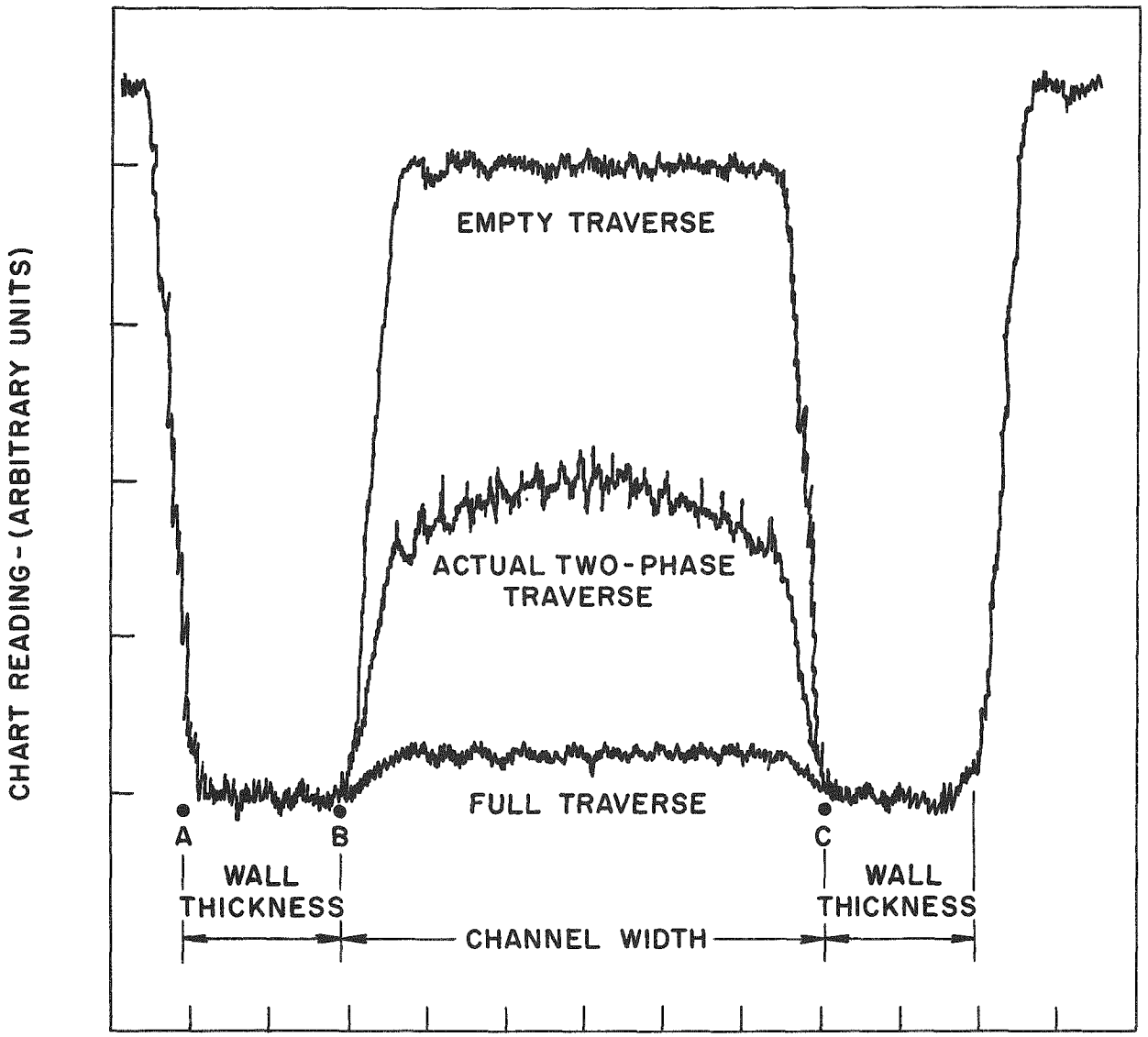

FIG. 3.3 SCHEMATIC DRAWING OF STRIP CHART ILLUSTRATING THE TRAVERSING TECHNIQUE

The reference point (A) was set at the instant the slot on the scintillation crystal moved entirely into the Lucite from the air. The beginning of the flow channel is point (B) and the end is point (C) on the empty traverse. The traverse of the actual two-phase fluid, v, lies in between the empty and full traverses.

The channel position and width was then laid out on the strip chart recording of the actual traverse, v, by measuring the distance from points A to B, and B to C as obtained from the empty traverse. All measured distances were cross checked by calculation, using the known speeds of both the traverse and strip chart and test section geometry. It is apparent that the accuracy of the traversing method depends very strongly on the ability to maintain a constant speed on the traversing carriage and recording instrument. The speeds were checked periodically during the course of the experimental investigation. The traversing carriage speed was 0.1875 in./min and the strip chart speed was 3 in./min.

The void fraction distribution was then calculated for a number of selected positions in the channel by using Eq. (3.30), and the mean void fraction was obtained by integration.

E. Discussion of Results

1. Data Procurement

A series of Lucite mock-ups, which simulated preferential phase distributions corresponding to various flow patterns encountered in two-phase flow, were made. The flow patterns selected for study were: (1) annular flow - central gas core; (2) local boiling distribution - gas layer at the wall with a liquid central core; (3) parabolic distribution; (4) a double annular vapor distribution; and (5) churn flow - vapor highly dispersed in liquid. The mock-ups of the various patterns are shown in Fig. 3.4.

The mock-ups were constructed from Lucite because of its close similarity to water in density and mass absorption cross section. The voids in the Lucite were simulated by machining predetermined geometric patterns to effect the desired simulated phase distribution.

The actual void volume fraction was obtained by calculation, using physical measurements of the Lucite mock-up. The calculated void volume fraction was checked by comparing the weight of the mock-up with the weight of an equally sized specimen of solid Lucite.

2. Comparison of "One-Shot" With Traversing Technique on Lucite Mock-Ups

A comparison of the calculated, with the measured, void distributions obtained by the traversing technique is shown in Fig. 3.5.

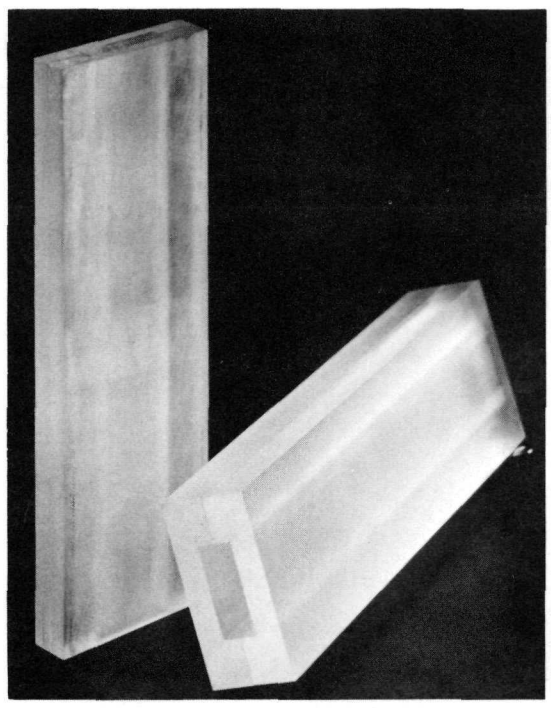

ANNULAR

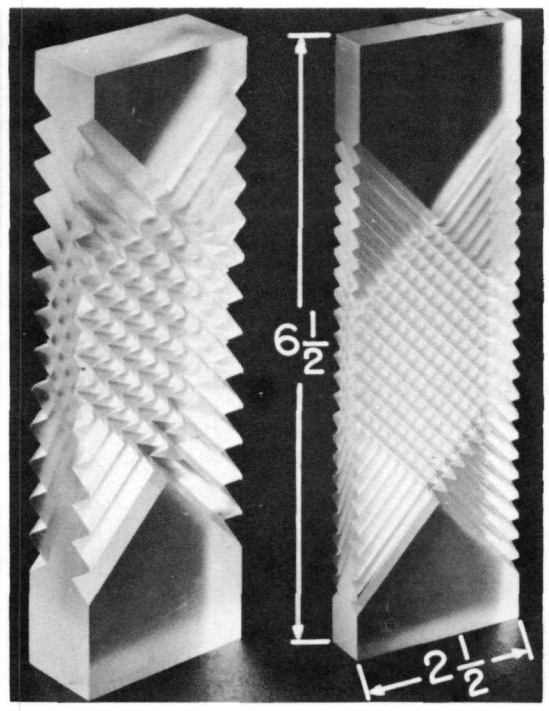

LOCAL BOILING

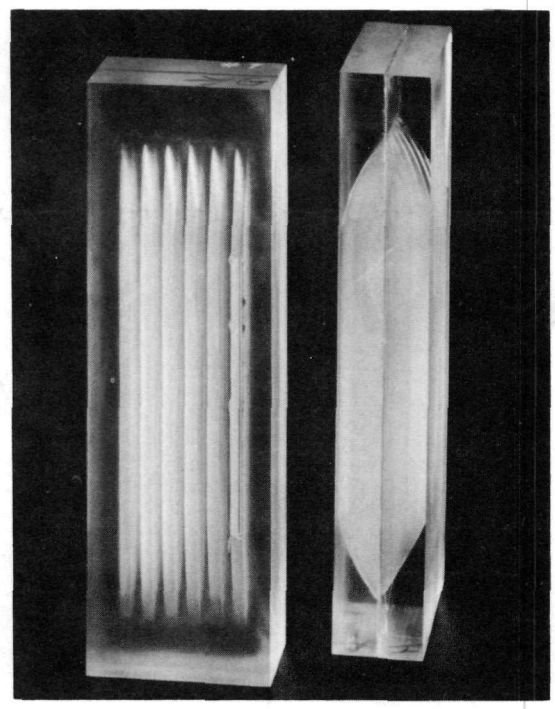

PARABOLIC

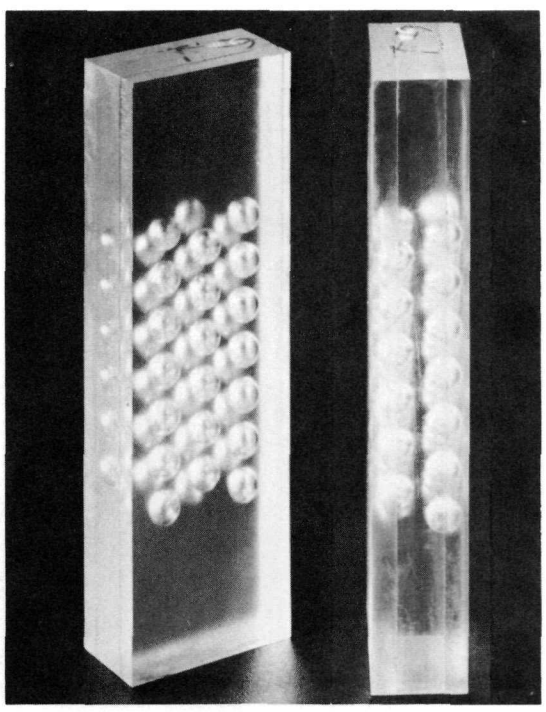

DOUBLE ANNULAR

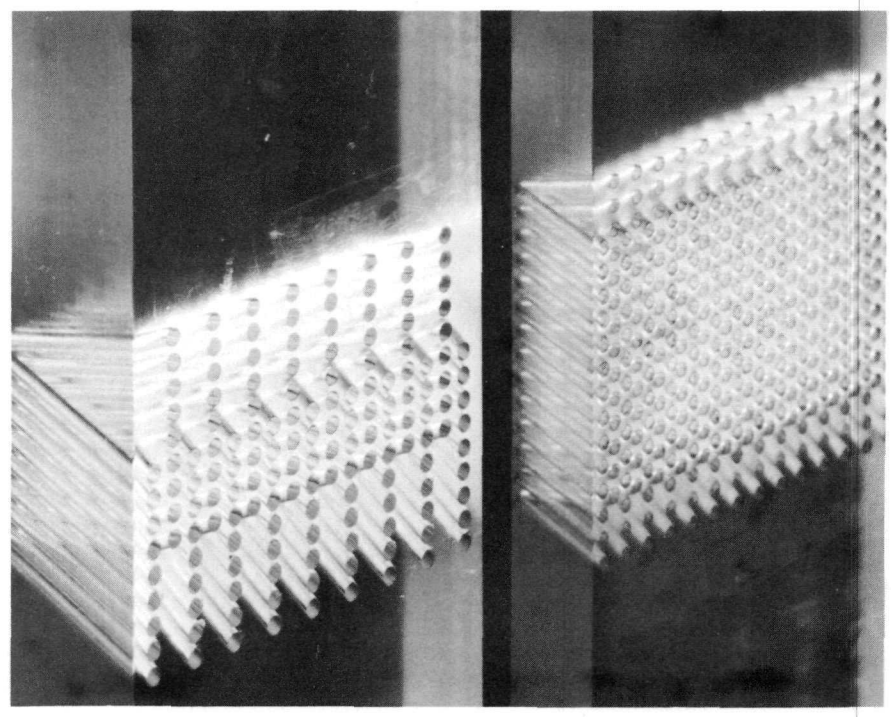

CLOSEUP VIEW OF CHURN
(HOMOGENOUS) FLOW

FIG. 3.4 LUCITE MOCK–UPS OF FLOW PATTERNS

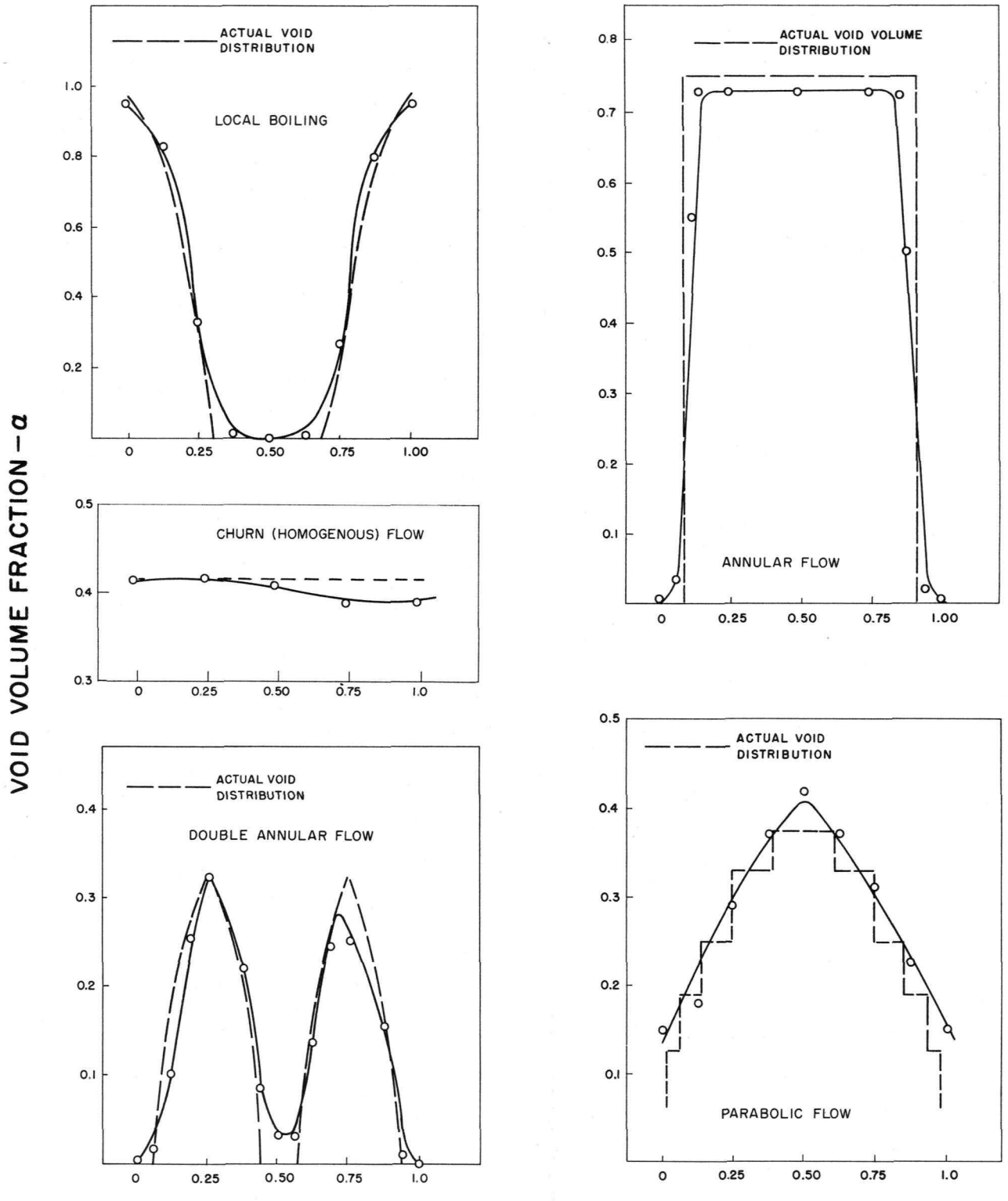

FIG. 3.5 COMPARISON OF VOID VOLUME FRACTION DISTRIBUTION MEASURED BY TRAVERSING TECHNIQUE, WITH ACTUAL VOID DISTRIBUTION FOR LUCITE MOCK-UPS OF VARIOUS FLOW PATTERNS

The mean value of the void volume fraction was then obtained by integration and the results compared with the value procured by the "one-shot" method and the actual void volume fraction. Typical results are shown in Table 3.1.

Table 3.1

COMPARISON OF VOID FRACTIONS OBTAINED BY TRAVERSING AND "ONE-SHOT" TECHNIQUES WITH ACTUAL VOID FRACTION

Simulated Phase Distribution in Mock-up	Lucite Mock-up Width, in.	Void Fraction		
		Traversing	"One-Shot" Method	Actual
Local Boiling	1	0.406	0.143	0.364
Annular Flow	1	0.164	0.324	0.203
Double Annular	1	0.151	0.181	0.166
Parabolic	1	0.286	0.322	0.267
Parabolic	1/2	0.350	0.567	0.345
Annular Flow	1/2	0.589	0.741	0.606
Local Boiling	1/2	0.401	0.161	0.345
Churn Flow	1/2	0.420	0.419	0.415

The void volume fractions measured by the traversing technique are in closer agreement with the actual void volume fraction than the values obtained by the "one-shot" method. The average per cent deviation of the "one-shot" method is 36.5% whereas the average error for the traversing technique is 7.3%.

A possible explanation for the larger error of the "one-shot" method for the wider channels may be due to the geometry of the test section-source - photomultiplier arrangement as schematically illustrated in Fig. 3.6. The source - photomultiplier system sees only a portion of the flow channel as depicted by the dotted lines. Therefore, if a preferential distribution of one phase occurs in the central region, the measurement of void volume fraction would be erroneous since the gamma radiation is passing through only a portion of the channel in which there is a greater concentration of one phase. The error may possibly be reduced by placing the source as far from the channel as feasible and by placing the scintillation crystal as close as possible. The error may be eliminated by using a larger source.

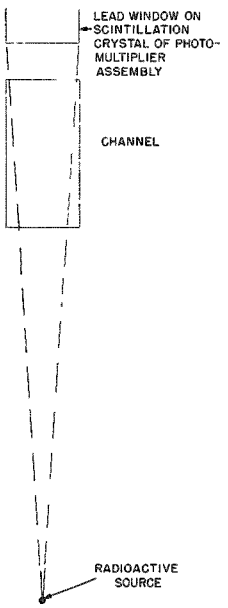

FIG 3 6 SCHEMATIC DRAWING OF SOURCE-TEST SECTION-PHOTOMULTIPLIER ASSEMBLY

The traversing technique appears superior to the "one-shot" method for void fraction measurement, especially for cases of highly preferential phase distributions and wide channel spacings.

3. Comparison of "One-Shot" and Traverse Method on Actual Two-Phase Fluid.

A series of runs were made in test sections of various channel widths to obtain a comparison between the traversing and "one-shot" methods on actual two-phase fluids. The results are presented in Fig. 3.7. As expected, the values checked very closely for the smaller channel spacings, but deviated as the channel spacing increased.

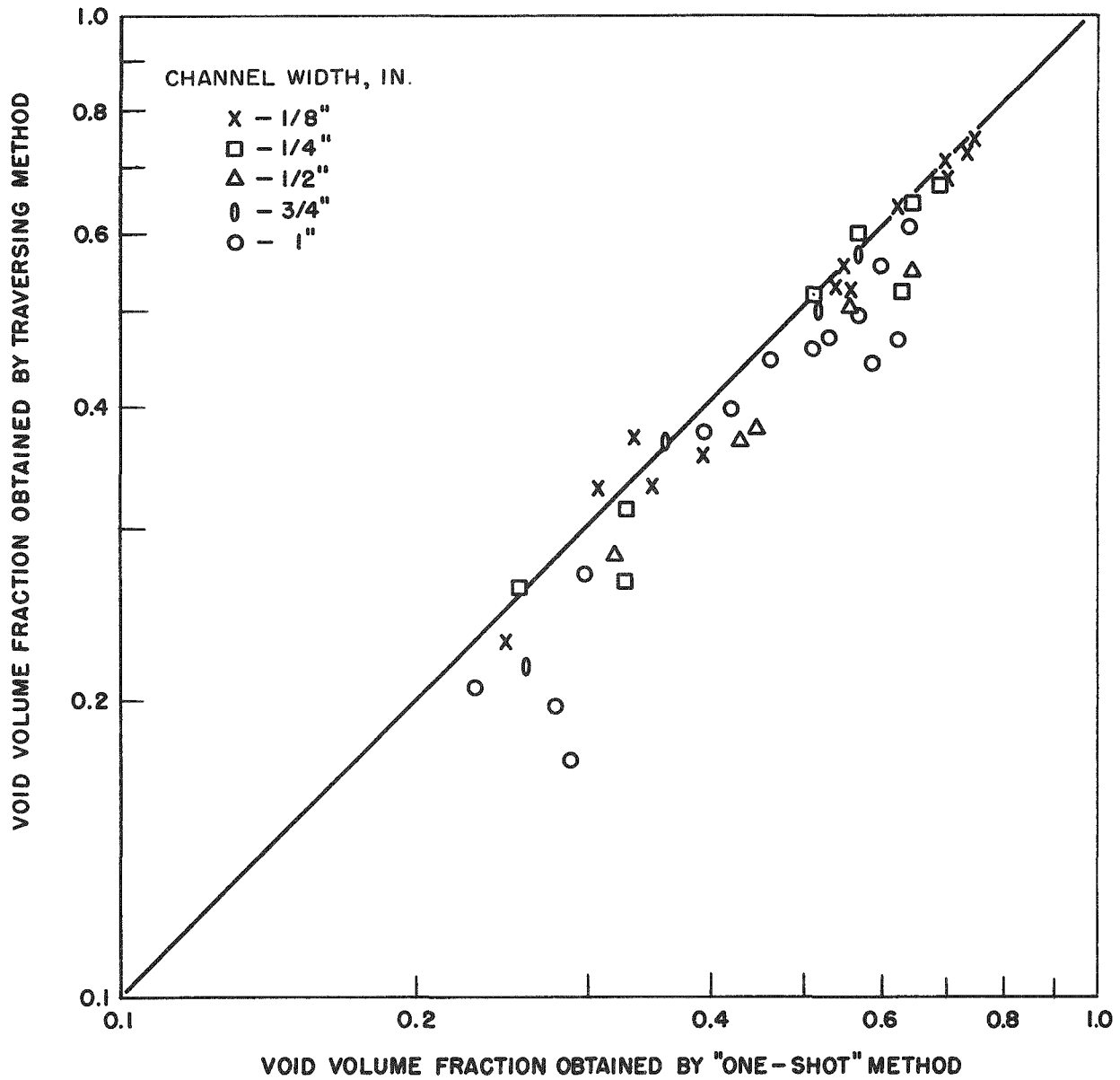

FIG. 3.7 COMPARISON OF THE "ONE-SHOT" AND TRAVERSING TECHNIQUES FOR VOID FRACTION DETERMINATION FOR VARIOUS CHANNEL WIDTHS

IV. EFFECT OF FLOW AREA CHANGES ON TWO-PHASE FLUID DENSITY

A. Introduction

Prediction of the density of an adiabatic two-phase fluid in motion is difficult because of inadequate information concerning the relative velocity between the gas and liquid phases. The gas volume fraction is interrelated with the velocity of the two phases and the gas weight fraction through the well-known continuity equation, which will be discussed later. At the present time, all the factors that affect the relative velocity or "slippage" between phases are not well established. There is meager experimental evidence which indicates that the relative velocity of the two phases is a function of the liquid flow rate, the gas weight fraction, pressure, and, possibly the geometry of the flow path.

Behringer[6] in a series of experiments on a static steam-water system showed that the relative velocity of the two phases decreases with increasing pressure. Marchaterre[7] observed a similar effect over a pressure range of 25 to 600 psi with a natural circulation system. He also noted an effect of liquid flow rate on the relative velocity of the two phases. Schurig[8] reported a marked influence of the circulation rate on the relative velocity. The recent data of Lottes, et al.,[9] for a natural, and for a forced, circulation boiling system shows both a flow rate and a quality effect on the "slippage" between the two phases. They obtained local two-phase density measurements by gamma-ray attenuation methods and readily converted the data to a slip ratio V_g/V_w. Cook,[3] on the basis of an extensive two-phase density study of steam-water in multisection rectangular channels, concluded: (1) an increase of V_g/V_w occurs with length along the heated channel; (2) the increase is a function of the rate of vaporization; and (3) with no vaporization, V_g/V_w is merely a function of geometry and the volume flow of the two phases. Dengler,[10] using a radioactive tracer technique, measured liquid holdups in a 1-in. diameter pipe and correlated them as a function of the mixture quality, X. Eddy[11] obtained local density values at atmospheric pressure for steam-water mixtures in a horizontal tube and showed the distribution of each phase in the tube. Sher[12] performed similar tests in a vertical tube. His vapor volume fraction-quality data were approximately 10% higher than the data of Martinelli, et al.

Zmola, et al.,[13] measured two-phase densities of an air-water system over a wide geometrical range of flow paths. These results checked with the data of Behringer in the high vapor volume fraction range. A radial parabolic distribution of the vapor volume fraction was observed in the various geometries. Schwarz[14] investigated the density and relative velocities of the water and steam phases in vertical and horizontal boiler tubes (2.36 ID). He also showed a radial parabolic distribution of the vapor volume fraction.

Up to the present no data has been published showing the liquid holdup variation due to a sudden change in flow area resulting from either an expansion or contraction. Utilizing presently available information on two-phase flow, it would be difficult to make a firm prediction as to whether a change in density of the two-phase mixture will occur with a change of flow area, let alone to estimate the magnitude of the change. Therefore, an experimental investigation was undertaken in an attempt to provide adequate information on the effect of changes of flow area on the two-phase fluid density and to explore further the factors which affect the relative velocity of the two phases.

B. Theory

The density of a two-phase mixture is given by:

$$\rho_m = (1 - \alpha)\rho_w + \alpha\rho_g \quad . \tag{4.1}$$

The relationship of the gas volume fraction with the relative velocity of the two phases and the gas weight fraction can be shown through the continuity equations as follows.

Under steady-state conditions, the amounts of gas and liquid flowing past a point in a channel are given by

$$W_w = V_w A_w \rho_w \tag{4.2}$$

$$W_g = V_g A_g \rho_g \quad . \tag{4.3}$$

The area relationship for each phase is

$$A_w = (1 - \alpha)\, A_T \quad ; \tag{4.4}$$

$$A_g = \alpha A_T \tag{4.5}$$

By definition,

$$W_w = (1 - X)\, W_T \tag{4.6}$$

$$W_g = (X)\, W_T \quad , \tag{4.7}$$

where

$$W_g + W_w = W_T \quad . \tag{4.8}$$

Substituting Eqs. (4.4), (4.5), (4.6) and (4.7) into Eqs. (4.2) and (4.3)

$$(1 - X)\, W_T = V_w\, (1 - \alpha)\, A_T \rho_w \tag{4.9}$$

$$X\, W_T = V_g\, (\alpha)\, A_T \rho_g \quad . \tag{4.10}$$

Dividing Eq. (4.10) by Eq. (4.9) and rearranging,

$$\frac{V_g}{V_w} = \left(\frac{X}{1 - X}\right)\left(\frac{1 - \alpha}{\alpha}\right)\left(\frac{\rho_w}{\rho_g}\right) \quad . \tag{4.11}$$

As mentioned previously, experimental evidence indicates that the relative velocity of the two phases is a function of both the circulation rate and the quality. For the case of an adiabatic system such as an air-water system, where the quality is a constant, α or the density of the two-phase mixture will vary only if the slip ratio changes. As a result, the density of a two-phase mixture will change, due to an expansion or contraction, only if the slip ratio is a function of the velocity.

Consider a change of flow area between two points as depicted below.

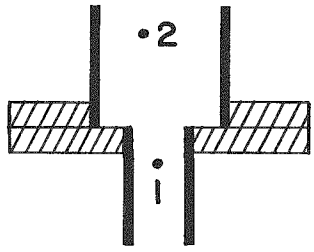

The gas volume fraction, α, can be expressed at each point by

$$\left(\frac{V_g}{V_w}\right)_1 = \left(\frac{X_1}{1 - X_1}\right)\left(\frac{1 - \alpha_1}{\alpha_1}\right)\left(\frac{\rho_w}{\rho_g}\right)_1 \tag{4.12}$$

$$\left(\frac{V_g}{V_w}\right)_2 = \left(\frac{X_2}{1 - X_2}\right)\left(\frac{1 - \alpha_2}{\alpha_2}\right)\left(\frac{\rho_w}{\rho_g}\right)_2 \quad . \tag{4.13}$$

Dividing Eq. (4.12) by Eq. (4.13) and rearranging,

$$\frac{(\alpha_1)/(1-\alpha_1)}{(\alpha_2)/(1-\alpha_2)} = \frac{\dfrac{(X_1/1-X_1)\,(\rho_w/\rho_g)_1}{(Vg/V_w)_1}}{\dfrac{(X_2/1-X_2)\,(\rho_w/\rho_g)_2}{(V_g/V_w)_2}} \quad . \tag{4.14}$$

Since for an adiabatic system

$$X_1 = X_2$$

and

$$(\rho_w)_1 = (\rho_w)_2 \quad ,$$

Eq. (4.14) becomes

$$\frac{\dfrac{\alpha_1}{1-\alpha_1}}{\dfrac{\alpha_2}{1-\alpha_2}} = \frac{\left(\dfrac{V_g}{V_w}\right)_2 (\rho_g)_2}{\left(\dfrac{V_g}{V_w}\right)_1 (\rho_g)_1} \tag{4.15}$$

Assume that

$$\frac{V_g}{V_w} = K\, V_{w_0}^N \quad . \tag{4.16}$$

Since

$$W = V_{w_0}\, A\, \rho \quad , \tag{4.17}$$

then

$$V_{w_0} = \frac{W}{A\rho} = \frac{K'''}{A} \tag{4.18}$$

for the constant total flow.

Substituting Eq. (4.18) into Eq. (4.16)

$$\frac{V_g}{V_w} = \frac{K''}{(A)^N} \quad ; \tag{4.19}$$

also

$$\frac{1}{\rho g} = \frac{R\,T}{P\,M} \quad , \tag{4.20}$$

so that

$$\rho g = K'P \quad . \tag{4.21}$$

Substituting Eqs. (4.19) and (4.21) into Eq. (4.15), and rearranging,

$$\alpha_2 = \frac{1}{\left\{(P_2/P_1)\left[(1/\alpha_1) - 1\right] / (A_1/A_2)^N\right\} + 1} \quad . \tag{4.22}$$

Based on forced circulation boiling studies at Argonne, the exponent N was set at 0.2 for the initial comparison with the experimental results (this is discussed more thoroughly in the presentation of results).

The static pressure ratio P_2/P_1 must be included because of the large changes in the specific volumes of the gaseous phase at the lower pressures. Thus, in addition to the change of the gas volume fraction due to the velocity effect, the gas volume fraction will also change due to the static pressure difference between positions. The latter effect will become negligible as the system pressure is increased ($P > 25$ psia).

C. Discussion of Results

1. Data Procurement

In order to investigate the effect of sudden changes of flow area on the density of a two-phase mixture, a series of expansion and contraction tests were made using rectangular Lucite sections, 2 in. wide and 4 ft long, with spacings of 1/8 in., 1/4 in., 1/2 in., 3/4 in. and 1 in., respectively. (All future reference to the sections will be with respect to spacing.)

Data on expansions were obtained with the following section combinations: 1/8 to 1/4 in.; 1/8 to 1/2 in.; 1/8 to 3/4 in.; 1/8 to 1 in.; 1/4 to 3/4 in.; 1/2 to 3/4 in.; and 1/2 to 1 in.

The section combinations used for obtaining data on contractions were: 1 to 3/4 in.; 1 to 1/2 in.; 1 to 1/4 in.; 1 to 1/8 in.; 3/4 to 1/4 in.; 1/2 to 1/4 in.; and 1/2 to 1/8 in. It was felt that the various geometric combinations investigated gave an adequate cross section of the expansion and contraction geometries possible.

The changes of flow area investigated ranged from a maximum of 8:1 using the 1-inch and 1/8-inch sections, and a minimum of 1.333:1 with the 3/4-inch and 1-inch sections.

A series of runs with varying air volume fractions were made for each geometry combination. The air volume fraction was varied from $\alpha = 0.2$ to $\alpha = 0.75$, primarily by adjusting the flow rate of air. Owing to the relationship between specific volumes of the two phases, the quality range corresponding to the air volume fraction range studied was very low ($X = 0.00055$ to $X = 0.0045$).

Measurements of the air volume fraction were taken at the exit of the lower section, and at positions 4, 8, 24 and 44 in. in the upper section. These positions were selected so that both the transition zone could be studied (using positions at 4 in. and 8 in.) and the actual over-all change in two-phase density could be determined (using positions at 24 in. and 44 in.)

The air volume fraction was measured and the data reduced by the methods described in Section III.

2. Air Volume Fraction Changes - Expansion of Flow Area

The air volume fractions are plotted as a function of the riser length in Fig. 4.1 for a series of expansions. The erratic behavior of the void volume fraction in the transition zone may be attributed to the varying degree of pressure drop which accompanies the expansion. A local low-pressure zone, whose magnitude will depend on the velocity, quality, and enlargement in flow area is created. The void fraction could therefore rise or fall abruptly in the transition zone due to the static pressure effect on the density-volume relationship of air at atmospheric pressure, and to possible cavitation effects, since the solubility of air in water is sensitive to pressure. The greatest increase in voids could be expected in the case of maximum area enlargement, such as from 1/8 to 1 in. and from 1/8 to 3/4 in., and at high qualities.

A decrease in voids would be expected in expansions which have a small frictional pressure drop and an actual pressure recovery (low velocities and qualities and a minimum area enlargement). Such results were obtained for expansions of from 1/2 to 1 in. and from 1/2 to 3/4 in.

The transition zone from a 1/8-inch section to a 1-inch section for various qualities is shown in Figs. 4.2 to 4.5. As the quality increases, the formation of a jet occurs over the first few inches; the jet immediately dissipates into a very turbulent flow region.

The change in the air volume fraction was calculated using Eq. (4.22), and the results were compared with the experimental data. Very good agreement is shown (Fig. 4.6) between predicted and measured values, with a maximum error of $\pm 10\%$ and an average deviation of 5%.

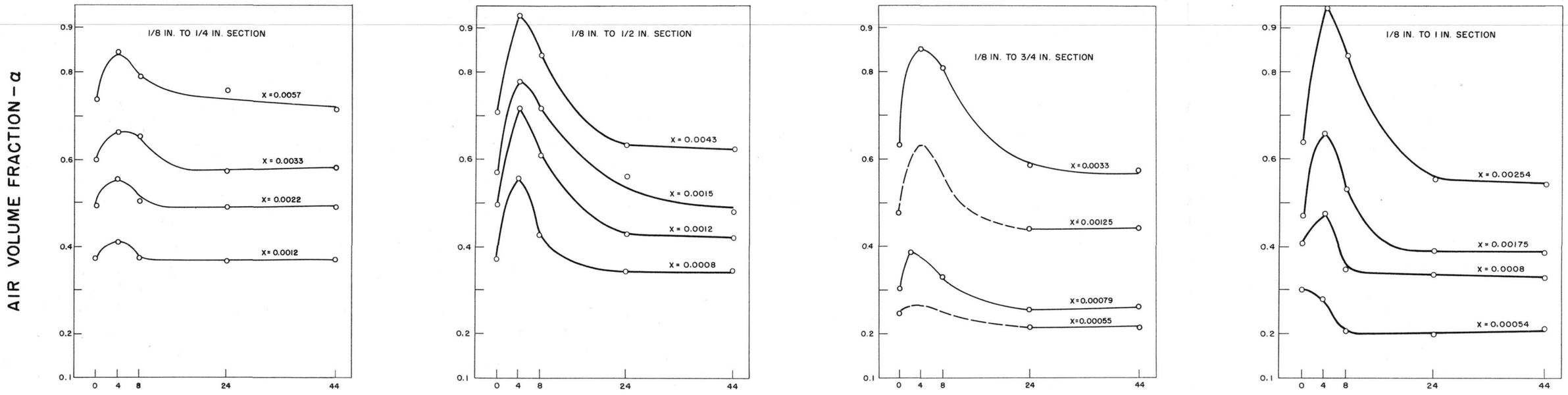

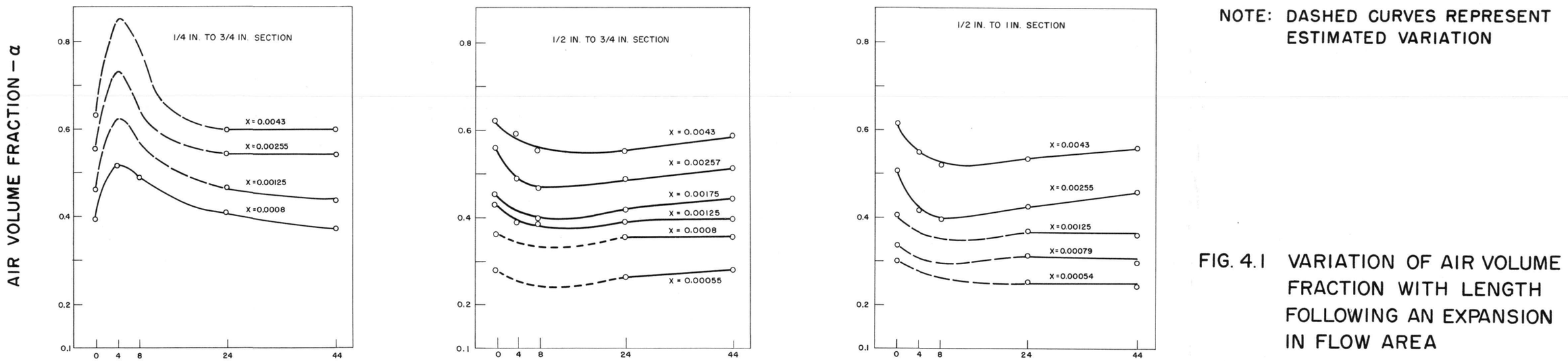

NOTE: DASHED CURVES REPRESENT ESTIMATED VARIATION

FIG. 4.1 VARIATION OF AIR VOLUME FRACTION WITH LENGTH FOLLOWING AN EXPANSION IN FLOW AREA

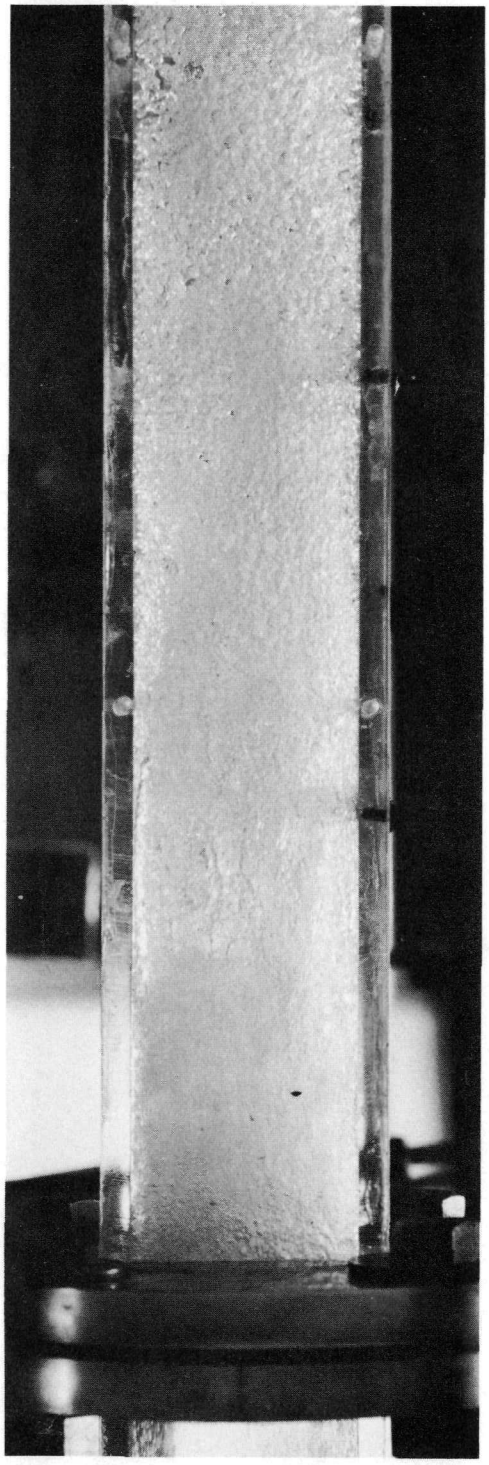

FRONT

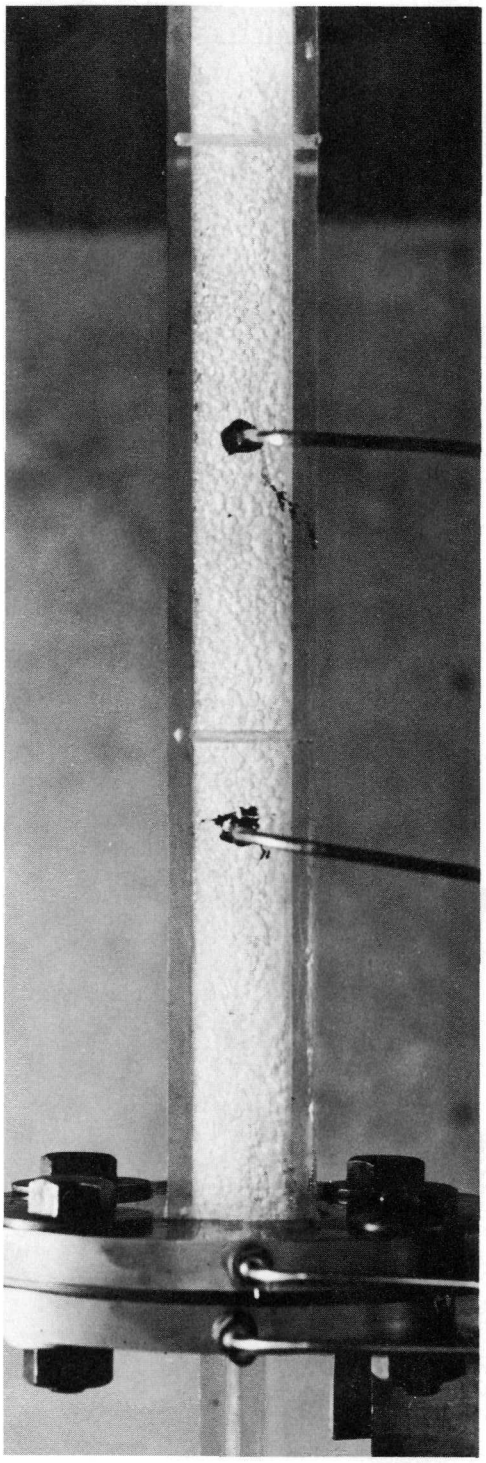

SIDE

FIG. 4.2 TRANSITION ZONE FOLLOWING AN EXPANSION FROM A 1/8-INCH SECTION TO A 1-INCH SECTION. QUALITY = 0.0008

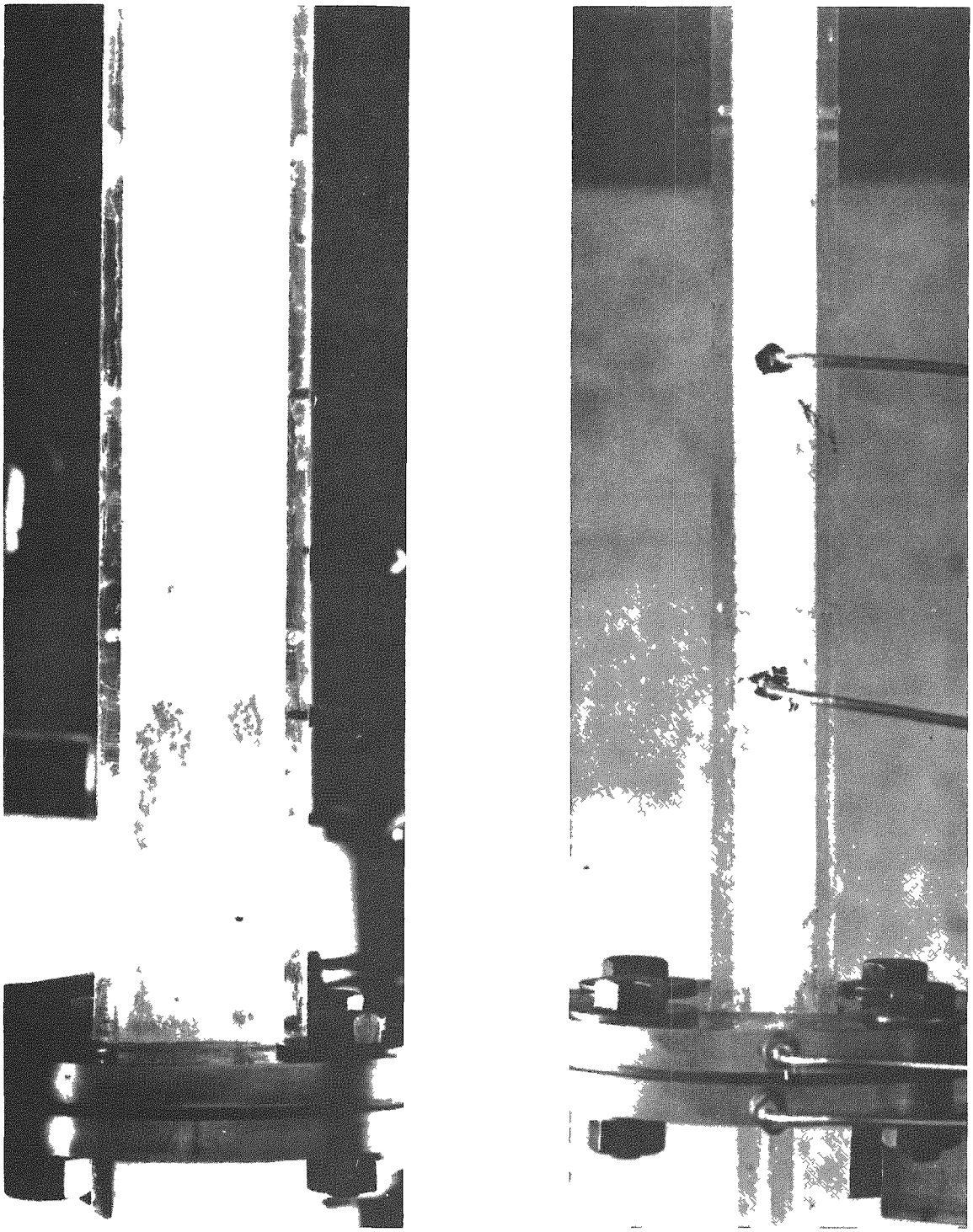

FRONT SIDE

FIG. 4.3 TRANSITION ZONE FOLLOWING AN EXPANSION FROM A 1/8-INCH SECTION TO A 1-INCH SECTION. QUALITY = 0.00175

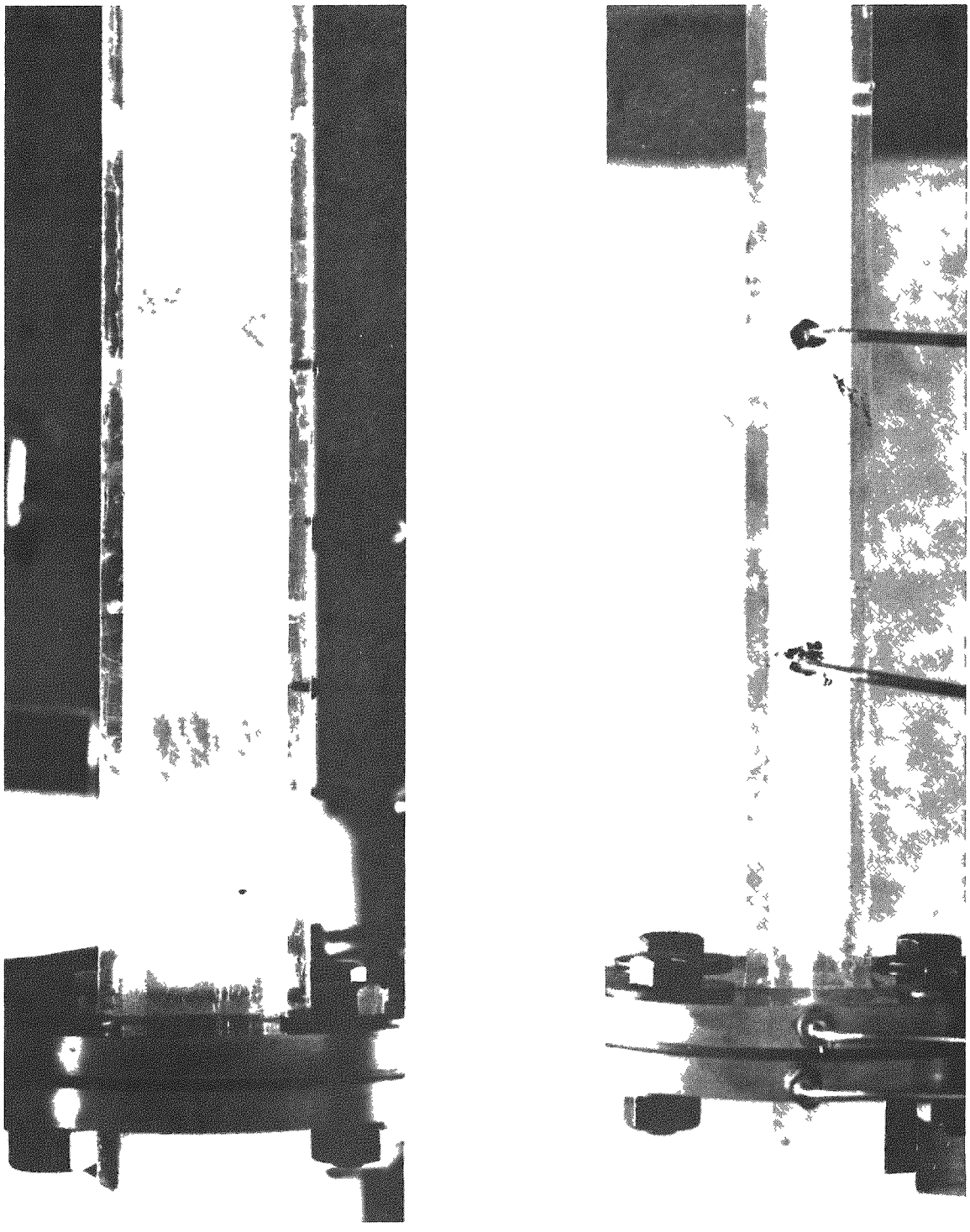

FRONT SIDE

FIG. 4.4 TRANSITION ZONE FOLLOWING AN EXPANSION FROM A 1/8-INCH SECTION TO A 1-INCH SECTION. QUALITY = 0.0033

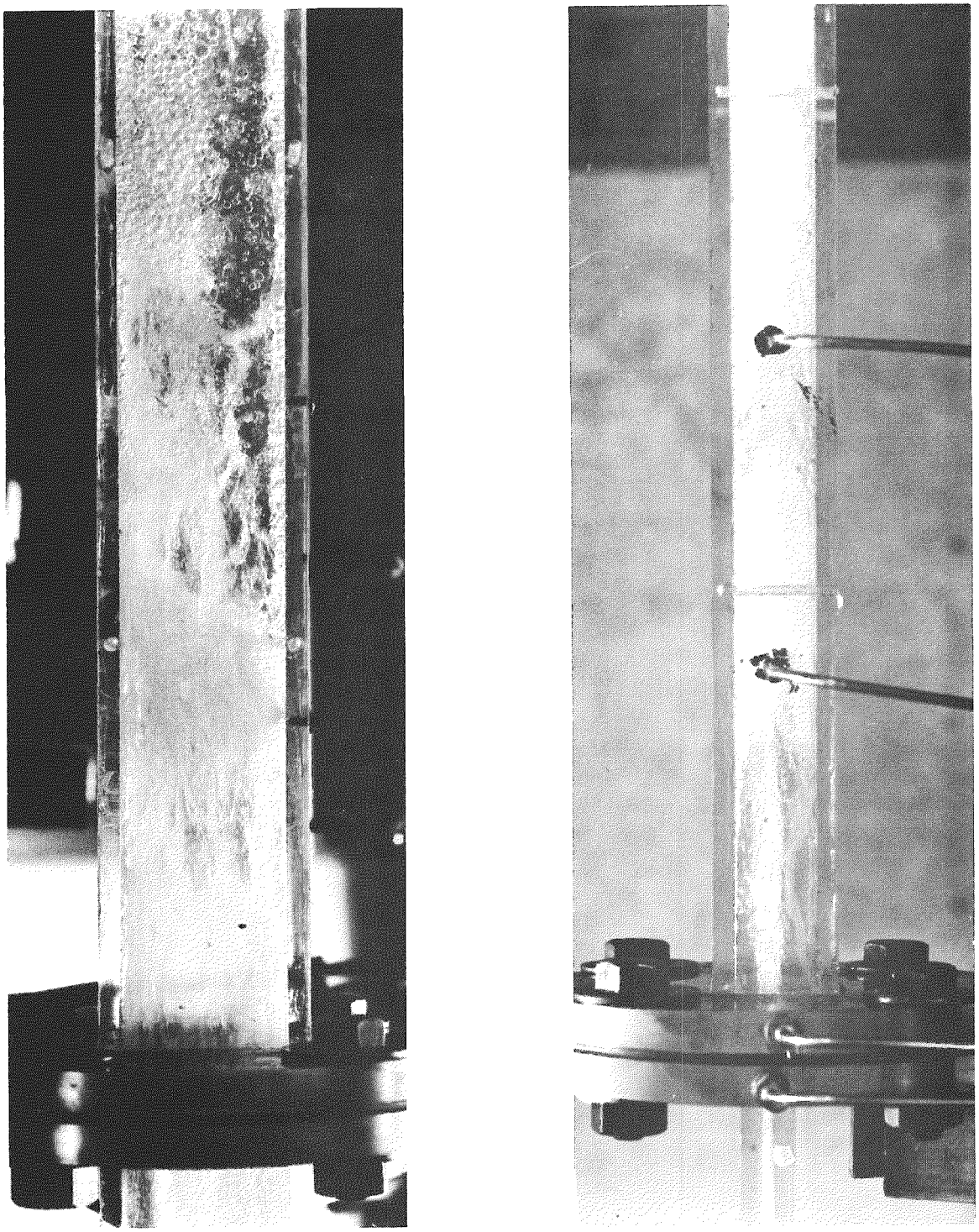

FRONT SIDE

FIG. 4.5 TRANSITION ZONE FOLLOWING AN EXPANSION FROM A 1/8-INCH SECTION TO A 1-INCH SECTION. QUALITY = 0.0043

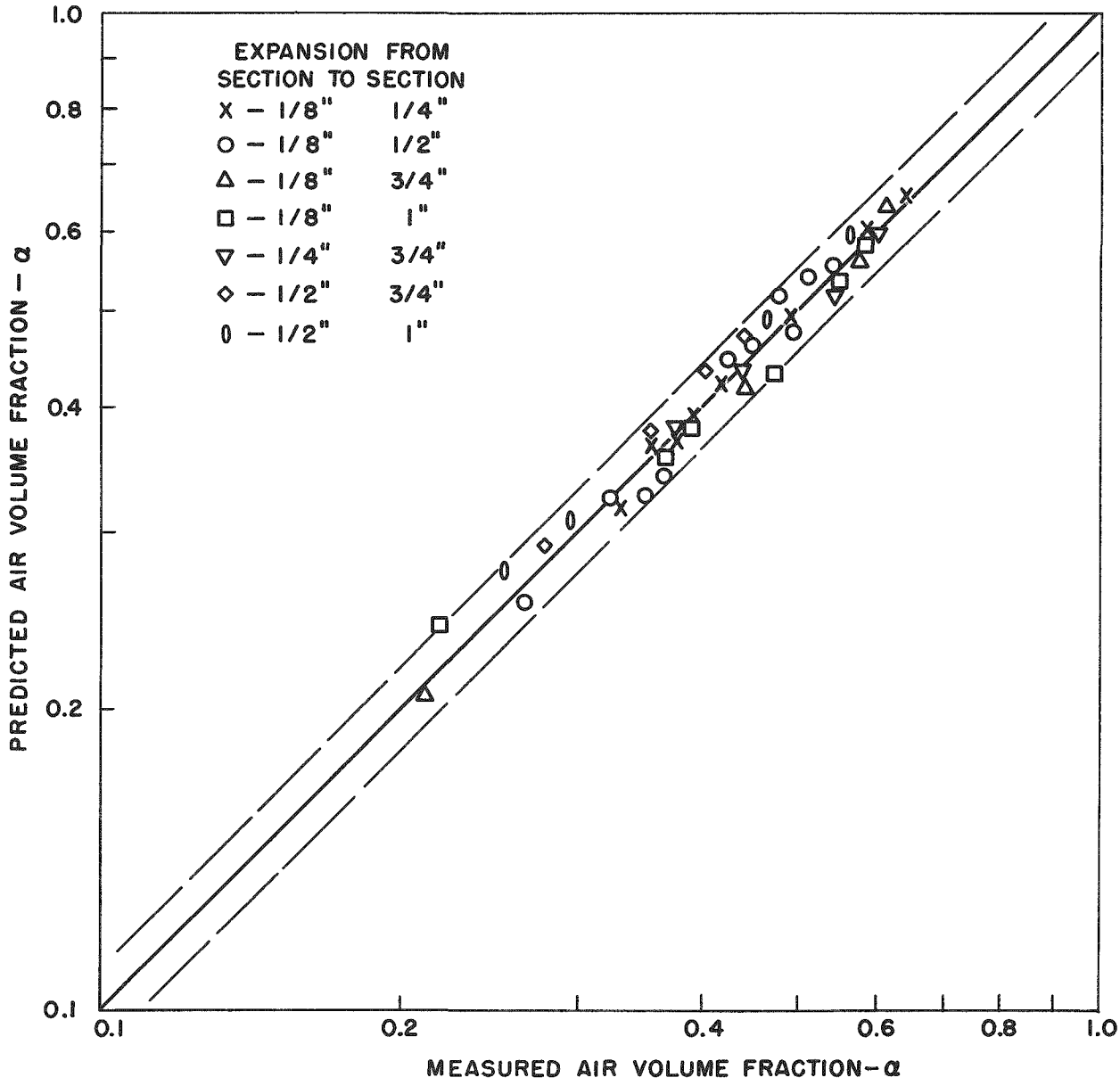

FIG. 4.6 COMPARISON OF THE PREDICTED AND MEASURED AIR VOLUME FRACTION FOR A SERIES OF EXPANSIONS

3. Air-Volume Fraction Changes - Contraction in Flow Area.

The variation of air volume fraction with length of riser, for the series of contractions studied, is plotted in Fig. 4.7. In general the transition zone appears to be very short and not as well-defined as in the case of expansion of flow area. The air volume fraction increases to a final value in the first few inches of riser length. In some contractions slight peaks occurred in the plots of air volume fraction vs. length of riser as was observed in the expansions. However, the magnitude of the peaks were within the accuracy of the air volume fraction measurements.

The short transition zone can also be seen in Fig. 4.8, which shows the contraction from 1-inch to a 1/8-inch section for increasing mixture qualities. The flow pattern in the riser tended to stabilize almost immediately after the contraction.

The apparent instability of the air volume fraction in the riser section for contractions of 1 in. to 1/8 in., and 1/2 in. to 1/8 in. as shown in Fig. 4.7 was due to the large static pressure changes in the 1/8-inch section which resulted from the excessive two-phase pressure drops. As the static pressure dropped along the riser length, the specific volume of the air changed markedly which, in turn, affected the air volume fraction. The static pressure dropped from 30 psia to 15 psia across the 1/8-inch section. Such a drop would approximately double the air volume fraction if a change in the relative velocities of the two phases did not occur. For the other series of contractions the static pressure change across the riser section was not severe, and therefore the air volume fraction stabilized fairly rapidly.

The change in the air volume fraction was calculated by Eq. (4.22) and compared with the data. The results are plotted in Fig. 4.9. Again, as for the expansions, the data is very well represented by Eq. (4.22), with a maximum deviation of $\pm 15\%$ and an average of 7%.

The maximum deviation occurred for contractions of from 1 to 1/8 in. and from 1/2 to 1/8 in., as shown in Fig. 4.10. This can be attributed to the large static pressure changes in the 1/8-inch section. As mentioned previously, experimental studies have shown that the relative velocities of the two phases decrease with increasing pressure. In addition, the exponent N in Eq. (4.22) also decreases with pressure (a lower value of N would tend to reduce the deviation between the measured and predicted values). Additional error in the predicted value of the air volume fraction was introduced from inaccurate static pressure readings obtained from the gauges. The flow pattern in the 1/8-inch riser section was a collapsing annular type, which resulted in very severe static

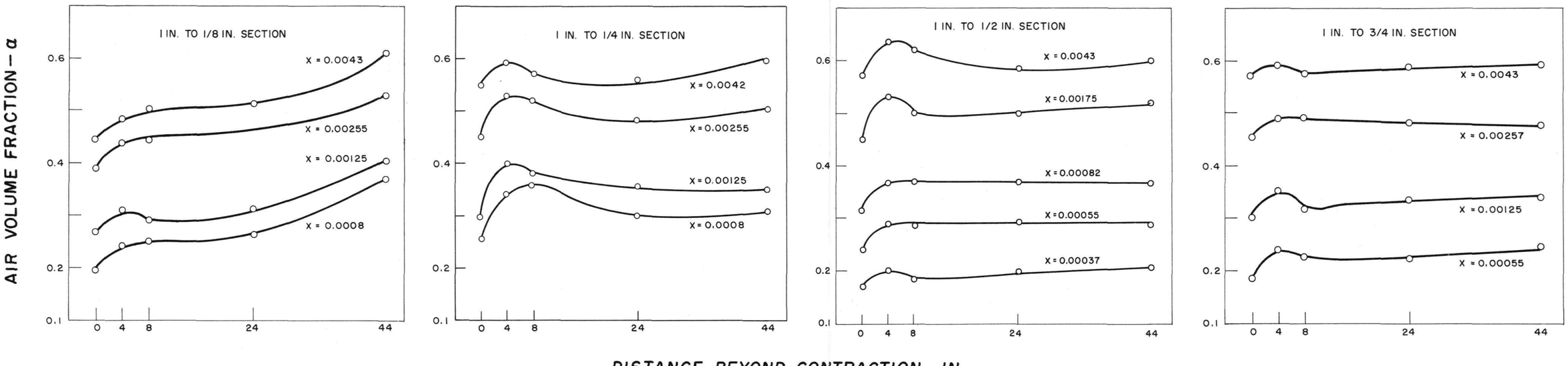

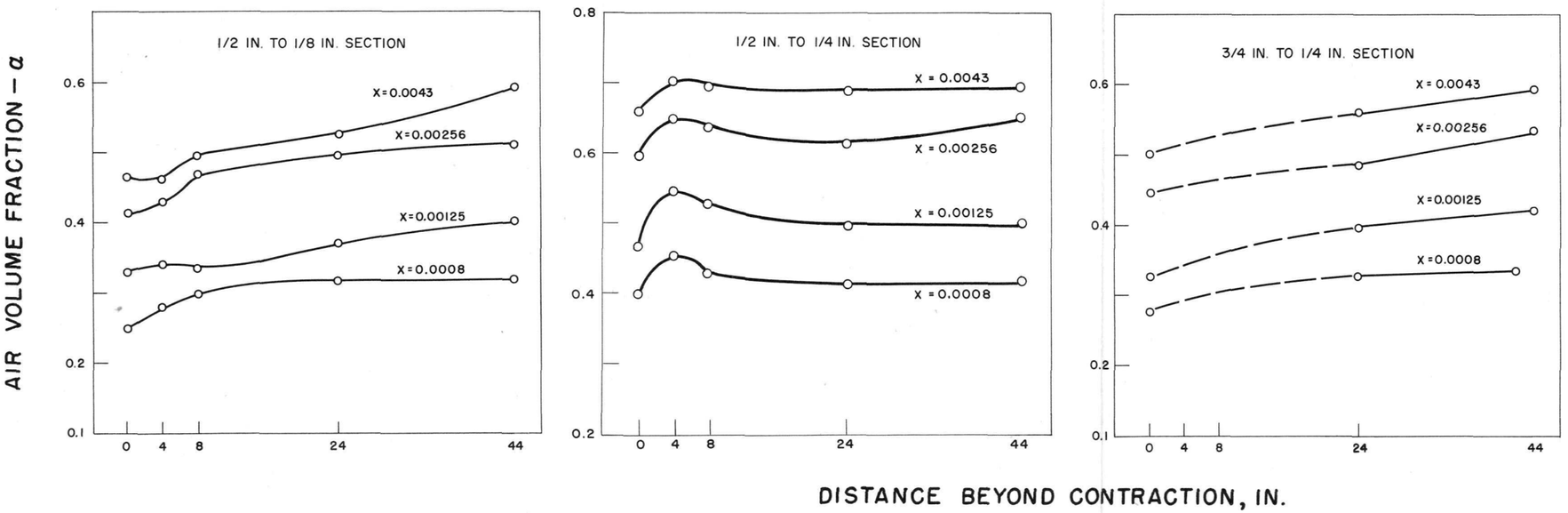

NOTE: DASHED CURVES REPRESENT ESTIMATED VARIATION

FIG. 4.7 VARIATION IN AIR VOLUME FRACTION WITH LENGTH FOLLOWING A CONTRACTION IN FLOW AREA

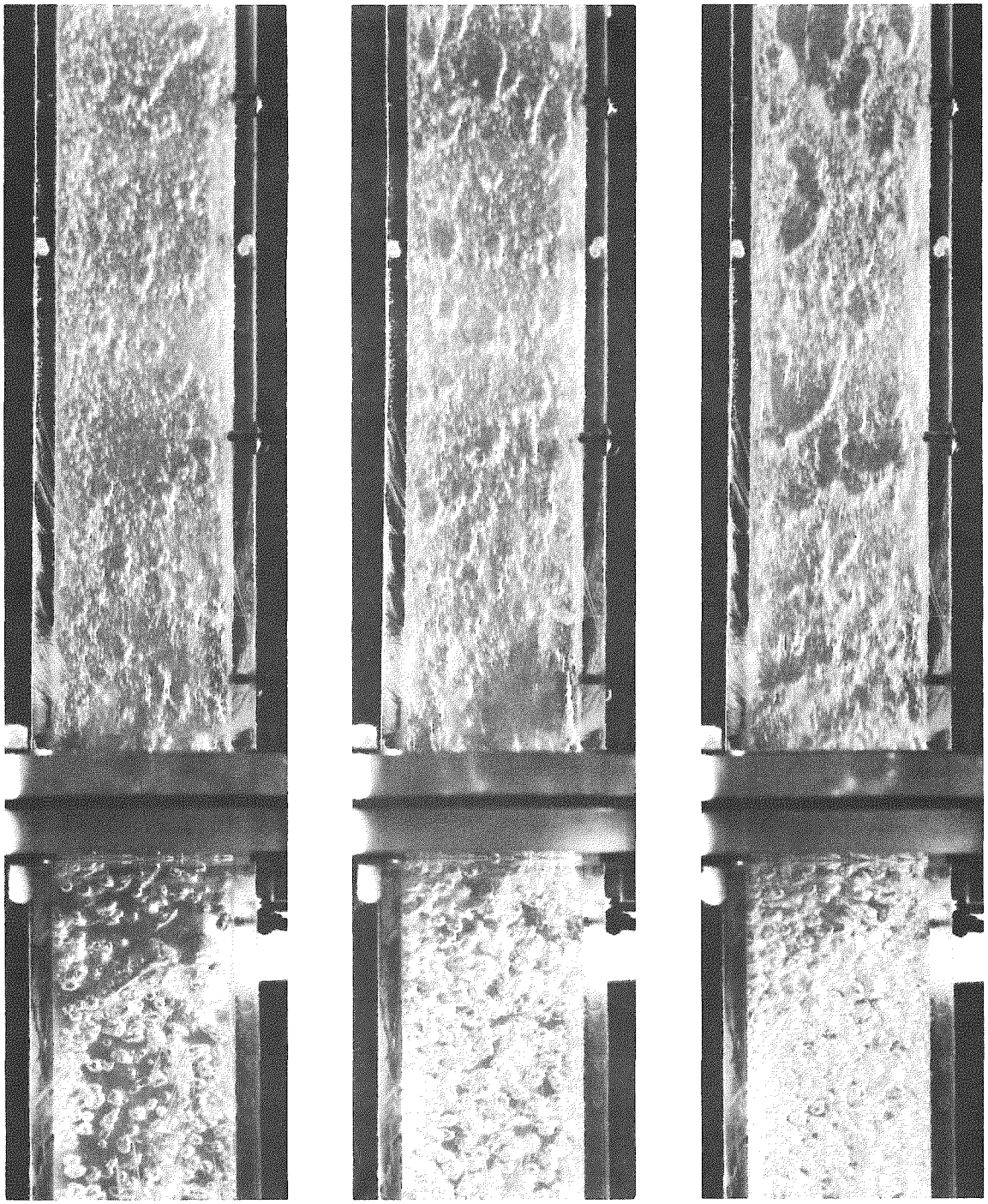

QUALITY = 0.0008 QUALITY = 0.00175 QUALITY = 0.0033

FIG. 4.8 TRANSITION ZONE FOLLOWING A CONTRACTION FROM A 1-INCH SECTION TO A 1/8-INCH SECTION

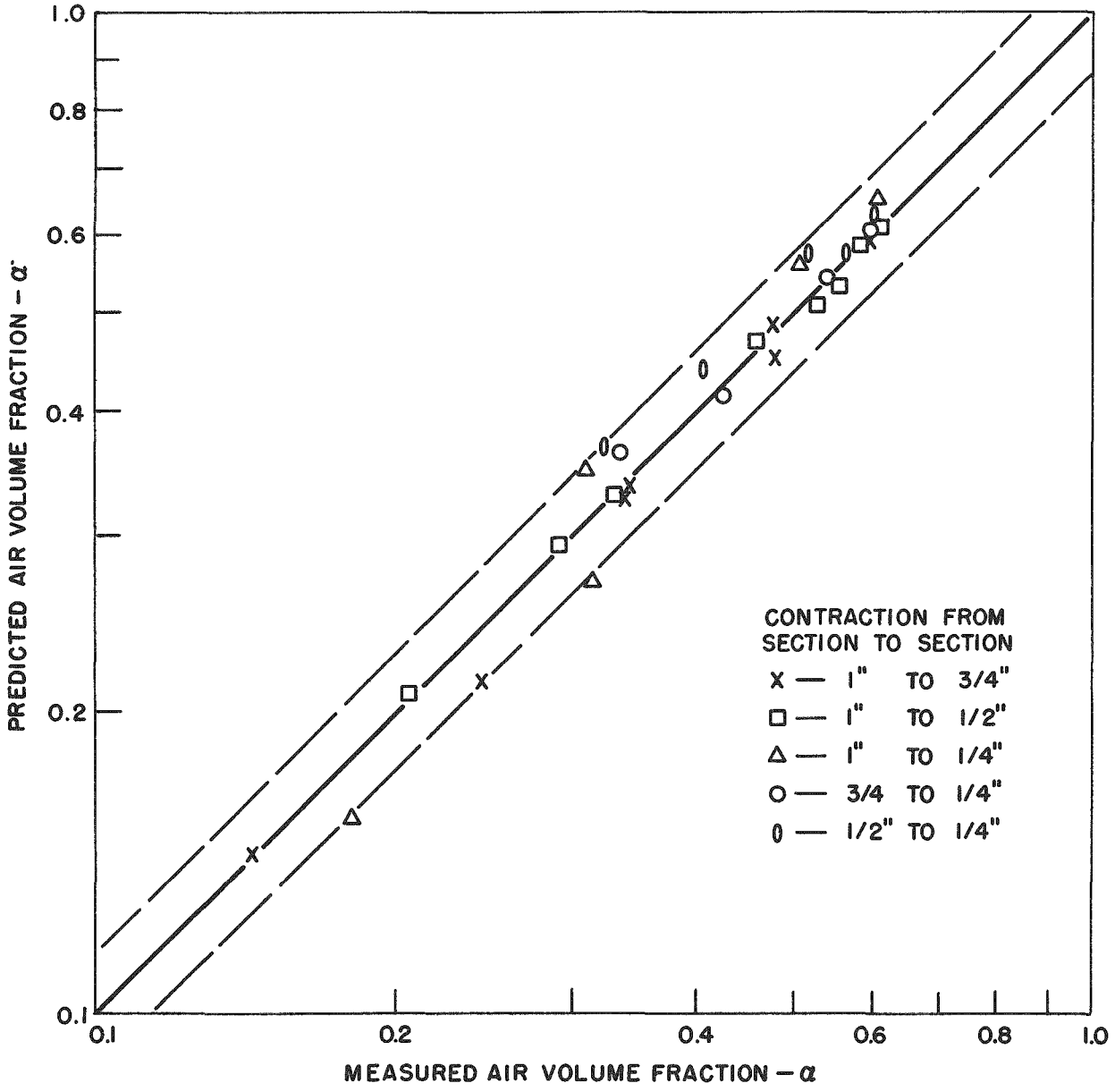

FIG. 4.9 COMPARISON OF THE PREDICTED AND MEASURED AIR VOLUME FRACTION FOR A SERIES OF CONTRACTIONS

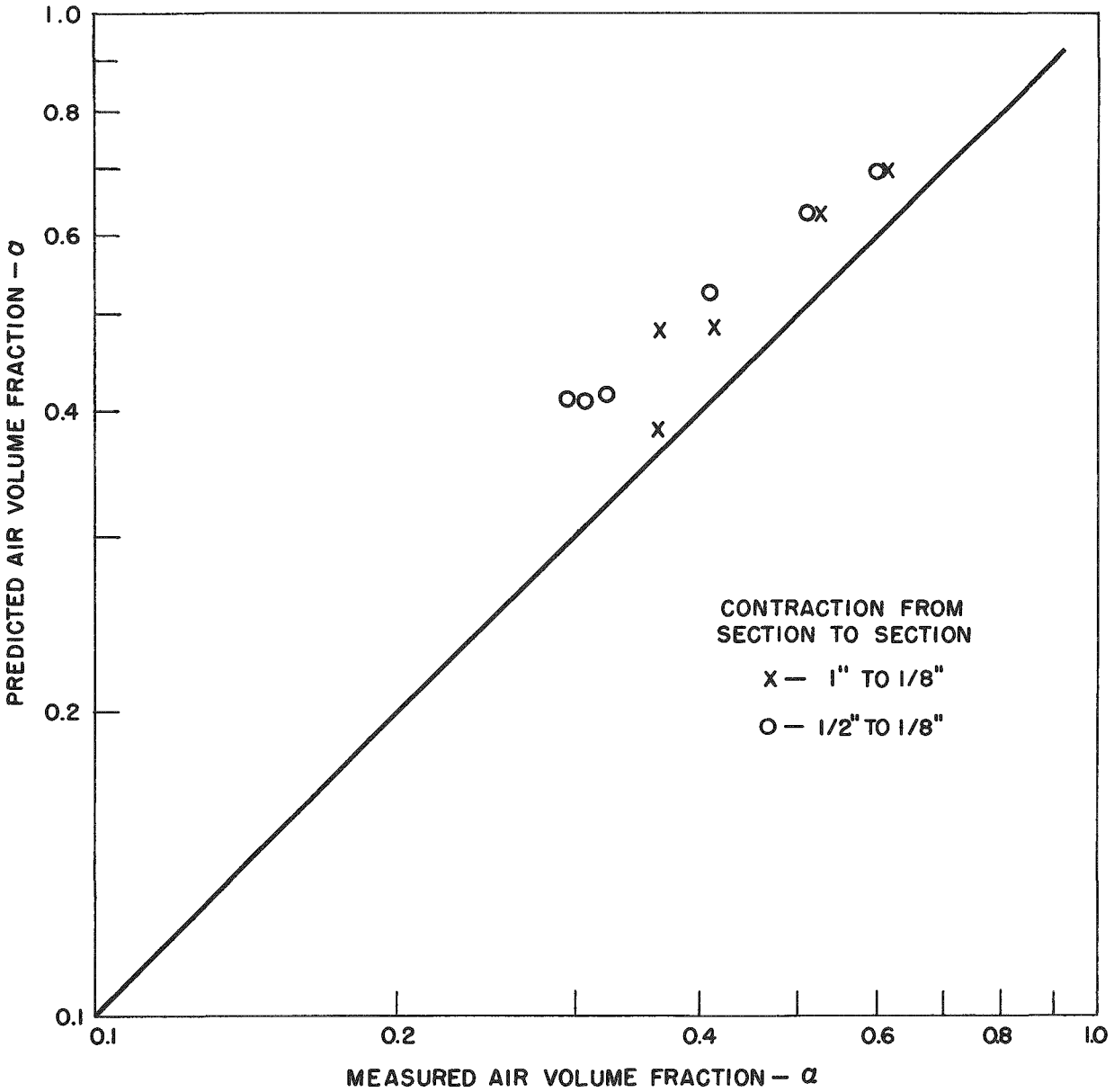

FIG. 4.10 COMPARISON OF THE PREDICTED AND MEASURED AIR VOLUME FRACTION FOR A SERIES OF CONTRACTIONS

pressure fluctuations. Since the magnitude of the fluctuations was, in most cases, beyond the range of the gauges, it was very difficult to obtain a mean static pressure reading; this, in turn, was reflected in the predicted air volume fraction change through the static pressure ratio P_2/P_1 (see Eq. (4.22)).

4. Relative Velocity of Gaseous and Liquid Phases.

The relative velocity of the two phases was calculated for a number of data points utilizing the measured air volume fraction and quality, and plotted in terms of slip ratio (V_g/V_w) vs. the water velocity V_{w_0} (based on section flow area) for a constant quality parameter. Figure 4.11 shows that the relative velocity of the two phases in a function of both the water velocity and the quality.

Since the slope of the quality parameters in the plot of (V_g/V_w) vs. V_{w_0} changed slightly, it was possible that the percentage deviations of the predicted and measured air volume fraction changes could be reduced if the exponent N in Eq. (4.22) were made a function of quality.

An interesting comparison is obtained between the data for an air-water system of this investigation and data obtained from boiling water studies at Argonne National Laboratory. The data for boiling water in a vertical rectangular channel at pressures of 150, 250, and 600 psi were reduced to slip ratios in an analogous manner and were plotted as (V_g/V_w) vs. V_{w_0}. Considerable scatter was obtained, due primarily to the quality effect. The mean functions representing the data for a quality range of X = 0.002 to X = 0.05 at 150 psi for the steam-water system, and X = 0.0043 at atmospheric pressure for the air-water system, are plotted in Fig. 4.12. There is a good agreement between the two sets of data even though the two systems are basically different. Extrapolation of the quality range of air-water data to coincide with the quality range of the boiling data would place the values of slip ratio further above the 150-psi data of the boiling system. This is in line with previous investigations which have shown that the relative velocity of the phases increases with decreasing pressure.

5. Extrapolation of Semi-Empirical Correlation for Predicting Changes in the Air Volume Fraction into the Higher Pressure Region.

The effect of changes of flow area on the vapor volume fraction for an adiabatic steam-water system would also be predicted by Eq. (4.22), since the basic analysis applies to either system.

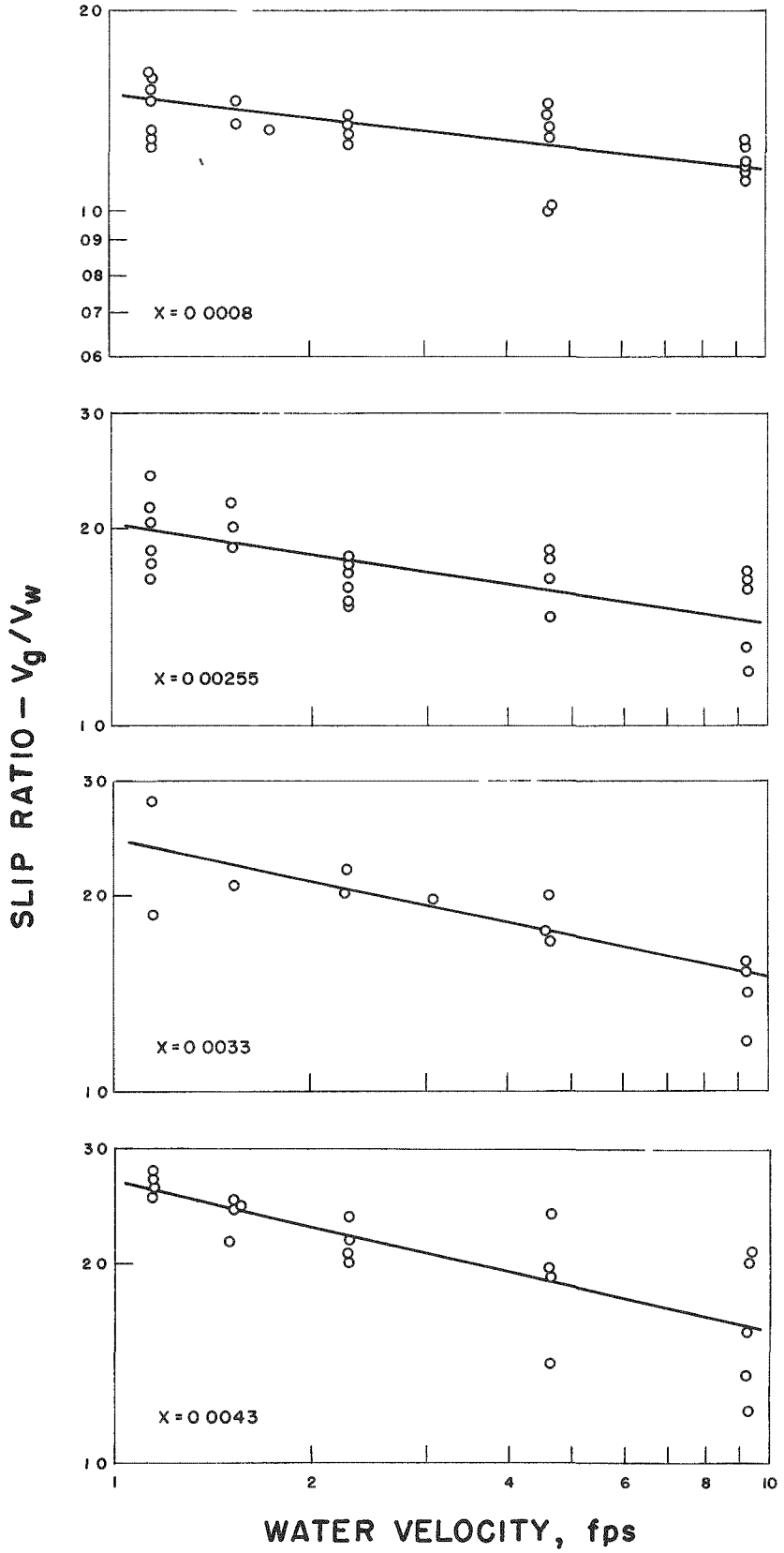

FIG. 4.11 VARIATION OF SLIP RATIO WITH WATER VELOCITY AND QUALITY

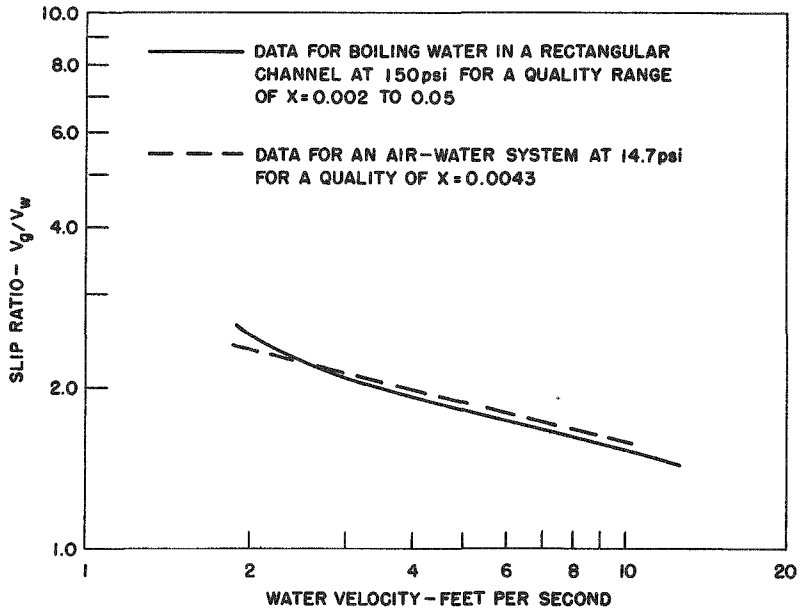

FIG. 4.12 COMPARISON OF THE SLIP RATIO FOR AN AIR-WATER SYSTEM AND A STEAM-WATER SYSTEM

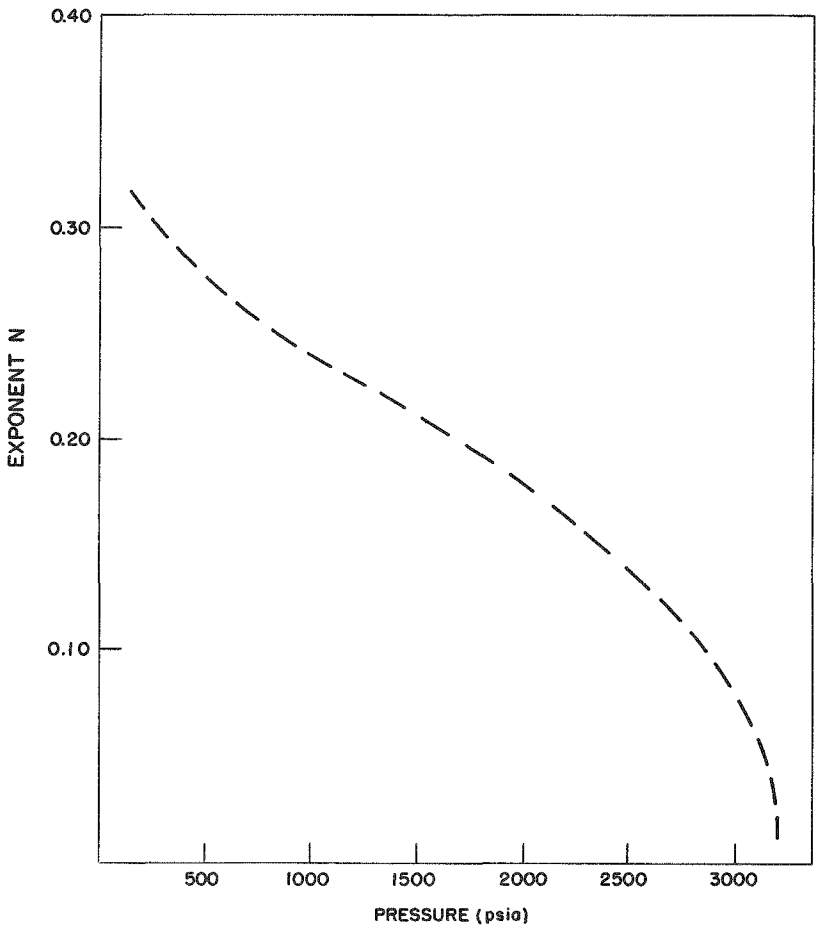

FIG. 4.13 EXTRAPOLATION OF EXPONENT N WITH PRESSURE

An estimation of the pressure effect on slippage between the two phases can be obtained by extrapolation into regions of higher pressure, utilizing the variation with pressure of the density difference $(\rho_w - \rho_g)$, which is a measure of the buoyancy forces, and the critical pressure as a guide. The densities of the steam and water phases approach a common value at the critical point and, therefore, the slip ratio, by definition, must be one.

The majority of the slip ratios used to develop the slip ratio - water velocity correlation for the steam-water system (Fig. 4.12) were obtained at the exit of the test section. It has been shown experimentally that the relative velocity of the steam and water at the exit of a section in which boiling occurs does not change when the fluid passes into an adiabatic riser section of equal flow area. Therefore, the two-phase data plotted for the boiling system also applied to an adiabatic steam-water system over a quality range of 0.002 to 0.05. The exponent N in Eq. (4.22) was therefore assumed to be 0.31 for a pressure of 150 psi. Figure 4.13 shows an extrapolation of the exponent N with pressure. Thus Eqs. (4.22) and Fig. 4.13 can be used to estimate the change in the vapor volume fraction (for a quality range of X = 0.2 to 0.05) due to sudden changes of flow area for a steam-water system. Further experimental work is being carried out to check the extrapolation at the higher pressures.

6. Phase Distributions.

The extensive air volume fraction data (obtained with the traversing technique) shows a parabolic distribution of the air in the liquid. In general, the average to maximum ratio of the air volume fraction $(\alpha_{avg}/\alpha_{max})$, which characterizes the distribution, varied with the quality of the mixture and the channel spacing. Figure 4.14 shows typical air-liquid distributions in 1/2-inch and 1-inch sections at various qualities. In general, the distributions are symmetrical with respect to the vertical axis.

Some interesting air volume fraction distribution pattern changes for expansion occurred in the riser section. A typical example is shown in Fig. 4.15. A distribution pattern of the double annular type was formed at the midpoint of the riser. This phenomena was observed in all riser sections at low qualities or low air volume fractions ($\alpha < 0.4$). Except for rare instances, this type of flow pattern was not observed in sections with normal flow and no expansion of flow area. The exceptions may be due to the jet flow pattern which was shown to occur at the expansion.

Figure 4.16 shows the air volume fraction profile at a position four inches above the expansion. The depression of the air volume fraction in the center of the section is in line with the jet shown in the photograph (side view, Fig. 4.5).

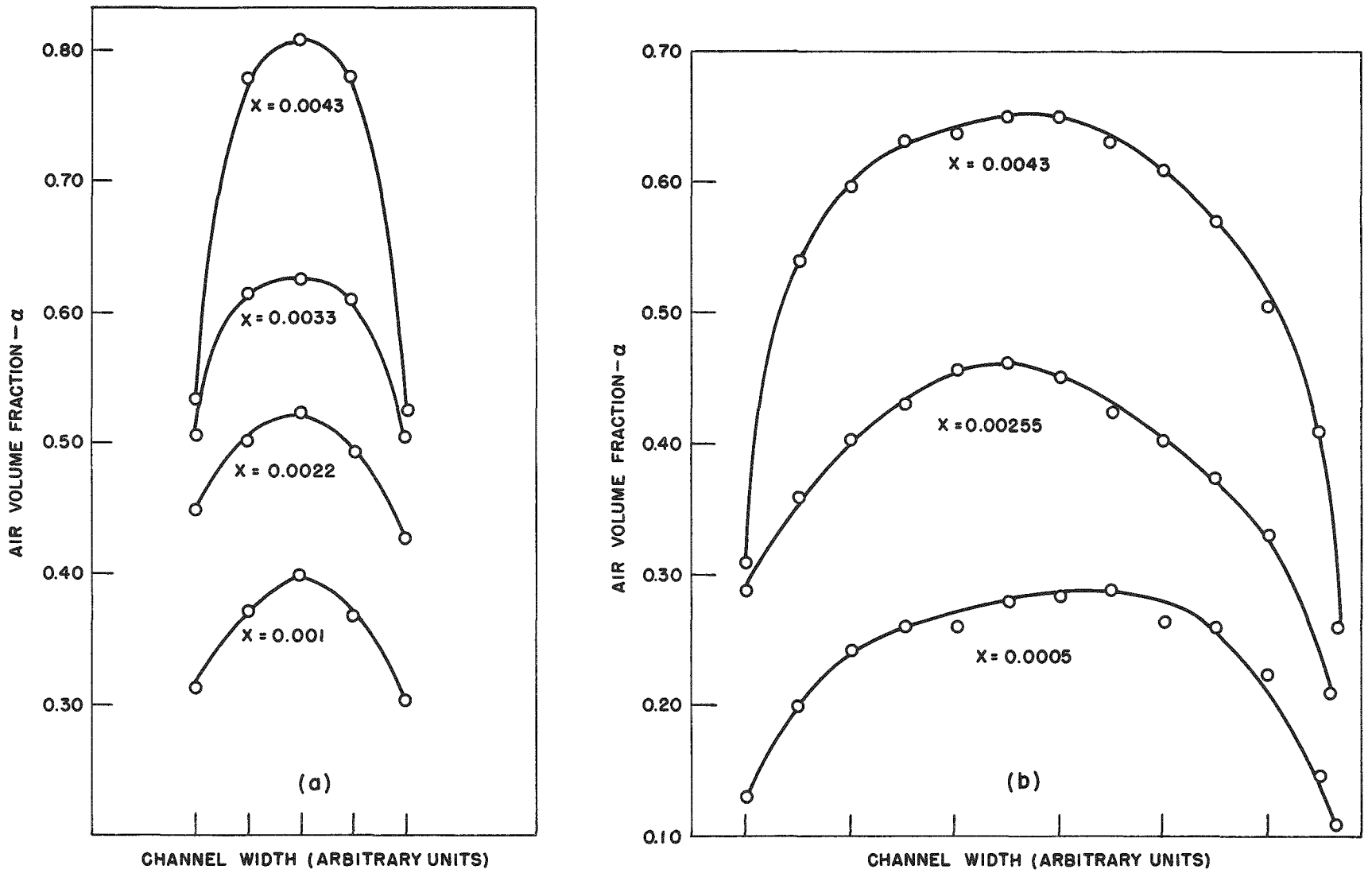

FIG. 4.14 DISTRIBUTION OF AIR IN WATER IN A 1/8-INCH SECTION (a) AND IN A 1-INCH SECTION (b) FOR VARIOUS QUALITIES

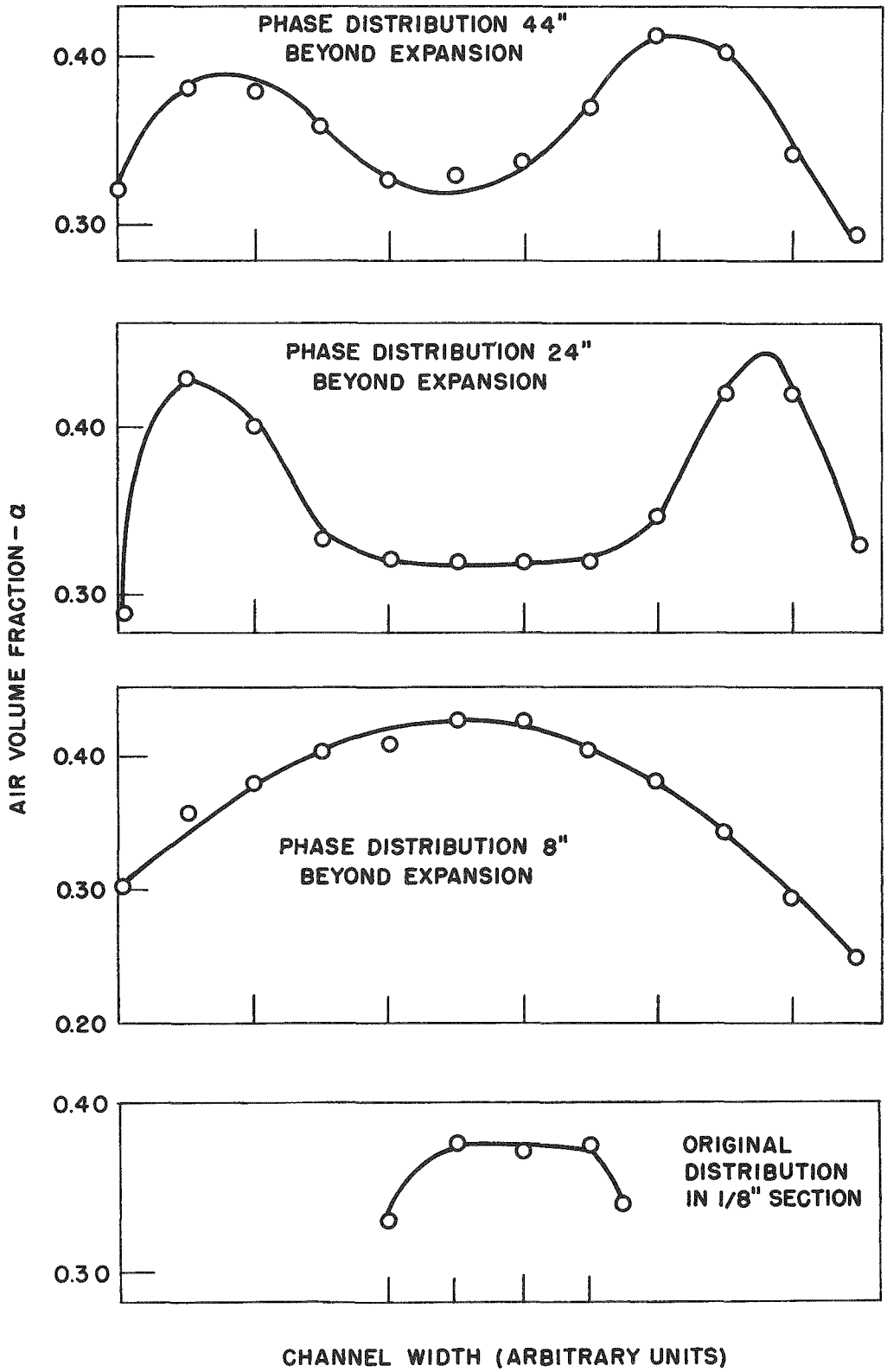

FIG. 4.15 FLOW PATTERNS IN A 1/2" SECTION FOLLOWING AN EXPANSION FROM A 1/8" SECTION

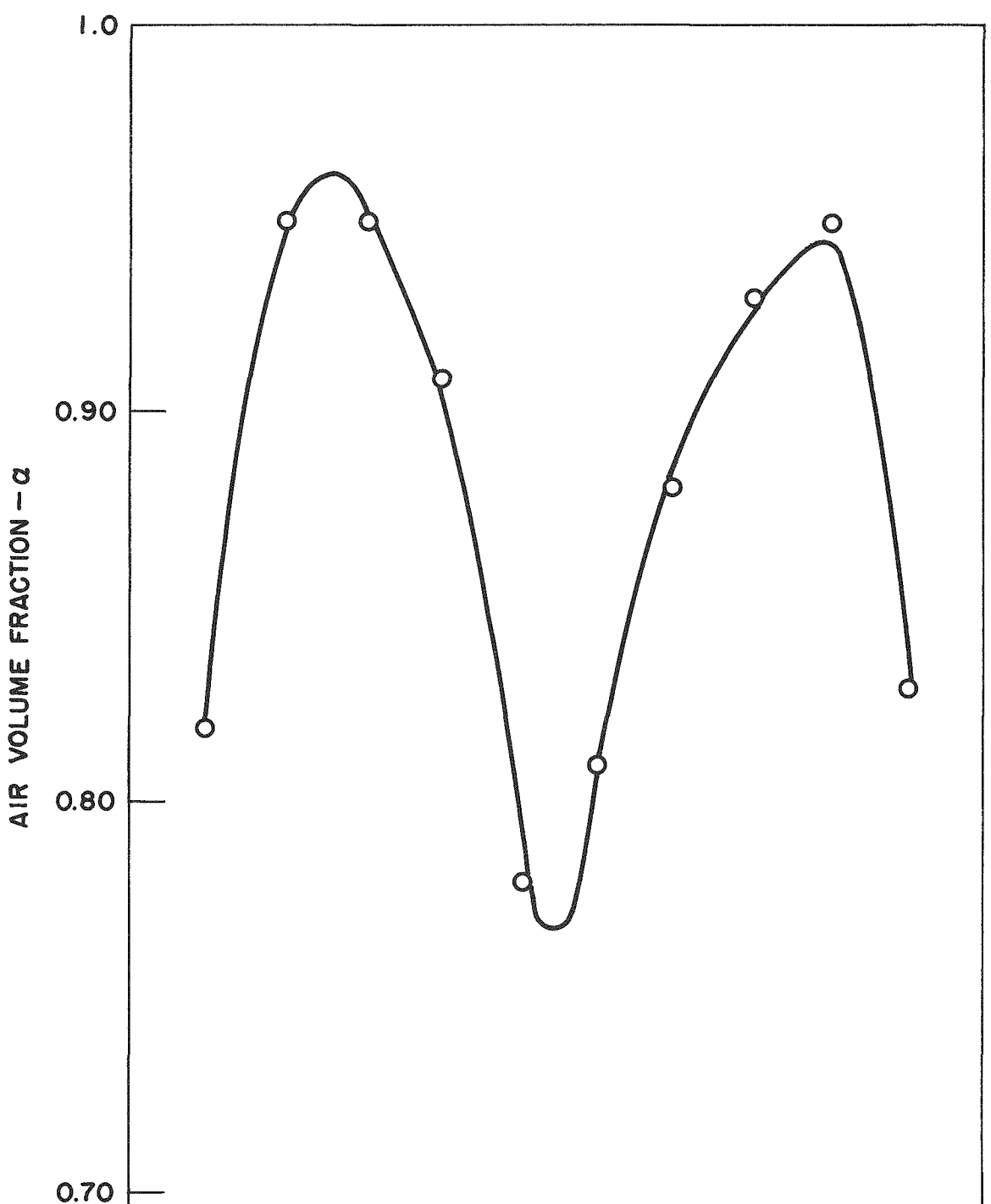

FIG. 4.16 AIR VOLUME FRACTION PROFILE AT A POSITION 4" BEYOND AN EXPANSION FROM A 1/8" SECTION TO A 1/2" SECTION

V. TWO-PHASE PRESSURE DROP STUDY

A. Introduction

Two-phase pressure drop is exceedingly more complex than single-phase pressure drop because of additional complicating factors, i.e., slippage between the two phases (relative velocity between liquid and vapor), interaction between the two phases, distribution of the phases in the conduit, etc.

Extensive experimental work has been carried out and several empirical and semi-empirical methods for calculating two-phase pressure drops have been published. The two most widely accepted methods are the Lockhart-Martinelli correlation and the friction-factor model. Because of the complexity of two-phase flow it is doubtful that a simple correlation for predicting two-phase pressure drop over all possible parameter ranges will be obtained as has been obtained for single-phase flow.

A comprehensive literature survey of two-phase flow has been published recently by Isbin[15] and Gresham;[16] therefore only selected references pertinent to this investigation are mentioned.

Visual studies have been made by a number of investigators[17-20] in an attempt to analyze the complexities of two-phase systems. Various flow patterns have been reported for both horizontal and vertical conduits; these can be categorized as follows:

(1) Bubble flow - Bubbles are dispersed in the liquid phase. The diameter of the bubble is a function of the mass of the two phases flowing.

(2) Plug or slug flow - Coalescence of the smaller bubbles into a large gaseous plug.

(3) Froth, churn, or turbulent flow - The gas phase is highly dispersed in the liquid phase and there is strong interaction between phases.

(4) Semi-annular - Unstable annular flow that periodically collapses down the conduit.

(5) Annular flow - Liquid film on the wall with a gaseous central core.

The flow patterns observed in vertical flow during the course of this investigation are shown in Fig. 5.1.

Several investigators have suggested that the frictional pressure drop of the two-phase flow should be related to the type of flow present. Based on his investigation, Alves[21] decided it was necessary to consider

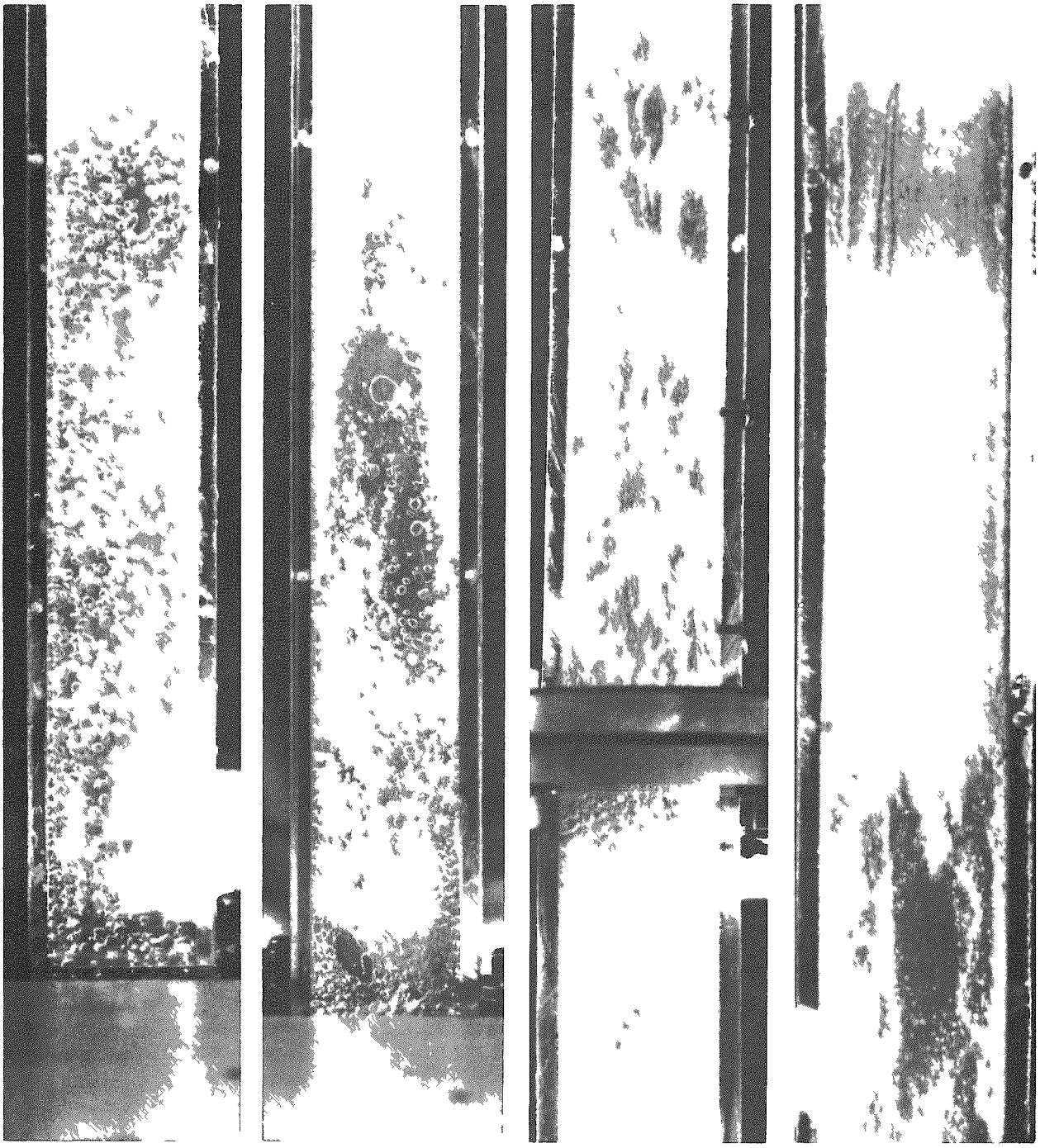

FIG. 5.1 VERTICAL FLOW PATTERNS

the flow pattern in order to predict the pressure drop. Radford[22] obtained different curves of the same general shape for various flow rates when plotting the pressure gradient vs. the exit air-water ratio. He also noted that various flow patterns were associated with certain portions of the curves and that the maximum pressure drop occurred in the froth-flow region.

As mentioned previously, the Lockhart-Martinelli correlation has become the most widely accepted method of calculating two-phase pressure drops. In the development of this correlation the authors did not account for the various flow patterns possible, but did attempt to incorporate various flow types by classifying the two phases individually as either turbulent or laminar. Impressive corroboration of this method of calculation can be found in numerous studies reported in the literature. Conversely, a number of investigators have also pointed out significant shortcomings.

Moen and Isbin[23] have demonstrated a sizeable mass flow rate parameter when plotting their data for steam-water mixtures in the form of Lockhart-Martinelli parameters. Johnson and Abou-Sabe[24] in their investigation with an air-water system showed that a more accurate correlation of their data could be obtained by introducing a liquid flow rate parameter. Gazley and Bergelin[25] concluded from their data on a 2-inch pipe that the Lockhart-Martinelli correlation was not adequate for stratified and wave flow. Baker[26] showed that the pipe diameter had an effect on the magnitude of the two-phase pressure drop. The data of Chisholm and Laird[27] for a rough tube show a strong effect of mass flow rate on a plot of the two-phase friction-factor multiplier vs. the vapor volume fraction. The highest pressure drop occurred with the lowest liquid mass flow rates and decreased with increasing liquid flow rate. However, their data for a smooth and galvanized tube did not show the same effect.

The data of Hoopes[28] on a vertical heated annulus with boiling flow showed a similar effect. Data for a 1/4-inch section were higher than for a 1/8-inch section when reduced to the Martinelli parameter (Φ_w^2) and plotted as a function of χ. No explanation was given. Thus, it appears that there is a definite mass flow rate parameter which is not adequately accounted for in the Lockhart-Martinelli correlation.

A number of other models and analytical treatments of two-phase flow have been presented in the literature.[29-31] In general, the basic assumptions of annular flow, no interaction between phases, etc., are essentially the same in each analytical treatment and represent an over-simplification of the actual physical picture. Although the analytical solutions have been helpful, their usefulness appears to be limited until a more thorough understanding of the interaction between phases and phase distribution is obtained.

Recently Lottes and Flinn[1] used a simple flow model to derive the following expressions for local two-phase pressure gradient, R, and the average two-phase friction factor, $\overline{R}$, over a boiling length:

$$R = \left(\frac{1 - X}{1 - \alpha}\right)^2 ; \tag{5.1}$$

$$\overline{R} = 1/3 \left[1\left(\frac{1 - X_e}{1 - \alpha_e}\right) + \left(\frac{1 - X_e}{1 - \alpha_e}\right)^2 \right] . \tag{5.2}$$

The derivation of Eqs. (5.1) and (5.2) is given in the Appendix. Their preliminary data for a 1/4-inch vertical rectangular channel with boiling showed fair agreement with the model, but the results were inconclusive. Therefore, a study of experimental two-phase flow pressure drop was undertaken to obtain additional information on the apparent mass flow parameter effect and to investigate the flow model of Lottes and Flinn, utilizing extensive local measurements of the liquid holdup.

B. Single-Phase Pressure Drop Results

A series of pressure drop runs were made on each rectangular section to obtain liquid-phase friction factors. The factors were required in the reduction of the two-phase pressure drop data to $\Delta P_{TP}/\Delta P_w$ ratios used in correlating the data. The channels were connected to an entrance cone which provided a smooth transition from the 4-inch pipe to the channel. Measurements of pressure drop were made over the last two feet of the channel; the initial two feet served as a calming section. The Reynolds number was varied (10,000 to 70,000) by adjusting the mass flow rate. The aspect ratio of the rectangular sections ranged from 2 (2 x 1-inch section) to 16 (2 x 1/8-inch section).

The calculated friction factors are compared with smooth tube factors in Fig. 5.2. The friction factors tend to separate for each channel geometry (aspect ratio), and individual lines with different slopes can be drawn to represent the data of each channel. The slopes of the lines were slightly less than the corresponding values for smooth tubes. Although the friction factor curves tended to separate with aspect ratio, there was a random orientation of the curves about the smooth tube function. Similar results were obtained by London[32] and Schiller,[33] who investigated a wide variety of geometries.

For all practical purposes the smooth-tube function adequately represented the data for all sections over the range of Reynolds Numbers studied. The maximum deviation of the data from smooth tube is +14% and -11%, with an average deviation of 6%.

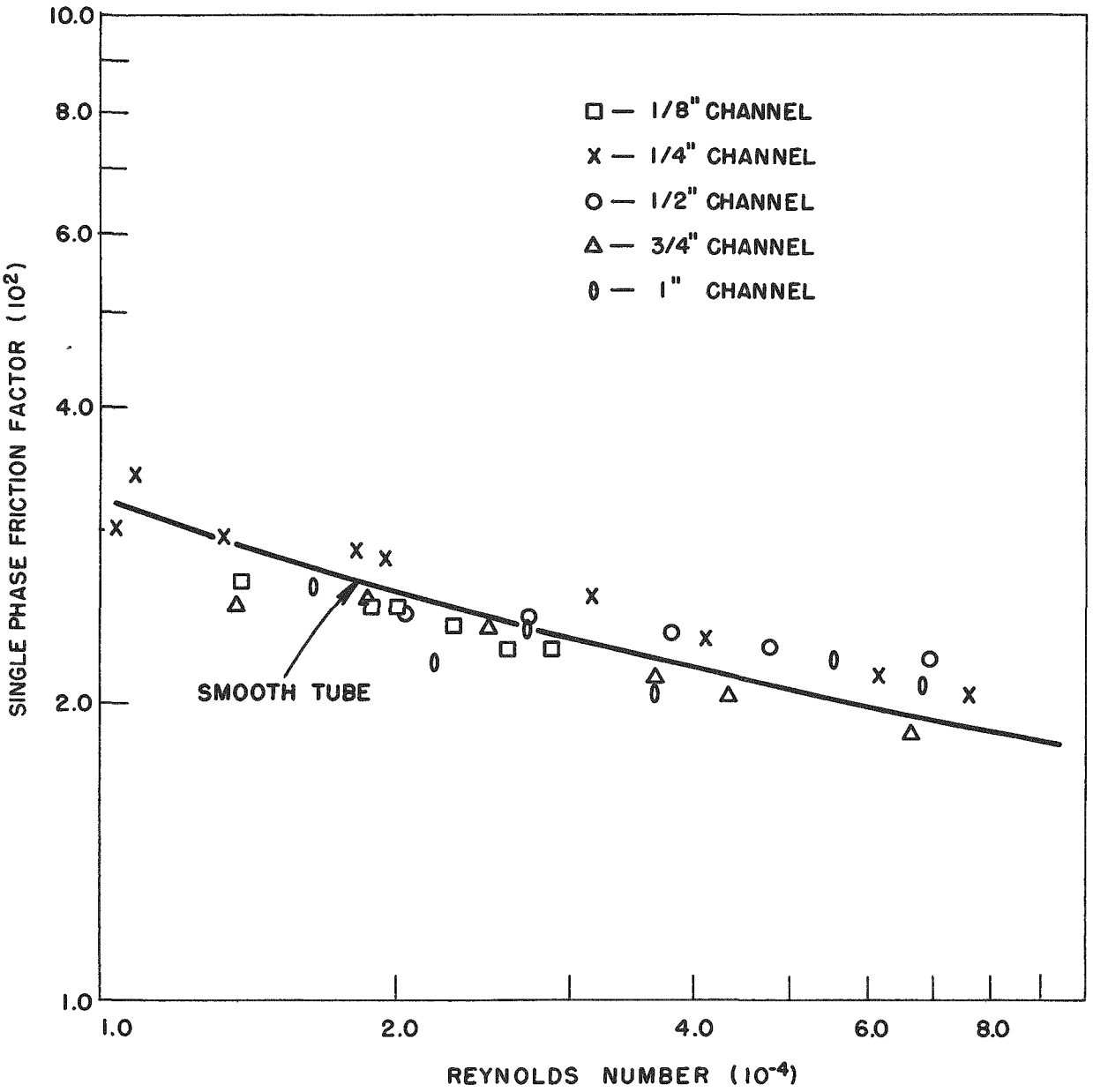

FIG. 5.2 SINGLE-PHASE FRICTION FACTORS VS. REYNOLDS NUMBER FOR RECTANGULAR CHANNELS WITH ASPECT RATIOS OF 2 TO 16.

C. Two-Phase Pressure Drop Results

1. Data Procurement and Reduction. The two-phase pressure drop data were obtained in three separate phases. The first set of data was taken in conjunction with the traversing vs. "one shot" void measurement study (see Section III). The major portion of the pressure drop data was obtained concurrently with the data on the effect of geometry changes on the air volume fraction. The balance of the data was procured in a separate set of pressure drop runs designed to study the mass flow rate effect in each channel.

The mass flow rate (G) was varied by either of two methods. In the first two series of runs, as described above, the total weight flow (W) was kept constant and the mass flow rate varied according to the cross-sectional area of each section. As a result, for the given section, the mass flow rate remained constant. In the third set of runs the mass flow rate was varied in each section by adjusting the total flow rate.

The ranges of variables studied were dictated primarily by interest in a specified range of the vapor volume fraction:

$$(X) = 0.00055 - 0.0043$$
$$(\alpha) = 0.20 - 0.75$$
$$(G) = 300{,}000 - 2{,}000{,}000 \text{ lb}/(\text{hr})(\text{ft}^2)$$
$$(D_e) = 0.24 \text{ to } 1.333 \text{ in.}$$

The limited range and magnitude of the quality studied is inherent with an air-water system at atmospheric pressure, due to the difference in specific volume for each component.

The reduction of two-phase pressure drop data in vertical flow was accomplished in the following manner. From the familiar mechanical energy balance, the pressure drop over a given length is

$$-\int_1^2 \frac{dP}{\rho_m} = \int_1^2 dL + \int_1^2 \frac{V dV}{g} + \int_1^2 dH_f \quad . \tag{5.3}$$

integrating,

$$P_1 - P_2 = \int_1^2 \rho_m \, dL + \int_1^2 \rho_m \frac{V dV}{g} + \int_1^2 \rho_m \, dH_f \quad . \tag{5.4}$$

For a two-phase mixture,

$$\rho_m = (1 - \alpha)\, \rho_w + \rho_g \ \alpha. \tag{5.5}$$

Since $\rho_w >> \rho_g$, Eq. (5.5) reduces, except when $\alpha \cong 1$, to

$$\rho_m = (1 - \alpha)\, \rho_w \quad . \tag{5.6}$$

Because the pressure drop data were taken only in portions of the section where α did not vary with length,

$$\int_1^2 \rho_m \, dL = \int_1^2 (1 - \alpha)\, \rho_w \, dL = (1 - \alpha)\, \rho_w \, L \quad . \tag{5.7}$$

For the same reason:

$$\int_1^2 \rho_m \frac{V dV}{g} = 0 \quad , \tag{5.8}$$

since the velocities of the two phases do not change. Therefore, Eq. (5.4) reduces to

$$P_1 - P_2 = (1 - \alpha)\, \rho_w \, L + \int_1^2 \rho_m \, dH_f \quad . \tag{5.9}$$

By definition,

$$\int_1^2 \rho_m \, dH_f = \Phi_w^2 \int_1^2 \rho_w \left(\frac{f_0 V_w^2}{2g\, D_e}\right) d\, L = \left(\frac{\Phi_w^2 \, V_w^2}{2g}\right) \left(\frac{L}{D_e}\right) \rho_w \quad , \tag{5.10}$$

where

$$\Phi_w^2 = \frac{\Delta P_{TP}}{\Delta P_w} \quad . \tag{5.11}$$

Substituting Eq. (5.10) into Eq. (5.9), and rearranging,

$$\Phi_w^2 = \frac{(P_1 - P_2) - (1 - \alpha)\, (\rho_w)\, (L)}{f_0 \left(\frac{V_w^2}{2g}\right) \left(\frac{L}{D}\right) \rho_w} \quad . \tag{5.12}$$

Examination of Eq. (5.12) shows that considerable scatter should be inherent in the calculated values of Φ_w^2 for the large equivalent diameter sections. The static head pressure drop approaches the total pressure drop in magnitude and, therefore, any slight error in the measurement of the air volume fraction α will produce a very large error in Φ_w^2. Ironically, the accuracy of void measurement also decreases with increased channel spacing. These observations were verified by the data of the one-inch by two-inch channel; it was impossible to obtain reliable pressure drop results that could be correlated with any degree of confidence. Further evidence of the anticipated increased scatter of the pressure drop results for the larger sections can be seen in Figs. 5.3 and 5.8. A definite decrease of scatter in the data is apparent as the equivalent diameter is reduced.

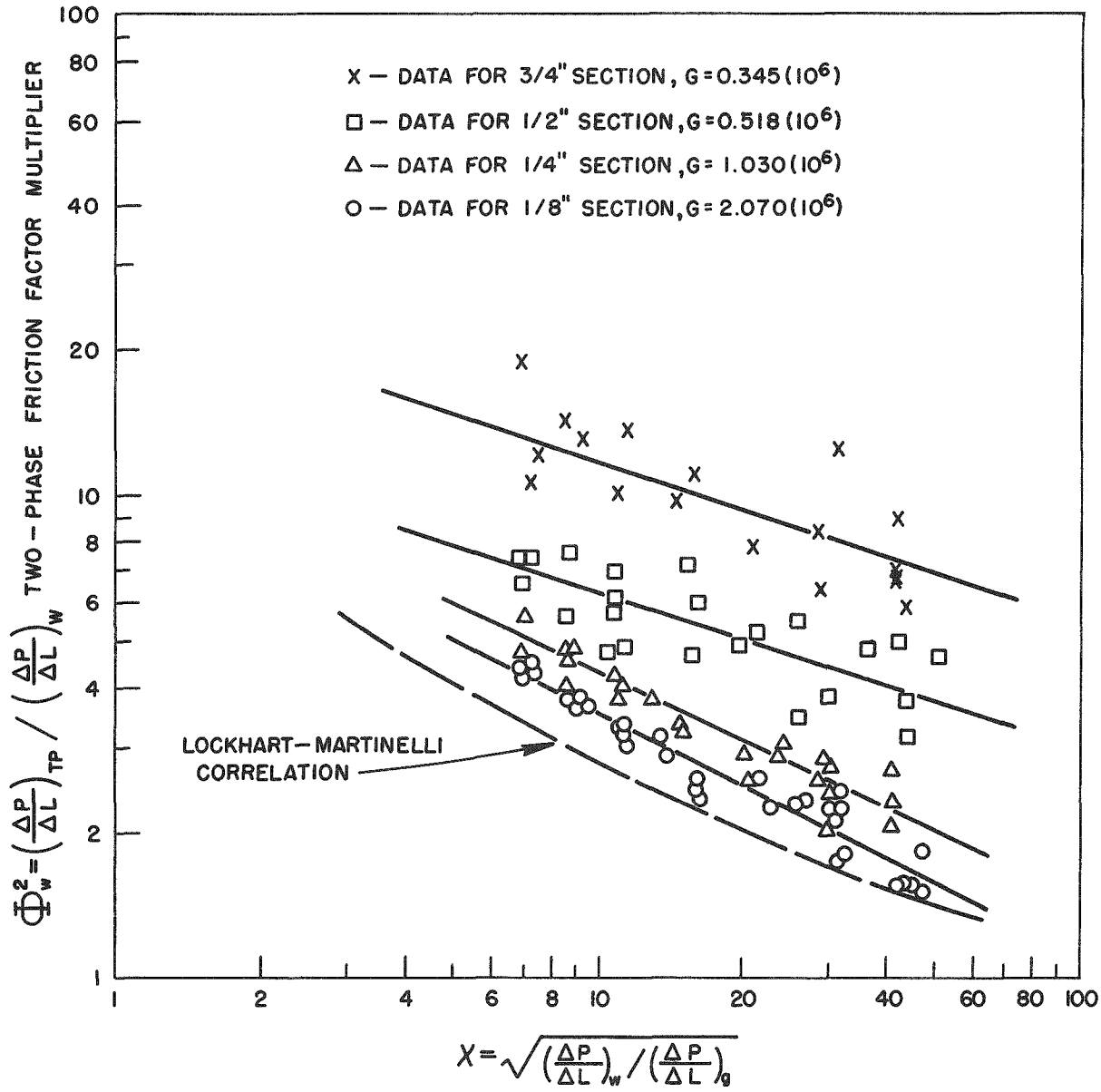

FIG. 5.3 COMPARISON OF PRESSURE DROP DATA WITH THE LOCKHART–MARTINELLI CORRELATION.

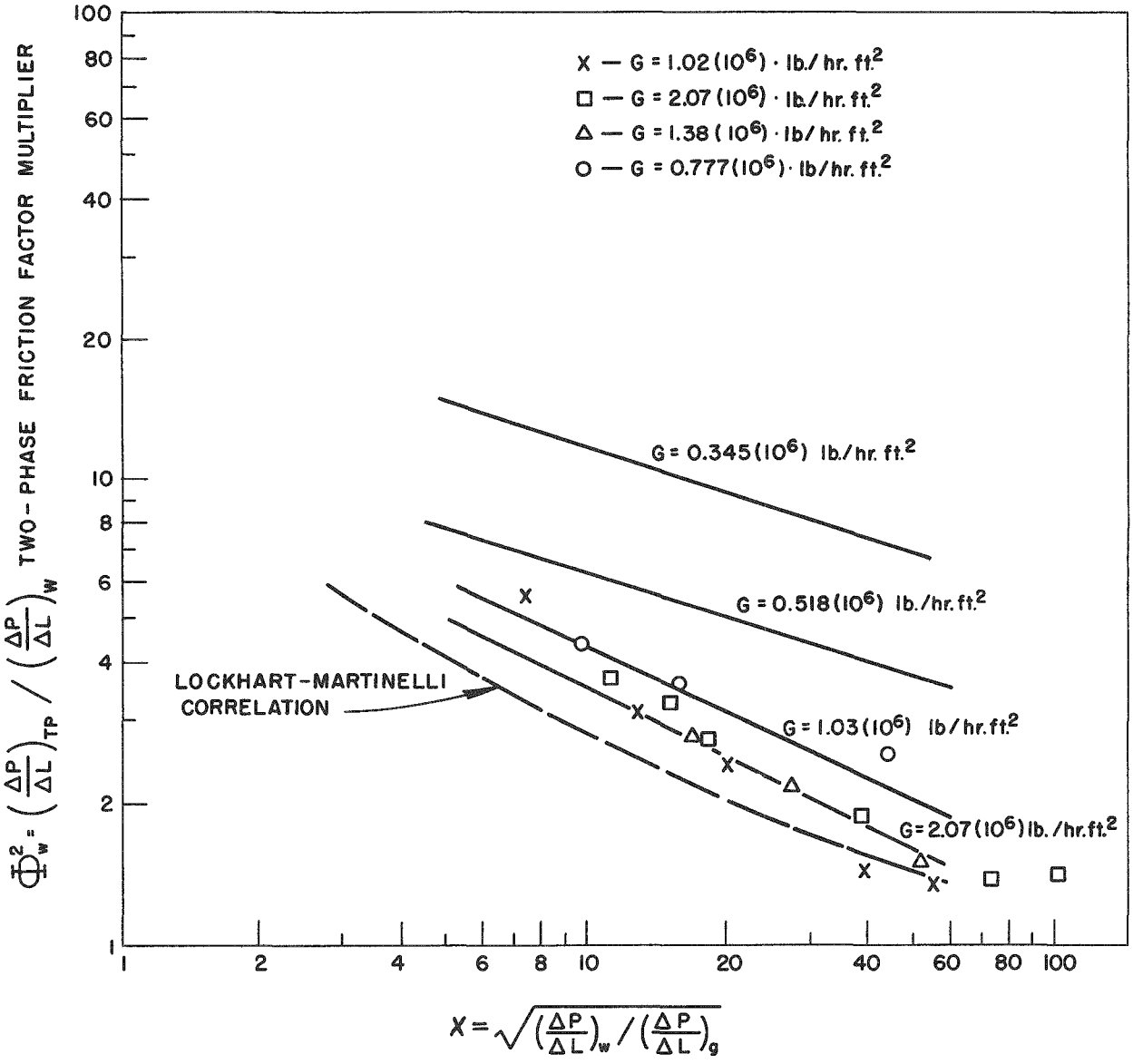

FIG. 5.4 EFFECT OF VARYING THE MASS FLOW RATE ON THE RELATIONSHIP BETWEEN THE TWO-PHASE FRICTION FACTOR MULTIPLIER AND THE LOCKHART – MARTINELLI FLOW PARAMETER, IN A 1/2" SECTION.

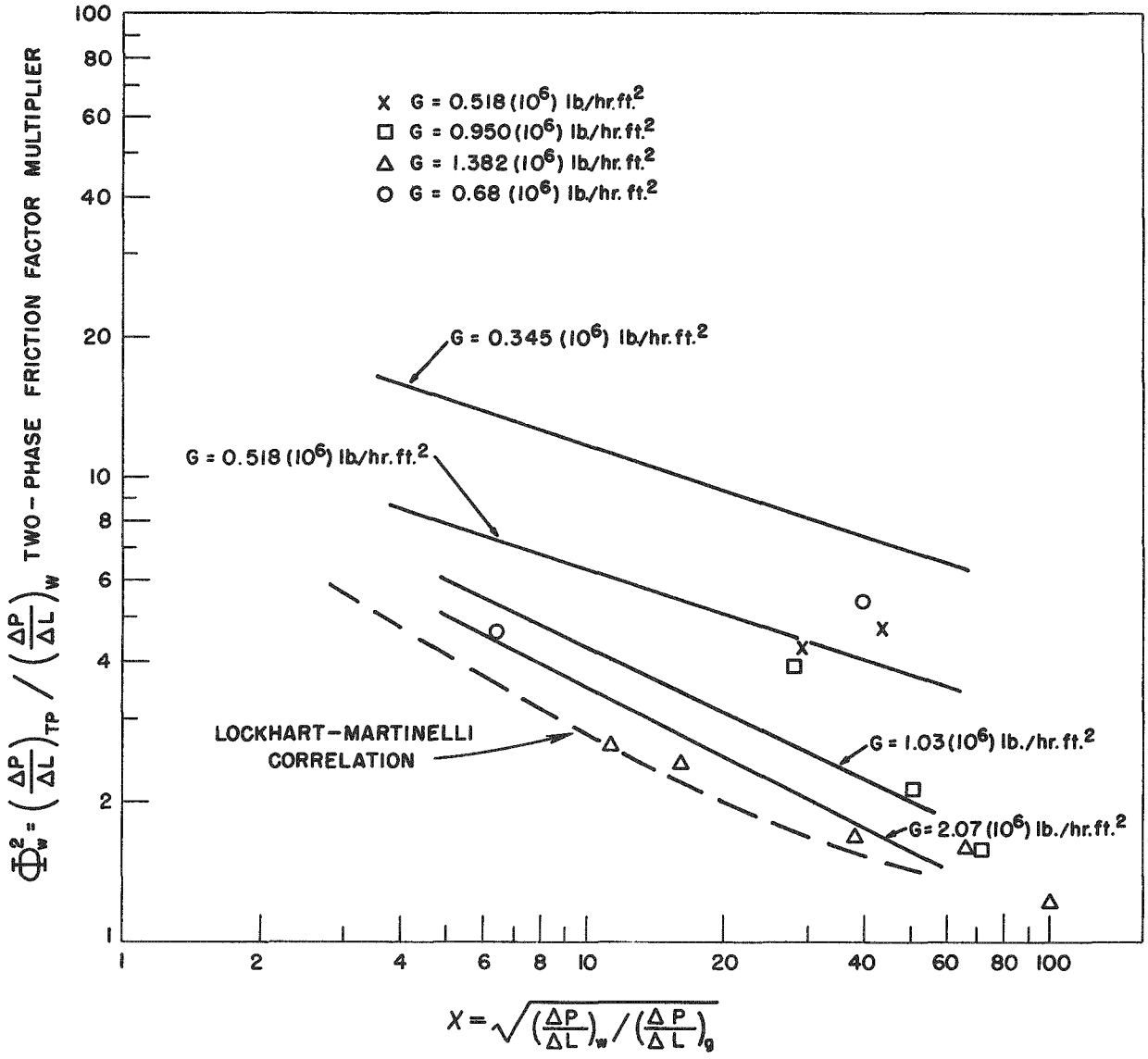

$$\Phi_w^2 = \left(\frac{\Delta P}{\Delta L}\right)_{TP} / \left(\frac{\Delta P}{\Delta L}\right)_w$$

$$X = \sqrt{\left(\frac{\Delta P}{\Delta L}\right)_w / \left(\frac{\Delta P}{\Delta L}\right)_g}$$

FIG. 5.5 EFFECT OF VARYING THE MASS FLOW RATE ON THE RELATIONSHIP BETWEEN THE TWO-PHASE FRICTION FACTOR MULTIPLIER AND THE LOCKHART-MARTINELLI FLOW PARAMETER, IN A 3/4" SECTION.

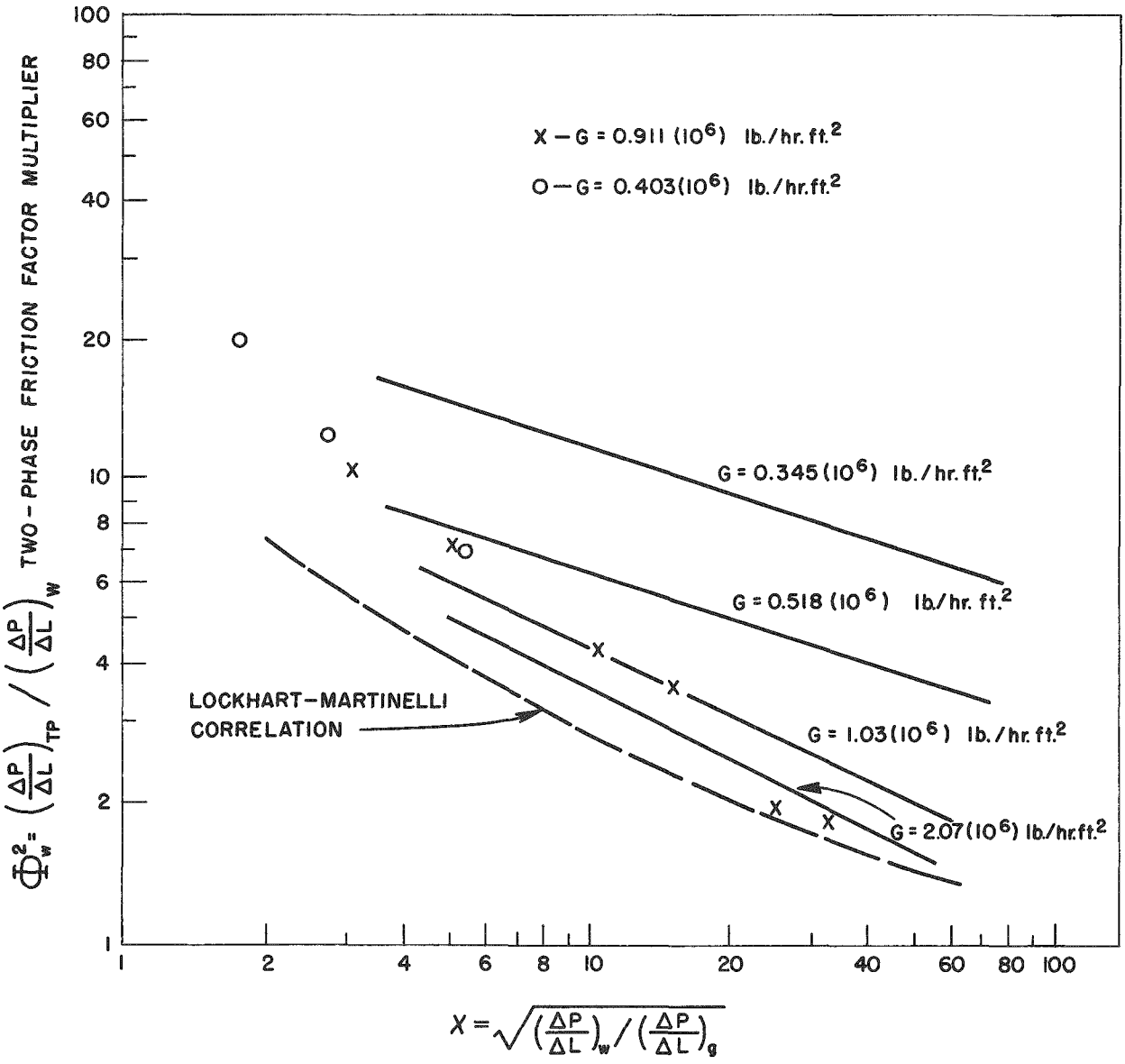

FIG. 5.6 EFFECT OF VARYING THE MASS FLOW RATE ON THE RELATIONSHIP BETWEEN THE TWO-PHASE FRICTION FACTOR MULTIPLIER AND THE LOCKHART-MARTINELLI FLOW PARAMETER, IN A 1/8" SECTION.

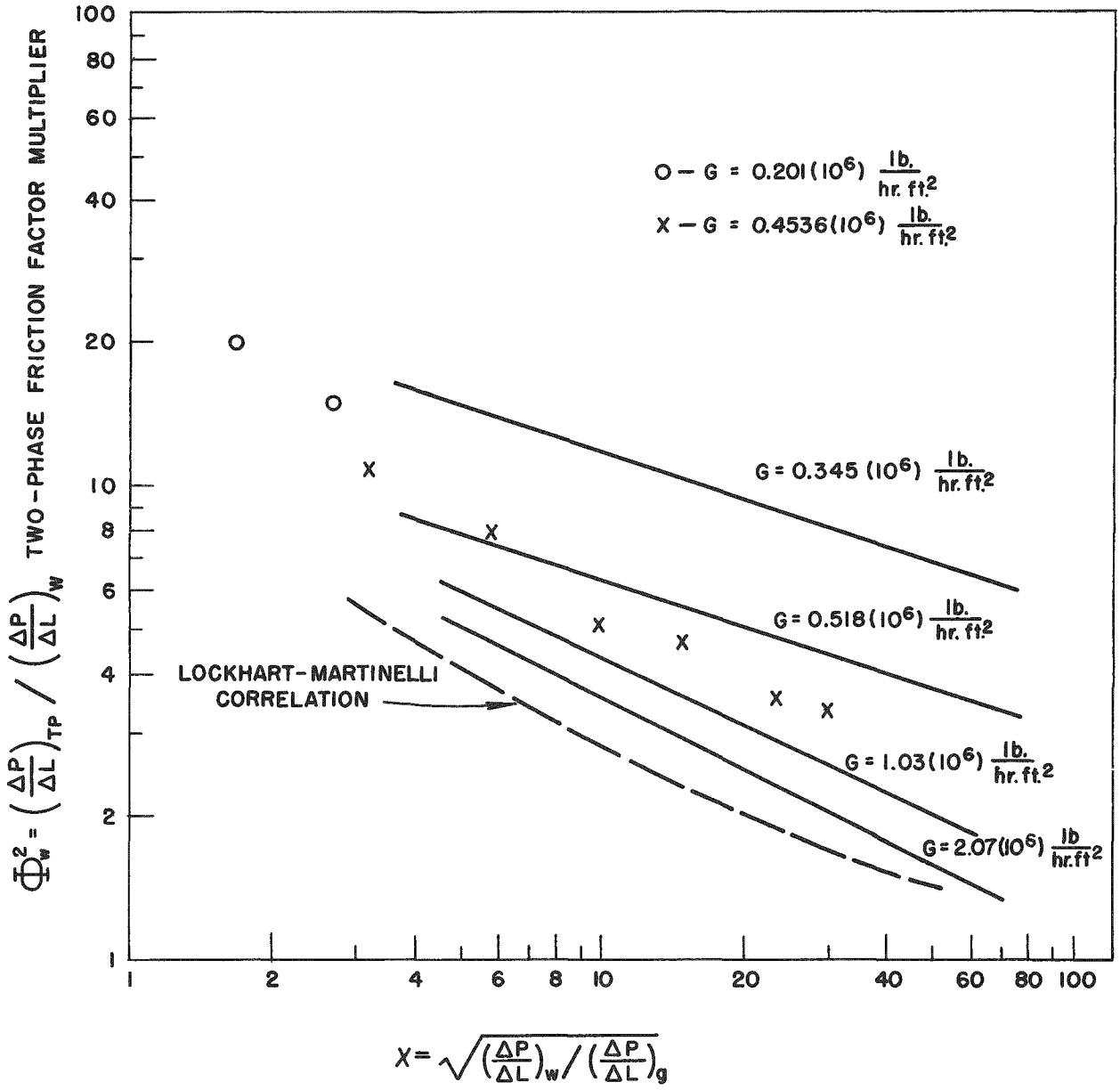

FIG. 5.7 EFFECT OF VARYING THE MASS FLOW RATE ON THE RELATIONSHIP BETWEEN THE TWO-PHASE FRICTION FACTOR MULTIPLIER AND THE LOCKHART—MARTINELLI FLOW PARAMETER, IN A 1/4" SECTION.

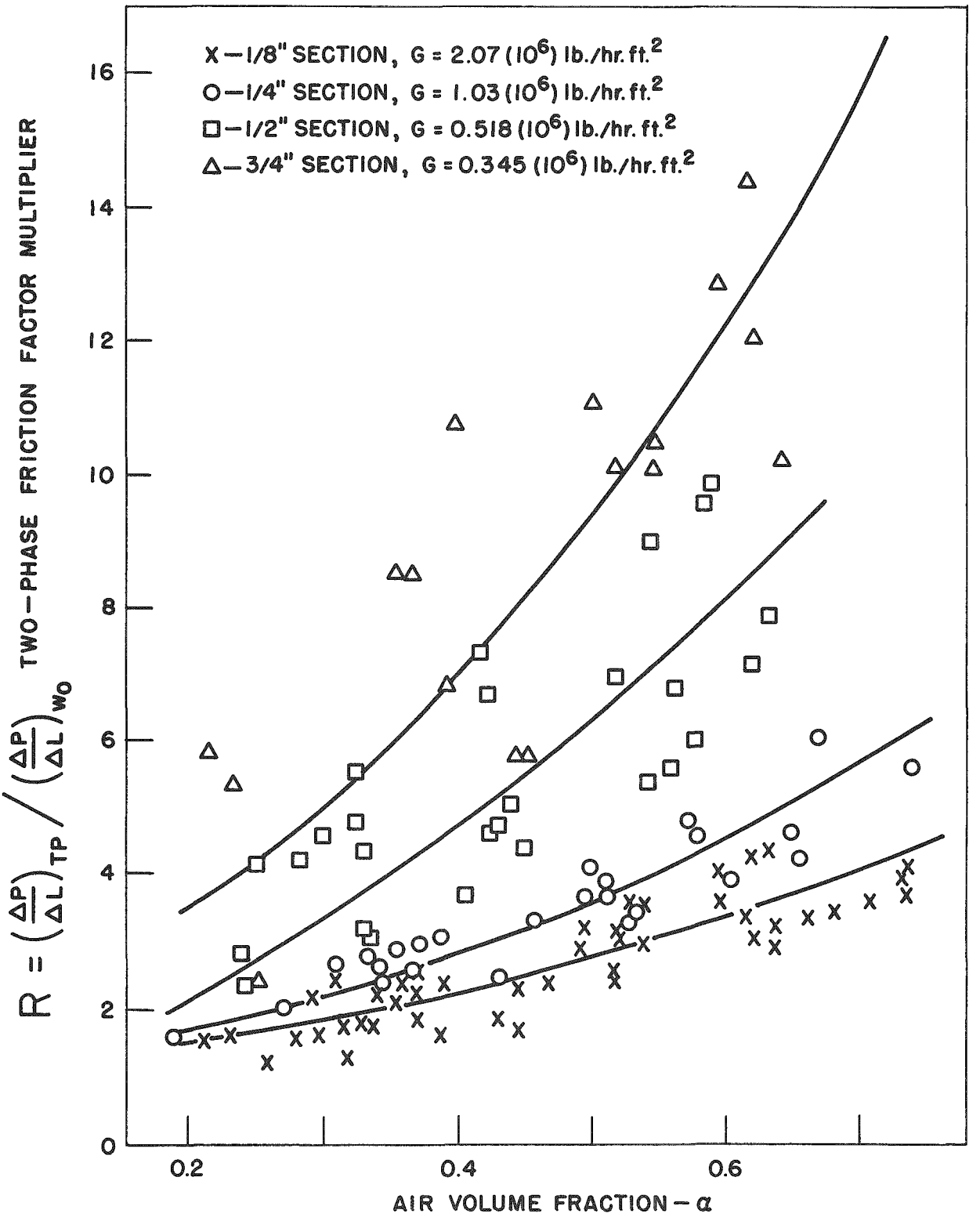

FIG. 5.8 TWO-PHASE FRICTION FACTOR MULTIPLIER VS THE AIR VOLUME FRACTION

2. Comparison of Two-Phase Pressure Drop Data With Martinelli, et al.

In the Lockhart-Martinelli correlation for two-phase frictional pressure drop data[34] each phase was classified into flow types (either turbulent or viscous), and a series of parameters were derived that were used in correlating the various two-phase flow combinations possible, i.e., liquid phase turbulent, gaseous phase viscous, etc.

The parameters are:

$$\Phi_w^2 = \frac{\left(\frac{\Delta P}{\Delta L}\right)_{TP}}{\left(\frac{\Delta P}{\Delta L}\right)_w} \quad ; \tag{5.13}$$

$$\Phi_g^2 = \frac{\left(\frac{\Delta P}{\Delta L}\right)_{TP}}{\left(\frac{\Delta P}{\Delta L}\right)_g} \quad ; \tag{5.14}$$

$$\chi^2 = \frac{\left(\frac{\Delta P}{\Delta L}\right)_w}{\left(\frac{\Delta P}{\Delta L}\right)_g} \quad . \tag{5.15}$$

The parameter χ can be shown to be a function of the physical properties and flow rates; it reduces to

$$\chi = \left(\frac{G_w}{G_g}\right)^{\frac{2-n}{2}} \left(\frac{\rho_g}{\rho_w}\right)^{0.5} \left(\frac{\mu_w}{\mu_g}\right)^{\frac{n}{2}} \quad , \tag{5.16}$$

where n is the exponent of the Reynolds number in the familiar expression for the friction factor:

$$f = \frac{C}{(N_{Re})^n} \quad . \tag{5.17}$$

From the single-phase data as shown in Fig. 5.2 the exponent n was taken to be 0.25. Therefore:

$$\chi = \left(\frac{G_w}{G_g}\right)^{0.875} \left(\frac{\rho_g}{\rho_w}\right)^{0.5} \left(\frac{\mu_w}{\mu_g}\right)^{0.125} \quad . \tag{5.18}$$

A plot of Φ_w^2 vs. χ is shown in Fig. 5.3 for the first two sets of data (mass flow rate varied with geometry). A very pronounced separation occurred with respect to channel geometry. As the mass flow rate decreased (large channels), the two-phase friction factor multiplier increased. The data for the 1/8-inch section showed good agreement with the Martinelli correlation for the turbulent viscous flow, which is the same type of flow obtained in the test sections.

The third set of pressure drop data was taken in an effort to determine whether the separation was due to an effect of geometry or to a mass flow rate phenomenon. The mass flow rates were varied in each section. The results are shown in Figs. 5.4 to 5.7. Figures 5.4 and 5.5 show a definite decrease of the two-phase friction factor multiplier, Φ_w^2, with increasing mass flow rate for the 1/2 and 3/4-inch sections. The data for the different mass flow rates tended to fall on and near the lines of equivalent mass flow rates shown in Fig. 5.3.

When the mass flow rate was reduced in the 1/8-inch and 1/4-inch sections, the factor Φ_w^2 increased as shown in Figs. 5.6 and 5.7. The data again tended to follow the same mass flow rate pattern as shown in Fig. 5.3.

The results obtained by the two different methods of varying the mass flow rate tended to prove that the observed separation phenomenon is due to a mass flow rate effect and not to a geometry factor. However, a more comprehensive experimental program will be required to substantiate this conclusion, since the scope of the latter set of pressure drop runs was limited in the range of variables investigated and number of runs.

Thus the Martinelli correlation is inadequate for predicting vertical flow, two-phase pressure drop over wide ranges of flow rate, particularly at the lower flow rates. However, the correlation appears to hold well at the higher mass flow rates [$G > 10^6$ lb/(hr) (ft^2)]. It should be noted that the majority of the experimental data used in developing the original Martinelli correlation, and the subsequent corroborating data, was obtained in horizontal conduits. This eliminated the necessity of evaluating the two-phase hydrostatic head which is inherent in vertical flow pressure-drop measurements.

It is conceivable that the mass flow rate effect may be more pronounced for vertical flow than for horizontal flow. Although the same basic flow patterns have been observed in both horizontal and vertical flow, the effect of gravity on phase distribution and interaction between phases will be different in each case, and thus the pressure drop characteristics would be somewhat different.

Visual observations during the course of the experimental investigation tended to show a relationship between flow pattern and pressure drop. Different flow patterns and varying degrees of turbulence and interaction between phases were noted with each section and varying mass flow rates. For example, turbulent or churn patterns were observed in the 1/2-inch and 3/4-sections with low mass flow rates. As the mass flow rate was increased, the flow pattern changed to a highly dispersed bubble flow (small diameter air bubbles). The factor Φ_w^2 decreased sharply when the flow pattern changed. The reverse effect was obtained with the 1/8-inch and 1/4-inch sections. As the mass flow rate was reduced, the flow patterns changed from a semi-annular to a wavy-type flow where there was considerably more interaction between phases and, as expected, the frictional pressure drop increased.

Since the flow patterns occurring in two-phase flow have been shown to be related to the mass velocity of each phase, it is possible that the mass flow rate effect is indirectly related to the flow patterns.

3. Correlation of Data With Air Volume Fraction. In a recent paper, Lottes and Flinn[1] presented two-phase pressure drop data for boiling water in a vertical rectangular channel; they correlated the data as a function of the vapor volume fraction (α). They postulated a simple flow model which attributed the higher frictional pressure drops of two-phase flow primarily to the drag of the increased liquid velocity, due to the presence of the vapor phase. For constant values of the vapor volume fraction the ratio of the two-phase to single-phase pressure drop is given by:

$$R = \left(\frac{1 - X}{1 - \alpha}\right)^2 \quad . \tag{5.19}$$

Therefore the data obtained in this study was plotted as R vs α in Fig. 5.8. The same type of separation occurred with mass flow rate as noted previously when using the Martinelli parameters. Comparison with the theoretical R function as given by Eq. (5.19) is shown in Fig. 5.9. There is close agreement between the theoretical R and the experimental R for the 1/4-inch and the 1/8-inch sections for $\alpha < 0.5$. As α becomes greater than 0.5, the theoretical R approaches the experimental R values for the 1/2-inch section. Thus the simple flow model of Lottes and Flinn does not hold over wide ranges and its use appears to be limited.

The pressure drop data in which the mass flow rate was varied in each section were also plotted as R vs α. Essentially the same results were obtained (Figs. 5.10 to 5.13). As the mass flow rate in the larger channels was increased, the two-phase friction factor multiplier R decreased; as the mass flow rate in the smaller channels was reduced, R increased.

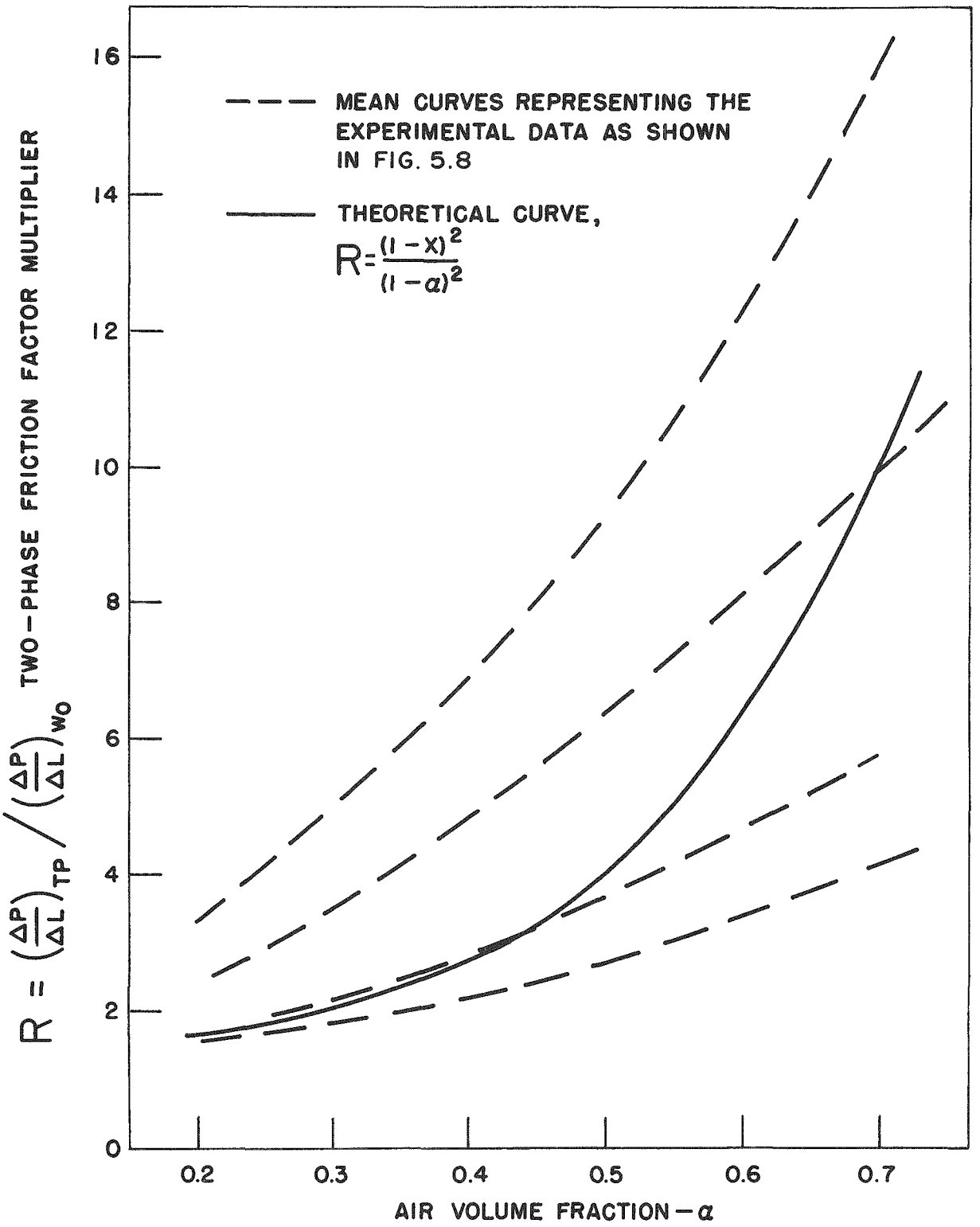

FIG. 5.9 COMPARISON OF THE EXPERIMENTAL AND THEORETICAL TWO-PHASE FRICTION FACTOR MULTIPLIER

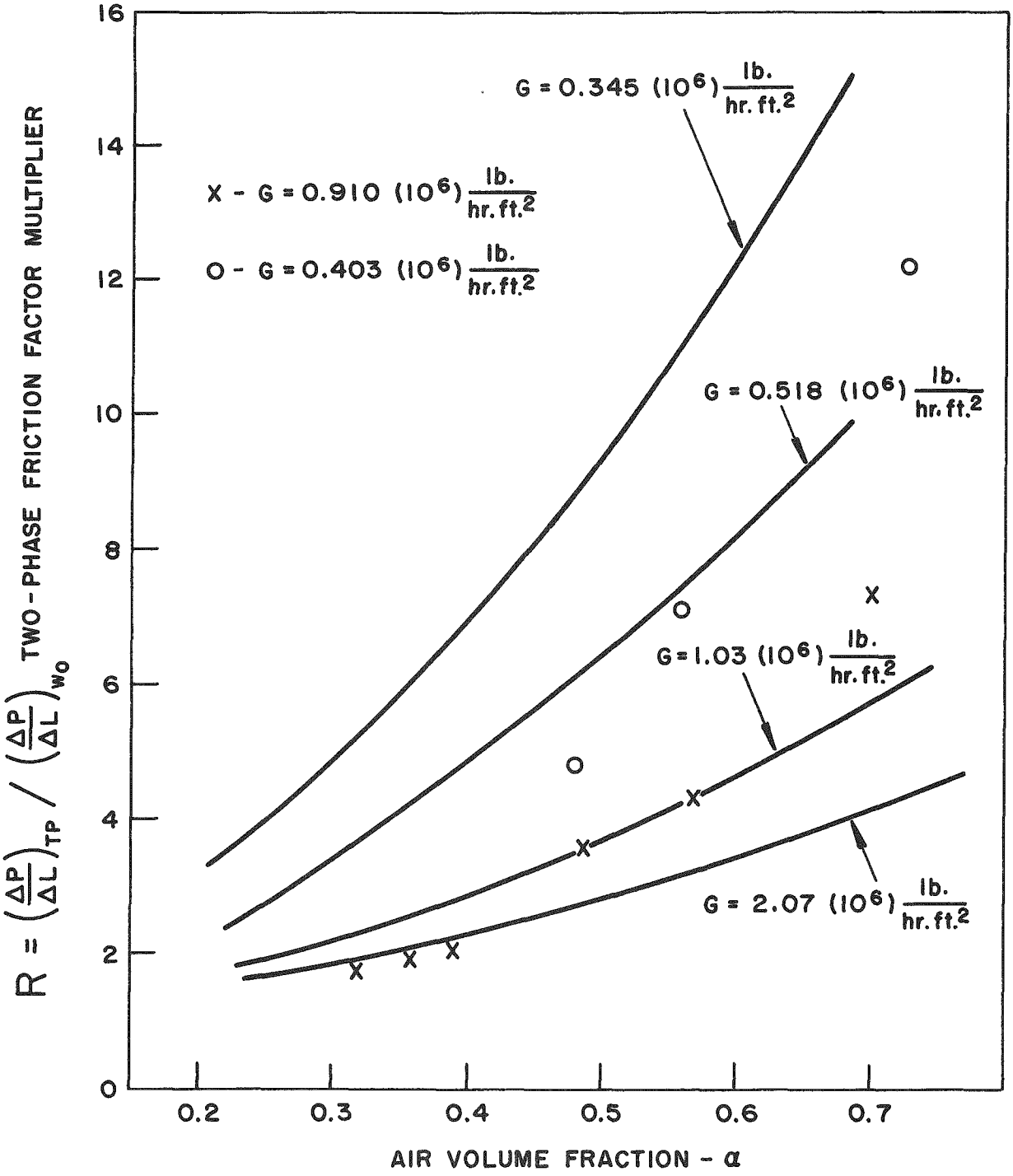

FIG. 5.10 EFFECT OF VARYING THE MASS FLOW RATE ON THE RELATIONSHIP BETWEEN THE TWO-PHASE FRICTION FACTOR MULTIPLIER AND THE AIR VOLUME FRACTION IN A 1/8" SECTION

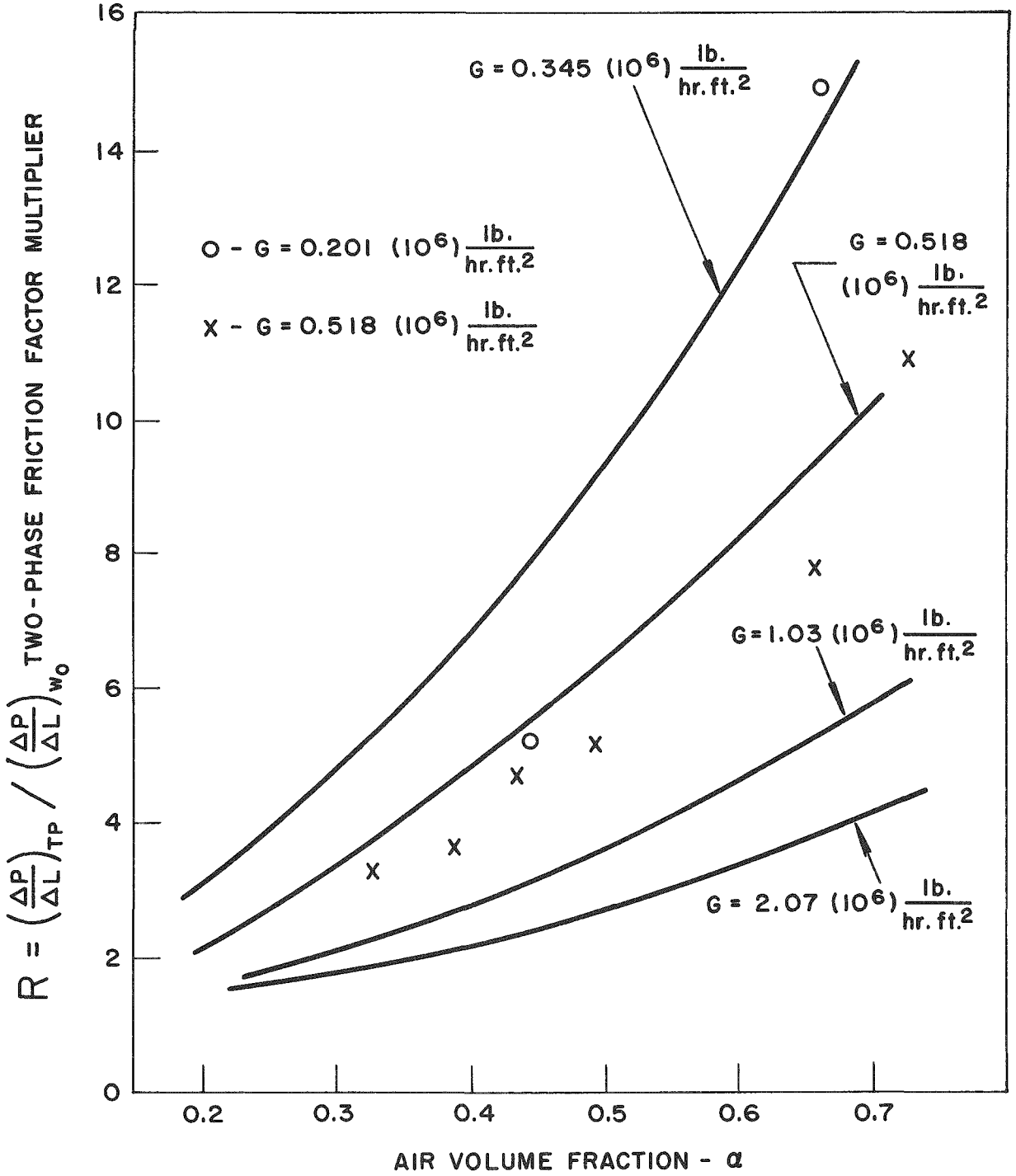

FIG. 5.11 EFFECT OF VARYING THE MASS FLOW RATE ON THE RELATIONSHIP BETWEEN THE TWO-PHASE FRICTION FACTOR MULTIPLIER AND THE AIR VOLUME FRACTION IN A 1/4" SECTION

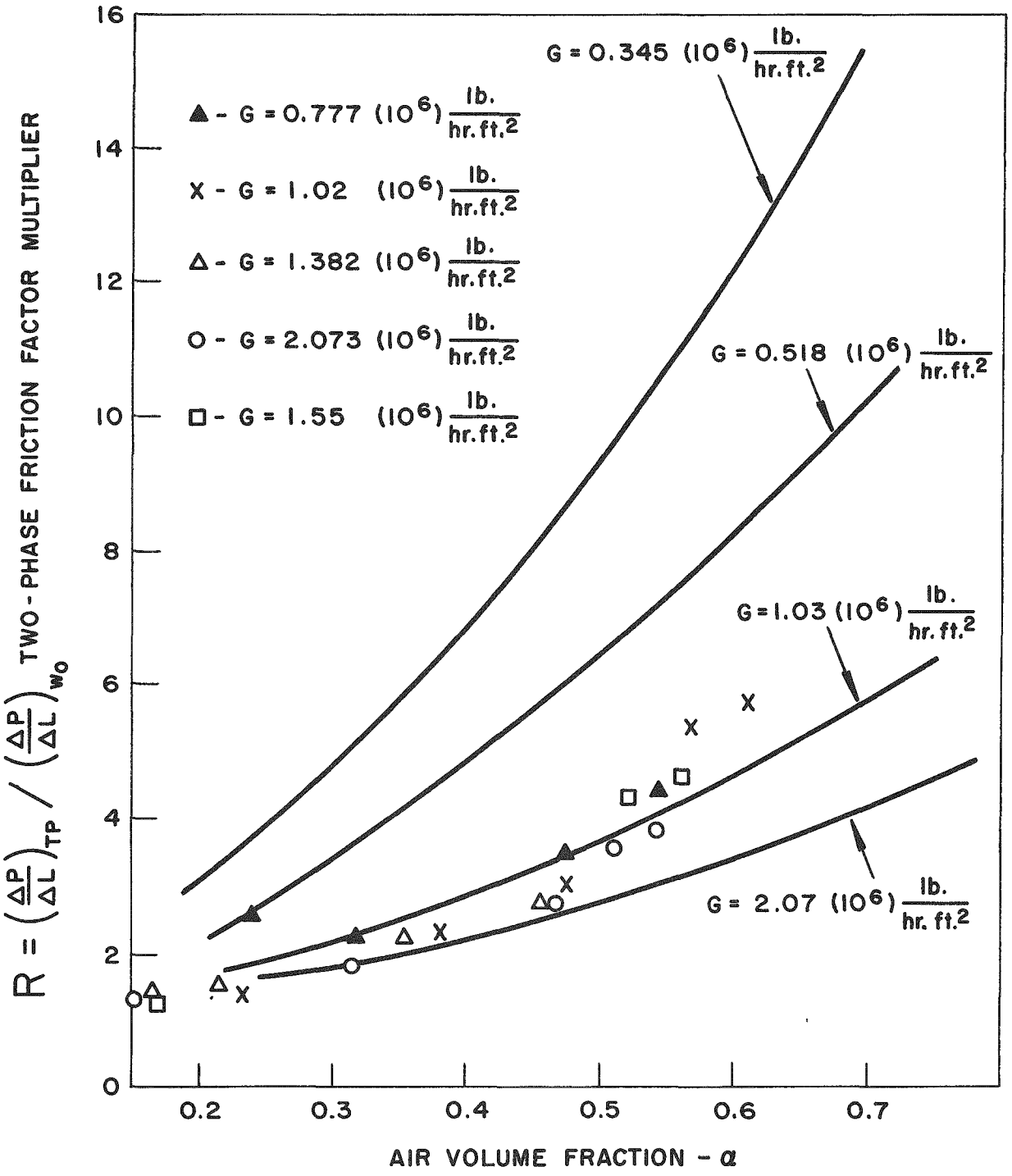

FIG. 5.12 EFFECT OF VARYING THE MASS FLOW RATE ON THE RELATIONSHIP BETWEEN THE TWO-PHASE FRICTION FACTOR MULTIPLIER AND THE AIR VOLUME FRACTION IN A 1/2" SECTION

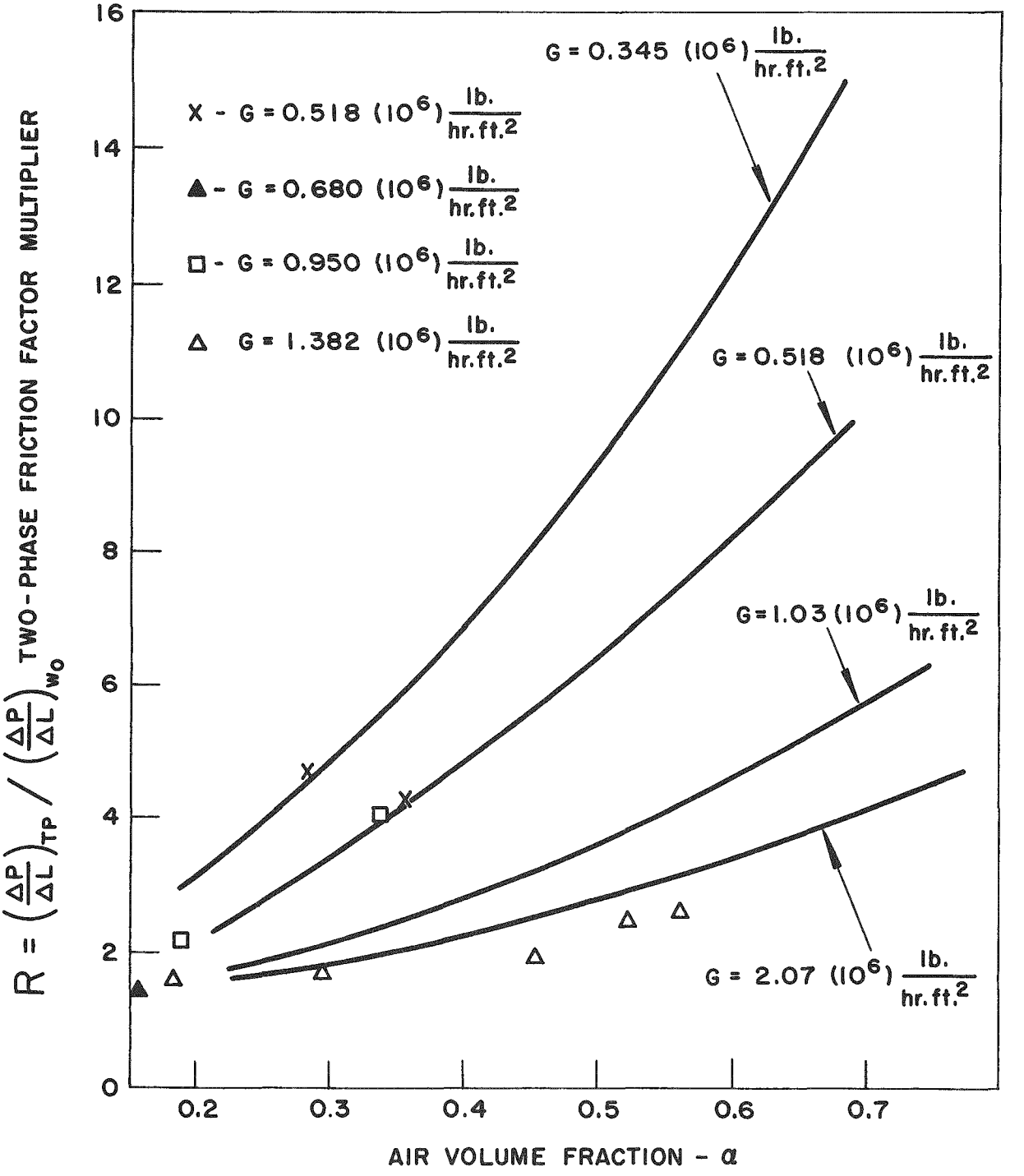

FIG. 5.13 EFFECT OF VARYING THE MASS FLOW RATE ON THE RELATIONSHIP BETWEEN THE TWO-PHASE FRICTION FACTOR MULTIPLIER AND THE AIR VOLUME FRACTION IN A 3/4" SECTION

VI. CONCLUSIONS

The following conclusions can be drawn from this experimental investigation, and are listed according to the appropriate Section headings.

Section III: Radiation Attenuation Method of Measuring the Density of a Two-Phase Fluid

1. Lucite mock-up studies have shown that the radiation attenuation method is a simple, accurate technique for obtaining local density measurements of two-phase fluids.
2. The "one-shot" method can be used for measuring the densities of two-phase fluids in narrow rectangular channels (spacing <0.5 in.).
3. The traversing technique is a more accurate method of measuring the densities of two-phase fluids and can be used for wide rectangular channels.
4. Phase distributions can be accurately obtained by the traversing technique.

Section IV: Effect of Flow Area Changes on Two-Phase Fluid Density

1. The void volume fraction, and hence density, of an air-water mixture changes during an expansion and a contraction. The magnitude of the change at atmospheric pressure can be estimated by the following equation.

$$\alpha_2 = \frac{1}{\frac{\frac{P_2}{P_1}\left(\frac{1}{\alpha_1}\right)}{\left(\frac{A_1}{A_2}\right)^{0.2}} + 1}$$

2. The relative velocity of a two-phase (air-water) fluid is a function of water velocity and the mixture quality.
3. The length of the transition zone following an expansion is a function of quality, mass flow rate and the area ratio.
4. The transition zone following a contraction is not as pronounced as for an expansion and is also a function of the quality, mass flow rate and area ratio.
5. The distribution of the air phase in the water phase was parabolic in nature, but the ratio of $\alpha_{max}/\alpha_{avg}$ which characterizes the distribution varied at random.

Section V: Two-Phase Pressure Drop Study

1. The isothermal single-phase friction factors for rectangular channels with aspect ratios of 2 to 16 are represented by the smooth-tube function as given on the Moody friction factor plot with a maximum deviation of +14% and -11%, and an average deviation of 6%.

2. The Lockhart-Martinelli correlation does not adequately predict two-phase pressure drop for mass flow rates $G < 10^6$ lb/(hr)(ft^2).

3. The two-phase friction factor multiplier Φ_w^2 or R is a function of the mass flow rate.

4. The mass flow rate effect on the two-phase pressure drop is related to the flow pattern existing in the two-phase fluid.

5. The proposed flow model of Lottes and Flinn does not adequately correlate the two-phase pressure drop data over wide ranges of mass flow rate.

APPENDIX

DERIVATION OF THEORETICAL TWO-PHASE FRICTION FACTOR MULTIPLIER

The flow model proposed by Lottes and Flinn[1] is one where most of the liquid phase is in contact with the channel walls and most of the steam is flowing down a central core. This essentially is the same as the Martinelli flow model for turbulent flow of both the liquid and vapor phases. The difference in the method of describing the behavior is that the present flow model is discussed on a steam volume fraction basis rather than on a steam weight flow fraction basis. It is proposed that the friction of the mixture may be found by calculating the frictional drag of the water phase along the channel wall, taking into account the change in velocity of the water phase along the channel:

$$\Delta P_{TP} = \frac{f\ \rho_w}{2g\ D_e} \int V_w^2\ dL \quad . \tag{1}$$

From a mass balance, the inlet velocity is related to the local liquid velocity by the equation

$$\frac{V_w}{V_{w_0}} = \frac{1 - X}{1 - \alpha} \quad . \tag{2}$$

Defining an isothermal local two-phase friction factor multiplier as

$$R = \left(\frac{\Delta P_{TP}}{\Delta P_0}\right) \quad , \quad , \tag{3}$$

substituting Eq. (2) into Eq. (1), and combining with Eq. (3),

$$R = \left(\frac{1 - X}{1 - \alpha}\right)^2 \quad . \tag{4}$$

As shown in Section IV, from a mass balance

$$\frac{V_g}{V_w} = \left(\frac{X}{1 - X}\right)\left(\frac{1 - \alpha}{\alpha}\right)\frac{\rho_w}{\rho_g} \quad . \tag{5}$$

For boiling water in a channel of uniform heat addition, if it is assumed that the slip ratio is independent of boiling length, steam voids, power density and quality, Eqs. (2) and (5) may be combined to give

$$\frac{V_w}{V_{w_0}} = 1 + \left(\frac{\rho_w V_w}{\rho_g V_g} - 1 \right) X \quad . \tag{6}$$

By assuming a constant slip ratio and constant pressure in Eq. (5), the slip ratio V_g/V_w is a linear function of X; for the case of uniform heat generation it will also be a linear function of channel length.

Define an average two-phase friction factor multiplier as

$$\overline{R} = \frac{\Delta P_{TP}}{\Delta P_0} \quad , \tag{7}$$

where $\overline{R}$ is the ratio of frictional pressure drop over the boiling length to the frictional drop over the same channel at the same mass flow rate with no boiling. Under these conditions Eqs. (1) and (7) may be combined to give

$$\overline{R} = \frac{1}{L} \int_0^L \left(\frac{V_w}{V_{w_0}} \right)^2 dL \quad . \tag{8}$$

Since the liquid velocity is linear with length, Eq. (8) becomes

$$\overline{R} = \frac{1}{L_T V_{w_0}^2} \int_0^{L_T} \left[V_{w_0} + (V_{w_e} - V_{w_0}) \frac{L}{L_T} \right]^2 dL \quad , \tag{9}$$

where V_{w_e} is the liquid velocity at the exit of the channel and L/L_T is the position in the boiling channel.

Upon simplification, Eq. (9) reduces to

$$\overline{R} = \frac{1}{3} \left[1 + \frac{V_{w_e}}{V_{w_0}} + \left(\frac{V_{w_e}}{V_{w_0}} \right)^2 \right] \quad . \tag{10}$$

Combining Eq. (2) and (10),

$$\overline{R} = \frac{1}{3} \left[1 + \left(\frac{1 - X_e}{1 - \alpha_e} \right) + \left(\frac{1 - X_e}{1 - \alpha_e} \right)^2 \right] \tag{11}$$

It is interesting to note that by definition

$$R = \left(\frac{1 - X}{1 - \alpha}\right) = \Phi_w^2 (1 - X)^2 \quad . \tag{12}$$

Since the quality range studied in this experimental investigation is so small, Eq. (12) becomes

$$R = \Phi_w^2 \tag{13}$$

BIBLIOGRAPHY

(1) Lottes, P. A. and W. S. Flinn. "A Method of Analysis of Natural Circulation Boiling Systems," Nuclear Science and Engineering, Vol. 1, No. 6, (December 1956).

(2) Grace, H. P. and C. E. Lapple. "Discharge Coefficients of Small-Diameter Orifices and Flow Nozzles," Trans. ASME (July, 1951).

(3) Cook, W. H. "Boiling Density in Vertical Rectangular Multi-channel Sections with Natural Circulation," ANL-5621 (November, 1956).

(4) Egen, R. A., D. A. Dingee, and J. W. Chastain. "Vapor Formation and Behavior in Boiling Heat Transfer," BMI-1163 (February 4, 1957).

(5) Hooker, H. H. and G. F. Popper. "A Gamma-Ray Attenuation Method for Void Fraction Determination in Steam-Water Mixtures," ANL-5766 (To be published).

(6) Behringer, P. "Velocity in Rise of Steam Bubbles in Boiler Tubes," Verein deutscher Inginieure, Forschungsheft 365B, 4 (1934).

(7) Marchaterre, J. F. "Effect of Pressure on Boiling Density in Multiple Rectangular Channels," ANL-5522 (February, 1956).

(8) Schurig, W. "Water Circulation in Boilers and Movement of Liquid Gas Mixture in Tubes," Verein deuscher Inginieure, Forschungsheft 365B, 13 (1934).

(9) Lottes, P. A., W. S. Flinn, R. J. Weatherhead, and M. Petrick. "Natural Circulation Boiling Studies," ANL-5735 (To be published)

(10) Dengler, C. E. "Heat Transfer and Pressure Drop for Evaporation of Water in a Vertical Tube," Unpublished Sc. D. Thesis, Massachusetts Institute of Technology (1952).

(11) Eddy, K. D. "Pressure Ratios in Two-Phase Flow," Unpublished M.S. Thesis, University of Minnesota (1954).

(12) Sher, N. C. "Liquid Holdup in Two-Phase Steam Water Flow," Unpublished Thesis, University of Minnesota (1954).

(13) Zmola, P. C. and R. V. Bailey. "Power Removal from Nuclear Reactors," Unpublished paper presented at ASME meeting, Boston, Massachusetts (1955).

(14) Schwarz, K. "Investigation Density Distribution, Water and Steam Velocities, as well as Pressure Loss in Vertical and Horizontal Upflow Boiler Tubes," Verein deutscher Inginieure, Forschungsheft 445B, 1 (1954).

(15) Isbin, H. S., R. H. Moen, and D. R. Mosher. "Two-Phase Pressure Drops," AECU-2994 (November, 1954).

(16) Gresham, W. A., P. A. Foster, and R. J. Kyle. "Review of the Literature on Two-Phase (Gas-Liquid) Fluid Flow in Pipes," WADC-TR-55-422 (June, 1955).

(17) Kirschbaum, E., B. Kranz, and D. Starck. "Heat Transfer with a Vertical Vaporizing Tube," Zeitschrift des Vereines Deutscher Inginieure, Forschungsheft 375 (1935).

(18) Badger, W. L. "How Long. Tube Evaporator Works," Chem. and Met. Eng., Vol 46, 640 (1939).

(19) Lewis, W. Y. and S. A. Robertson. "The Circulation of Water and Steam in Water Tube Boilers, and the Rational Simplification of Boiler Design," Proc. Inst. Mech. Eng., (London), Vol. 143, 147 (1940).

(20) Martinelli, R. C., L. M. K. Boelter, T.H.M. Taylor, E. G. Thomsen, and E. H. Morrin. "Isothermal Pressure Drop for Two-Phase Two-Component Flow in a Horizontal Pipe," Trans. ASME, Vol. 66, 139 (1944).

(21) Alves, G. E. "Co-Current Liquid-Gas Flow in a Pipeline Contactor," paper presented at San Francisco meeting of A.I.Ch.E., (September 14, 1953).

(22) Radford, B. A. "Gas-Liquid Flow in Vertical Pipes - A Preliminary Investigation," M.S Thesis, University of Alberta (1949).

(23) Moen, R. H. and H Isbin. Personal Communication, University of Minnesota.

(24) Johnson, H. A. and A. H. Abou-Sabe. "Heat Transfer and Pressure Drop for Turbulent Flow of Air-Water Mixtures in a Horizontal Pipe," Trans. ASME, Vol. 74, 977, (1952).

(25) Bergelin, O. P. and C. Gazley. "Co-Current Gas-Liquid Flow, I, Flow in Horizontal Tubes," Heat Transfer and Fluid Mechanics Institute, Berkeley, California (1949).

(26) Baker, O. "Design of Pipelines for Simultaneous Flow of Oil and Gas," The Oil and Gas Journal (July 26, 1954).

(27) Chisholm, D. and A. D. K. Laird. "Two-Phase Flow in Rough Tubes," ASME Paper No. 57-SA-11, presented at Semi-Annual Meeting, San Francisco, California (June 9-13, 1957).

(28) Hoopes, W. H. "Flow of Steam-Water Mixtures in a Heated Annulus and Through Orifices," A.I.Ch.E. Journal Vol. 3, No. 2 (1957).

(29) Levy, S. "Theory of Pressure Drop and Heat Transfer for Two-Phase Two-Component Annular Flow in Pipes," Ohio State Univ. Eng. Exp. Station Bul. No. 149.

(30) Gazley, C. "Co-Current Gas-Liquid Flow - III - Interfacial Shear and Stability," Heat Transfer and Fluid Mechanics Institute, Berkeley, California Meeting, (1949).

(31) Harvey, B. F. and A. S. Foust. "Two-Phase One-Dimensional Flow Equations and their Applications to Flow in Evaporator Tubes," Chem. Engr. Progress Symposium Series, No. 5, Vol. 49, "Heat Transfer - Atlantic City," Publ. by Am. Inst. Chem. Engrs., 91, (1953).

(32) London, A. L. and W. M. Kays, "Compact Heat Exchangers," The National Press, Palo Alto, California (1955).

(33) Schiller, L. Zit. S. 131, Z. angew. Math. Mech. Bd. 3 (1923) S. 2. Z. VDI Bd 67 (1923) S. 623.

(34) Lockhart, R. W. and R. C. Martinelli, "Proposed Correlation of Data for Isothermal Two-Phase, Two Component Flow in Pipes," Chemical Engineering Progress, 45, 39 (1949).

(35) Sher, N. C. "Estimation of Boiling and Non-Boiling Pressure Drop in Rectangular Channels at 2000 PSIA," WAPD-TH-301.